Hybrid Control Schemes for Permanent Magnet Synchronous Generator Wind Turbines

by

Ahmed Selman Hadi Al-Toma

Department of Electronic and Computer Engineering

College of Engineering, Design and Physical Sciences

Brunel University London

United Kingdom

This thesis is submitted in partial fulfilment for the degree of

Doctor of Philosophy (PhD) in Electrical Power Engineering

September 2017

To my family

Parents..

Sister ..

My wife..

and Children..

I introduce this effort

. . .

Abstract

Wind turbines require continuous monitoring and control in order to maintain the power output as the wind speed varies. Traditional control techniques using conventional equipment and devices have been used in small scale generators at a commercial or residential level. A range of techniques have been developed and used to control generation output and to satisfy grid code requirements. Such techniques have demonstrated good performance with constant wind speed and linear system parameters.

At the same time classical control techniques, based on the linear Proportional Integral controller and low band-width modulation, present several technical issues during lower switching frequency operation as well as slow response to uncertainty in system parameters.

It is important to note that wind turbines are non-linear in nature and therefore require robust controllers that can adjust to the changes in the external environment as well as operational conditions and disturbances. For this reason, advanced control schemes have been proposed to mitigate the effects of potential system disturbances.

A variety of advanced control methods have recently been applied in response to wind energy conversion problems, such as fuzzy logic, slide mode, adaptive and predictive that have been applied to solve some of these problems. Such techniques are only valid for a specific operational range and do not cover the whole operational region with regard to rate of change of wind speed. Therefore, when considering large scale power generation from wind energy, high turbulence wind velocities and uncertainty in system parameters require the development of new hybrid controllers in order to address such problems. In order to improve

the system performance and deal with uncertainties under different operational conditions, advanced control techniques such as model reference control and model predictive control are combined with fuzzy logic control.

This thesis presents detailed analyses, modelling and simulation of novel and hybrid control schemes for variable speed wind turbines as operated in small or large scale such as 2 MW grid-connected Permanent Magnet Synchronous Generators. The proposed controllers show a reduction of steady state errors, reduced overshoot of the rotor speed and an increase in the active power that is generated. The results are compared to conventional controllers such as Proportional Integral controller in order to demonstrate the improved performance and the robustness of system.

Declaration

I declare that this thesis is my own work and is submitted for the first time to the Post-Graduate Research Office. The study was originated, composed and reviewed by myself and my supervisors in the Department of Electronic and Computer Engineering, College of Engineering, Design and Physical Sciences, Brunel University London UK. All the information derived from other works has been properly referenced and acknowledged.

by

Ahmed Selman Hadi Al-Toma

September 2017

Acknowledgements

Firstly, I would like to express my appreciation and gratefulness to the Ministery of Higher Education and Scientific Research, University of Karbala and Iraqi Cultural Attaché-London for sponsorship and funding my PhD study and managing the student affairs.

I would like to thank my supervisor Professor Gareth A. Taylor for his advice and guidance during the PhD period and valuable assistance over the last three years.

I am so thankful to my second supervisor Dr. Maysam Abbod for his support and encouragement. My gratitude goes also to my colleagues in the Smart Power Networks theme and Brunel Institute of Power Systems, who have been supportive throughout this period.

I would like to acknowledge the great attitude of all the staff members that I have interacted with at Brunel University and specifically in the department of Electronic and Computer Engineering.

I am very grateful to all my friends who always show their care and support.

Finally, to my parents, sister and wife: I would like to thank you for being beside me as a source of care, love, encouragement and motivation which fill me with patience and commitment.

Abbreviations

ANN	Artificial Neutral Network
COE	Cost Of Energy
DSP	Digital Signal Processors
DTC	Direct Torque Control
DPC	Direct Power Control
ES	Expert Systems
ETO	Emitter Turn-Off thyristor
FACTS	Flexible AC Transmission System
FOC	Field Oriented Control
FLC	Fuzzy Logic Control
FPC	Fuzzy Predictive Control
FPGA	Field Programmable Gate Array
FRT	Fault Ride-Through
GA	Genetic Algorithm
GCT	Gate Commutated Thyristor
GSC	Grid Side Converter
GTO	Gate Turn-Off thyristor

HAWT	Horizontal Axis Wind Turbine
HCS	Hill Climbing Searching
IG	Induction Generator
IEGT	Injection-Enhanced Gate Transistor
IGBT	Insulated Gate Bipolar Transistor
IGCT	Insulated Gate Commutated Thyristor
IPPM	Interior Pole Permanent Magnet
LV	Low-Voltage
LVRT	Low-Voltage Ride-Rhrough
MCT	MOSTET-Controlled Thyristor
MOSFET	Metal-Oxide Semiconductor Field Effect Transistor
MPC	Model Predictive Control
MPPT	Maximum Power Point Tracking
MRFC	Model Reference Fuzzy Control
MSC	Machine Side Converter
MTE	Minimum Transmission Energy
MV	Medium-Voltage
NMPC	Non-Linear Model Predictive Control
OPC	Optimum Power Conversion
PSO	Particle Swarm Optimization
RB	Reverse Blocking IGBT
SCR	Silicon-Controlled Rectifier
SGCT	Symmetrical Gate Commutated Thyristor
SISO	Single Input Single Output

SIT	Static Induction Thyristor
STATCOM	Static Compensator
TSR	Tip Speed Ratio
VOC	Voltage Oriented Control
VSC	Voltage Source Converter
VSWT	Variable Speed Wind Turbine
WECS	Wind Energy Conversion System
WRSG	Wound Rotor Synchronous Generator
ZCD	Zero Cross Detection
ZVRT	Zero Voltage Ride-Through

Table of contents

Abstract **vii**

Abbreviations **x**

List of figures **xiv**

List of tables **xviii**

1 Introduction **1**

1.1 General Background 1

1.2 Research Motivation 3

1.3 Aim of the thesis 4

1.4 Thesis Contribution 5

1.5 Thesis Organisation 6

1.6 Publications 7

1.6.1 Journals 8

1.6.2 Conferences 8

2 Wind Energy Conversion System **10**

2.1 Introduction 10

2.2 Overview of Wind Energy Conversion Systems 12

2.2.1 Main Parts of Wind Energy Conversion System 12

2.2.2 Operating Voltages of Wind System Configuration 16
2.2.3 Grid Code Regulations 17
2.3 Classification of Wind Energy Conversion Systems 17
2.3.1 Type 1: Fixed Speed Wind Turbine Concept 17
2.3.2 Type 2: Variable speed wind turbine with variable rotor resistance . 19
2.3.3 Type 3: Doubly-Fed Induction Generator Wind Turbine 20
2.3.4 Type 4: Variable Speed Wind Turbine with Full-Scale Converter . . 21
2.3.5 Comparison between WECS types 23
2.4 Overview of Power Converters 23
2.4.1 General Classification of Power Converters 24
2.4.2 Technical Requirements for Power Converters 25
2.4.3 Back-To-Back Converters 28
2.5 Overview of Control Schemes 30
2.5.1 Wind Turbine Controller Techniques 31
2.5.2 Developed Configurations Studies of Control Systems 40
2.6 Summary 42

3 Modelling and Control of Wind System 43
3.1 Introduction 43
3.2 Mechanical Modelling of WECS 45
3.2.1 Wind Turbine Model 45
3.3 Electrical Modelling of WECS 48
3.3.1 PMSG Model 48
3.3.2 Voltage Source Rectifier Model 53
3.3.3 Back-To-Back Converter Model 55
3.3.4 Grid Model 55
3.4 Control System Schemes 58

3.4.1 Reference Frames for Control Schemes 58
3.4.2 Control Schemes of Variable Speed Generator 59
3.4.3 Machine Side Converter Control 61
3.4.4 Grid Side Converter Control 68
3.4.5 Phase Locked Loop 71
3.4.6 Pitch Angle Control 72
3.5 Simulations and Results 73
3.5.1 Wind Turbine Control Simulations 75
3.5.2 Generator Current Control Simulations 75
3.5.3 Grid Current Control Simulations 77
3.6 Summary 80

4 Advanced Control Schemes of Wind System 83

4.1 Introduction 83
4.2 Fuzzy Logic Controller 86
4.2.1 Fuzzy Logic System 86
4.3 Analysis of Fuzzy Logic Controller 87
4.3.1 Fuzzification 88
4.3.2 Inference Engine 90
4.3.3 Defuzzification 90
4.4 Application of Fuzzy Logic in Control Scheme 91
4.4.1 Direct Fuzzy Logic Controller 91
4.4.2 Model Reference Fuzzy Controller 92
4.5 Simulation and Results 94
4.5.1 Simulation Using PI Controller 96
4.5.2 Simulation Using FLC 99
4.5.3 Simulation Using MRFC 102

4.5.4 Comparison Between Controllers 104
4.6 Summary 109

5 Fuzzy Predictive Control Schemes 111
5.1 Introduction 111
5.2 Model Predictive Controller 112
5.2.1 Control Strategy of MPC 112
5.2.2 MPC Control Principle 113
5.3 Analysis of Fuzzy Predictive Control 115
5.4 Structure of the Proposed Technique 118
5.4.1 Machine Side Control System 118
5.4.2 Grid Side Control System 122
5.5 Simulation of the Proposed Controller 125
5.5.1 Machine Side Converter Simulations 126
5.5.2 Grid Side Converter Simulations 127
5.5.3 Analysis of Results 130
5.5.4 Comparison between FPC and traditional PI controller 132
5.6 Summary 137

6 Conclusions and Future Works 138
6.1 Conclusions 138
6.2 Future Works 141

Bibliography 142

List of figures

2.1 Development in commercial wind turbine sizes 11
2.2 Basic structure of a grid connected wind turbine 12
2.3 Type 3 grid-connected Fixed speed SCIG WECS 18
2.4 Type 2 grid-connected semi-variable speed WRIG WECS 19
2.5 Type 3 grid-connected semi-variable speed DFIG WECS 20
2.6 Type 4 grid-connected variable speed WECS 22
2.7 Classification of power converters [11] 27
2.8 Classification of Back-to-Back converters [11] 29
2.9 Development of control techniques and the percentage of their researches [98] . . 40

3.1 Schematic diagram of grid connected WECS model 44
3.2 Variation of power cofficient with TSR 47
3.3 Cross section of different synchronous generator types [162] 49
3.4 abc-dq axis. 51
3.5 Phasor diagram and equivalent circuit of PMSG 52
3.6 AC to DC diode rectifier 54
3.7 Back to Back IGBT converters 55
3.8 Representation of the symmetrical three-phase voltage 56
3.9 Schematic Diagram of PMSG Control Scheme 59
3.10 Classification of Control Schemes of PMSG 60

3.11 Field Oriented Control Schematic Diagram 62
3.12 Synchronous reference frame control loops 66
3.13 Control architecture provided by SISO tool 66
3.14 q-axis current loop 67
3.15 Schematic diagram of grid side converter configuration 68
3.16 Current control of grid side converter 69
3.17 DC voltage loop control 70
3.18 Schematic diagram of the pitch angle control method 73
3.19 Power Output fo a Wind Turbine Generator[201] 74
3.20 Wind speed variation with time 75
3.21 Rotational rotor speed and reference speed with time 76
3.22 Tip Speed Ratio TSR 76
3.23 Variation of power coefficient with time 77
3.24 Generated 3-phase current with respect to time 78
3.25 DC link voltages during wind variation with time 78
3.26 Grid side 3-phase Current 50 Hz with respect to time 79
3.27 Grid side 3-phase active, reactive and mechanical power with time 79
3.28 3-phase active power losses with time 80
3.29 mechanical and electromagnetic torque variation 80
3.30 Grid side Frequency Variation 81
3.31 3-phase Grid voltage 81

4.1 Structure of Fuzzy Logic Controller 88
4.2 Membership Function of FLC for the input variables 89
4.3 Membership Function of FLC for the output variable 90
4.4 FOC scheme using FLC for current variable 92
4.5 MRFC scheme using FLC with model reference for current variable 95

4.6 Wind speed variation with respect to time 97
4.7 3-phase generator currents applying PI 97
4.8 Direct and quadrature axis currents variation applying PI 98
4.9 Variation of reference and rotor speeds applying PI 98
4.10 Variation of mechanical and electromagnetic torques applying PI 99
4.11 3-phase Generator current variation using FLC 100
4.12 Direct and quadrature axis currents variation using FLC 100
4.13 Variation of reference and rotor speeds using FLC 101
4.14 Variation of mechanical and electromagnetic torques using FLC 101
4.15 3-phases Generator currents variation using MRFC 102
4.16 Direct and quadrature axis currents variation using MRFC 103
4.17 Variation of reference and rotor speeds applying MRFC 103
4.18 Variation of mechanical and electromechanical torques using MRFC 104
4.19 Variation of rotor speed for in case of step change for all controllers 106
4.20 Variation of rotor speed for steady state for all controllers 106
4.21 Variation of electromechanical torques in case of step change for all controllers . . 107
4.22 Variation of electromechanical torques in case of steady state for all controllers . . 108
4.23 Variation of steady state quadrature axis current for all controllers 109

5.1 Timing diagram of the execution of the MPC algorithm 114
5.2 Structure of Fuzzy Logic Controller 116
5.3 Membership Function of FLC for the input variables 117
5.4 Membership Function of FLC for the output variables 117
5.5 FPC - MSC Schematic Diagram for the Machine Side 119
5.6 FPC - GSC for the Grid Side 123
5.7 Variation of wind speed 127
5.8 Variation of the generator speed 127

5.9 Variation of mechanical torque and electromagnetic torque 128
5.10 Variation of the generator currents 128
5.11 Variation of DC link voltage 129
5.12 Variation of grid voltage and current for a specific period of time 129
5.13 Variation of grid current with respect to time 130
5.14 Variation of grid frequency 130
5.15 Variation of grid active and reactive power 131
5.16 Variation of grid active power losses 131
5.17 Variation grid frequency compared to PI controller 134
5.18 Variation rotor speed compared to PI controller 134
5.19 Variation electromagnetic torque compared to PI controller 135
5.20 Variation of ΔP_e of FPC compared to PI controller 136
5.21 Variation of ΔV_{dc} for both controllers 137

List of tables

2.1 Comparison of LV and MV Operation Wind Turbines 30

4.1 Rule base table of the Fuzzy Controller 89

4.2 Standard deviation in variations of the power coefficient and rotor speed . . 105

4.3 Calculation of change response for rated rotor speed for different controllers 105

4.4 Calculation of torque variation 108

5.1 Rule base table of the Fuzzy Controller 116

5.2 Switching states and corresponding output voltages $V^{j}_{sdq(j=0...7)}$ 121

5.3 Variation of active power with respect to wind speeds for PI controller . . . 132

5.4 Variation of active power with respect to wind speeds for FPC 132

5.5 Calculation of some metrics standard deviations for both controllers 133

5.6 Calculation of some metrics mean values for both controllers 133

5.7 Calculation of change response for rated rotor speed for different controllers 133

5.8 Standard deviation of the variation in DC voltage and active power 136

Chapter 1

Introduction

1.1 General Background

It is believed that the ancient human being has utilised the movement of the wind for 3000 years. The use of wind power has been more developed since the beginning of the last century to provide mechanical power to grind grain or pump water [1].

At the beginning of industrial revolution, utilization of the unstable or swing wind energy resource have been replaced and exchanged by fossil fuel for firing the machines to produce the electrical energy, which delivered a more consistent adjustable power source in acceptable price and high efficiency.

Fossil fuel sources cover more than 80% of the world's energy absorption which are being depleted at a faster rate than they can be regenerated. Generally, the consumption of fossil fuels has bad side effect for the Earth's atmosphere and surface such as climate change and global warming, which related to the anthropogenic release millions of tons of carbon dioxide (CO_2) every year. This problem causes a huge amount of pollution and high costs of fuel in generation.

To overcome this problem, reliable and cost effective renewable energy such as wind energy which have been applied in developed countries and finally commercially traded in

several developing countries. Renewable energy production is rapidly increased during the last decades concerns about limited fossil resources and the associated environmental issues.

Due to the fast development of wind energy generation and penetration into the electrical power market, many issues related to the stability and security of operational environment is growing as well as the development of protection and control in the electric power system. Nowadays grid codes may form a crucial point to acquire in many countries that contain grid connected large scale wind turbines operated instantaneously in large areas of wind farms [2]. Global demand for renewable energy have been raised during 2014, then it provided an estimated 19.2% of global energy consumption [3].

Various categories with different types of generators are utilized with a lot of advantages and drawbacks in operation. The power electronic devices have been used commercially in wind turbines design since the beginning of grid connected operation, and this technology has changed dramatically over the past three decades [4].

Recently, various combinations of wind generators and power electronic devices have been applied in wind turbines operation and control to obtain different values of rotational speed operation. The latter has raised as a successful configuration to improve the system efficiency of wind energy conversion and then increase the quality of injected grid power. The power converter and its control are very crucial in the successful and efficient operation of variable-speed wind turbines [5].

In practice, the widely used electrical machine drive systems are permanent magnet synchronous machine due to the attractive features such as high energy density, low torque ripple, higher efficiency, higher reliability, lower cost of maintenance and operation at low rotational speed [6]. Furthermore, there is a wide range of variety to control the output powers, voltages, current and frequency in all parts of the system.

Generally, control schemes manage different variables such as generator currents and voltages, pitch angle of the blade in the turbine, DC link voltage, and grid side variables such

as frequency, active and reactive powers as well as the output voltages and injected currents to the grid. Different types and techniques have been used and developed to achieve the control schemes requirements and implement in practice using power electronic devices.

Furthermore, traditional control techniques using simple equipments and devices have been used in small size generators which cover a domestic area or residential. These have a good performance during constant wind speed and assumption of linearity in the system parameters. A lot of issues have been discussed in research rather than in practice such as variable wind speed, non linearity of the system, behaviour of the system during faults or mechanical damage and the main issues of power system network such as load flow, stability analysis and constancy of voltage and frequency [7].

Operation of the system under constant voltage and frequency need further precise and robust techniques by developing control schemes to satisfy stable penetration of power during the operational periods. A new techniques use an intelligent system such as Fuzzy Logic Control (FLC) in combination with other controller to overcome the problems of the uncertainties and improve the profile of output current. These models are Model Reference Fuzzy Control (MRFC) and Fuzzy Predictive Control (FPC) that can be used in different parts in the system [8–10].

This thesis described the impacts of these techniques and the effect of their combination on the output profile of the currents to maintain the voltage and frequency constant during wind speed variations.

1.2 Research Motivation

Designing, modelling and simulation are very important processes that enable the efficient operation of the wind system and control strategies. The developed devices of power electronics supports control operation and enables wind energy conversion to adequately enhance the electric power penetration. Increase in grid code requirements lead to develop

modern wind turbines capable to follow the designing of robust, advanced and intelligent control schemes for variable speed wind turbine depending upon the potentials of power electronic interface.

This thesis deals with designing a grid connected variable speed wind energy conversion system, their modelling, analysis and control. The design also controls wind system operation in various values of wind system parameters using novel hybrid controllers that satisfy different issues such as maximum power extraction from the wind. Modelling of a three phase voltage source converter with traditional controller such as proportional integral controller or hysteresis current controller are commercially employed in power markets. Furthermore, advanced controller such as fuzzy are recently used to improve the output profiles of voltages and currents.

This design can be developed using an alternative model for voltage source rectification and inversion switching circuit using a hybrid control that can be efficiently applied.

In addition to that, the new control scheme can mitigate the effect of sudden change and disturbances in wind speed during operation and the effect of uncertainties of the system due to change of the system parameters.

1.3 Aim of the thesis

The main aim of the presented thesis is to design an advanced control scheme for wind generator to satisfy stable performance of the systems and constant voltage and frequency. This can be achieved by analysing the system behaviour under different operational conditions using following steps:

1. Design and simulate a variable speed wind energy conversion system using permanent magnet synchronous generator to mitigate the effect of wind speed disturbances and satisfy maximum power tracking during wind speed variation.

2. Investigate the system states to different wind speeds and loading conditions (stand alone load or the power grid).

3. Develop advanced control schemes using intelligent controller such as fuzzy logic control scheme to maintain the output voltage and frequency constant during any disturbance and operated in wide range of generator sizes.

4. Evaluate the effectiveness of the developed schemes for large scale system at different speeds and parameters variations.

1.4 Thesis Contribution

The principal contributions to knowledge, as discussed in this thesis, can be expressed briefly in the following summarized points:

1. Permanent magnet synchronous generators and control strategies are generally based on detailed voltage source back to back converters. Therefore, such a model has been developed and implemented using a fuzzy logic based algorithm in the design of the controller of the converter machine side to enhance the operation of the system by mitigating the effect of wind speed disturbances and satisfying maximum power extraction from the wind.

2. Development and implementation of a novel Model Reference Fuzzy Control scheme for the machine side converter. The design is based on using a fuzzy logic controller that improves the input to the system using the error between the model reference and the values of output variables. This controller is designed using expert knowledge which is activated in the event of plant parameter variations or external disturbances. The fuzzy controller is designed to preserve the desired model reference in order to

give more robustness and effectiveness to the proposed controller as demonstrated via simulation results.

3. Development and demonstration of a novel hybrid control scheme combining both fuzzy logic control and Model Predictive Control for both the machine side and grid side converters. The scheme reduces overshoot of the generator rotor speed, and maintains the output voltage and frequency within the rated values in cases of wind speed disturbances. This approach requires the determination of set values of currents in order to adjust the converter voltages. Fuzzy logic control performs this task by adjusting the input to the predictive controller and minimizing the cost function to maintain the output voltage constant.

1.5 Thesis Organisation

The chapters of this thesis can be organised as follows:

- Chapter 1 represents the general introduction of the thesis. It consists of background of the wind energy and research motivation, aims and objectives and thesis contributions. Finally, the publications that regarded with the thesis have been added.
- Chapter 2 shows the main background of the thesis which consists of the classification of wind energy conversion systems and issues that related to power energy and the literature survey to the references for the relevant issues of the main contributions.
- Chapter 3 represents the modelling and control of the Back to Back energy conversion system. It is defined by an introduction then mechanical modelling witch belongs to wind turbine structure, electrical modelling of wind energy conversion system which consists of the generator, converter and the grid. Other part of this chapter is the traditional control of the system which consists of the machine side converter and

the grid side converter control using proportional integral controller in field oriented scheme. The aim of the control system to achieve the proper values of currents and speed of the generator to satisfy Maximum Power Point Tracking to extract the maximum power of the wind.

- Chapter 4 is talking about one of the advanced control technique in the field oriented scheme to control the machine side converter. This type of control uses a Fuzzy Logic Control in currents and speed circuit to improve the rotor speed variation during variable wind speed. At the same time, setting values of rotor speed and direct axis current are also adjusted to satisfy the principle of maximum capturing power from the wind and maximum torque at low current during operation. Further improvement has been made using a combination of Fuzzy Logic Control with model reference to obtain Model Reference Fuzzy Control which addressed as a novel control scheme to overcome the problems of non-linearity of the system.

- Chapter 5 describes hybrid control scheme that use a combination of Model predictive control with Fuzzy Logic Control to form a Fuzzy Predictive control scheme. Descriptions of both controllers and their applications have been presented through and simulation and results for different values of wind speed are discussed. To prove the impact of this controller on the uncertainty of the system, two cases studied have been suggested for the change in generator resistance and inductance during the operation showing the output currents and power and system behaviour during this period.

- In chapter 6, conclusions followed by brief points of future work have been summarised.

1.6 Publications

The work in this thesis has been published in number of refereed publications as follows:

1.6.1 Journals

Journal papers submitted and in preparation at the time of submission of this thesis:

- A. Al-Toma, G. Taylor, and M. Abbod, "Robust Fuzzy Predictive Control Strategies for Grid Connected Variable Speed Permanent Magnet Synchronous Generator Wind Turbines", *IEEE Transactions on Control Systems Technology*. Submitted Aug. 2017, TCST-2017-0726.

- A. Al-Toma, G. Taylor, and M. Abbod, "Model Reference Fuzzy Control Scheme for Field Oriented Permanent Magnet Synchronous Generator Wind Turbines", *IEEE Transactions on Control Systems Technology*. In preparation.

1.6.2 Conferences

Conference papers that have published and accepted:

- A. Al-Toma, G. Taylor, and M. Abbod, "Modelling and simulation of load connected fixed blade wind turbine with permanent magnet synchronous generators", 50^{th} International Universities' Power Engineering Conference (UPEC2015). 1-4 September, University of Staffordshire, Stoke-On-Trent, UK, 2015.

- A. Al-Toma, G. Taylor, and M. Abbod, "Development of Space Vector Modulation Control Schemes for Grid Connected Variable Speed Permanent Magnet Synchronous Generator Wind Turbines", 51^{th} International Universities' Power Engineering Conference (UPEC2016). 6-9 September, Coimbra Institute of Engineering (ISEC), Coimbra, Portugal, 2016.

Paper have been submitted to the following conferences:

- A. Al-Toma, G. Taylor, and M. Abbod, "Intelligent Pitch Angle Control Scheme for Variable Speed Wind Generator Systems", 52^{th} International Universities' Power Engineering Conference (UPEC2017). Accepted April 2017.

- A. Al-Toma, G. Taylor, and M. Abbod, "A Comparison of PI and Fuzzy Logic Control Schemes for Field Oriented Permanent Magnet Synchronous Generator Wind Turbines", ISGT Europe 2017. Full paper accepted June 2017.

Chapter 2

Wind Energy Conversion System

This chapter introduces the fundamentals, principle of operation and control of Wind Energy Conversion System (WECS). General description to the principles and operation of WECS has been demonstrated by describing major components of grid connected WECS such as mechanical, electrical and control parts, operation voltage that the WECS work and finally the grid code requirements. Classification of WECS has been discussed in section showing all types of WECS and their applications detailed and mentioned the advantages and disadvantages of them. Power converters and their applications have been reviewed as well as the classification of applied control schemes which is used in WECS has been discussed briefly.

2.1 Introduction

Several technological advancement in both aerodynamic or electrical equipment design have been developed by wind energy markets during last decades in industry or commerce environments. These issues related to mechanical equipment, electric generators and power electronic devices, which cooperated the control equipment in power systems integration.

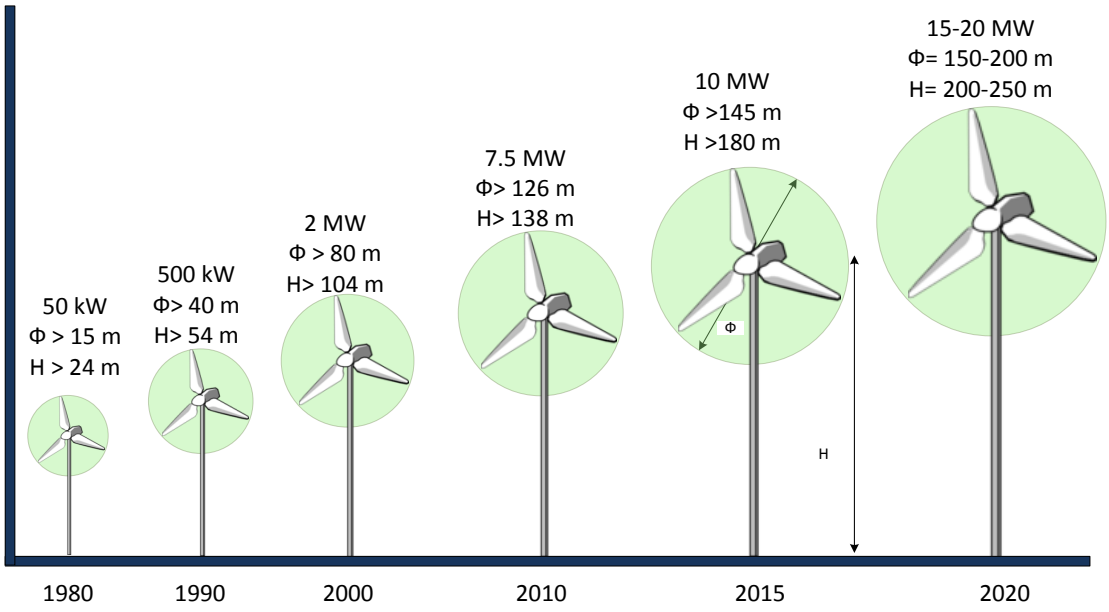

Fig. 2.1 Development in commercial wind turbine sizes

From the perspective of electrical engineering, the electric generators and power electronic converters have major interest in the operation of WECS.

Since the beginning of grid-connected wind system utilization in 1980s, different types of combinations of generators and equipment of power electronic converters have been applied and improved in modern wind turbines manufacturing companies to acquire fixed or variable rotational speed wind turbine system [11, 12]. The production of power which obtained by renewable sources in the world exceeded 1470 GW in 2012 representing nearly 19% of global energy consumption [13–15]. As a result, in 2013 the sizes of offshore and onshore wind turbines are stated approximately as 3.613 and 1.926 MW respectively [3].

Commercially the marketing of wind turbines expects that 10 - 20 MW of those turbines should be operated in large scale size in the future. These turbines have rotor diameters may exceed 150 m, that means double of the length of the air-plane Boeing 747. The development of wind turbine size during last three decades is shown in Figure 2.1. Statistical studies show that the industrial plants consume the largest amount of delivered energy; where expected to

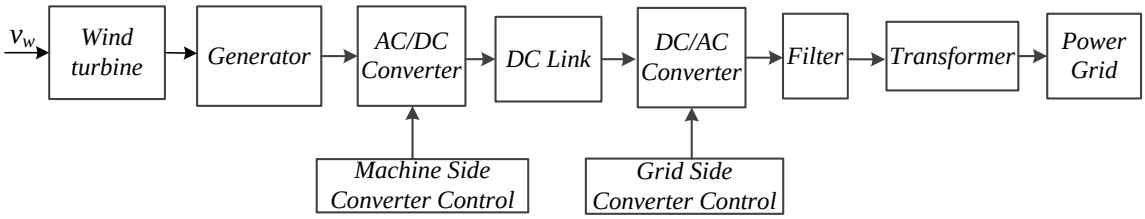

Fig. 2.2 Basic structure of a grid connected wind turbine

absorb over half of total supplied energy in 2040. Research show that the renewable energy is one of the world's rapidly growing sources of energy, increasing by 2.6% /year; nuclear energy grows by 2.3% /year, from 4% of the global total in 2012 to 6% in 2040 [3, 11].

In modelling, application and control of WECS many researchers have published various works focussing on the related topics. Some studies concentrated on designing using various types of generators and control schemes. These topics will be discussed in the next sections. To analyse the whole components of the system, it is important to concentrate on the fundamental and principles of operation of these components such as generation, conversion devices and control parts that represent the main topics of recent studies.

2.2 Overview of Wind Energy Conversion Systems

The following topics related to the main components of WECSs, the classification of these systems, ratings limits of voltages and currents, and the requirements of grid code have been described in this section.

2.2.1 Main Parts of Wind Energy Conversion System

The main configuration of grid-connected wind energy system is shown in Figure 2.2. The WECS consists of several components that manage the conversion process of kinetic energy

captured by the wind into electric energy penetrated to the grid in reliable pattern and efficient performance.

Generally the essential components of a WECS contain mechanical, electrical and control components. The main mechanical parts contain the structure of tower, rotor hub, nacelle,rotor blades, moving parts of pitch drivers, yaw rotating drivers, gearbox, drive-train, sensors of wind speed, and brakes. The electrical parts contain electric generator, connection wires, power converters and inverters and finally the collection point to the three-phase grid [2, 11, 16].

In some models the harmonic filters and transformer are shown in the system. Control techniques are used with both the mechanical and electrical equipment to manage the energy conversion process [17, 18, 12].

2.2.1.1 Mechanical Components

First of all the kinetic energy captured by wind turbine can be converted into mechanical energy by the aid of air-foil structured rotating blades. In the common types of wind turbines, a three blades configuration is more beneficial and stable for the conversion process [19, 20]. The efficiency of the energy conversion process depends upon many parameters like blade's angle, the structure of the rotor blades, air density, and velocity of wind [21].

Some electronic or mechanical sensors are used to measure the values and direction of wind speed, while the yaw is designed to rotate the blades with nacelle in the direction of the wind to obtain the maximum power extraction. When the turbine speed is increased over the rated limit, the blades angle will be varied to maintain the output electric power within the rated value of the generator [19].

The purpose of tower, nacelle and hubs is providing mechanical support to the structure of the blades. According to the aerodynamic properties, maximum electricity is generated by any particular turbine only within or above the rated value of wind speed [11, 22–24].

The large scale turbines usually operate at relatively high torque and low speed (6 - 20 rpm) due to huge construction of the turbine. The review of wind power markets shows that the diameter of the rotor and power rating of offshore wind turbines and generator are higher than the onshore wind turbines. A multi stage gearbox is used for coupling purpose to convert the low speed and high torque to the high speed low torque generator shaft. The gearbox shows several effective impacts such as highly cost, high audible noise, low life span and efficiency, and finally requiring a continuous maintenance [25].

These drawbacks leads to think in an appropriate design to eliminate the gearbox of the machine. By corresponding the turbine speed with the rotor speed, the existence of gearbox can be omitted. The elimination of gearbox; which is usually called as direct-drive or gear less; helps to reduce mechanical problems, particularly in the case of offshore wind turbines [26, 27].

Other mechanical equipment such as brakes can be mounted in the generator drive-train specially in those which have a shaft of high speed in order to break wind turbine in the case of unbalanced conditions such as fault or high wind gust during highly variable air flow.

2.2.1.2 Electrical Components

To convert mechanical energy to electric energy, an electric generator is the tool that can be used. Over the last three decades, many types of generators like the Squirrel-Cage Induction Generator (SCIG), Doubly Fed Induction Generator (DFIG), Wound Rotor Induction Generator (WRIG), Permanent Magnet Synchronous Generator (PMSG) and Wound Rotor Synchronous Generator (WRSG) have been studied and analysed in research for wind turbines manufacturing [28–30].

Growing up of these types began only with SCIG have been used in wind turbines, but recently the turbines incorporates both types of induction and synchronous generators. The

induction generators (IGs) mainly run at highly speeds compared to the synchronous which operated with wide range of speeds [31–33].

The output voltage and frequency of the generator are changed proportionally with the wind speed. It will be difficult to control these variables when the generator is directly connected the grid. To achieve a controllable values of output variables, the generator can be decoupled through a power electronic rectifiers and inverters, various types of converters topologies utilise the power switching devices usually connected to the DC-link equipment like capacitors or inductors. Harmonic filters can be applied in AC generator output converter or inverter to mitigate the harmonic of the switching process of power converters [5].

In the generator side part, the harmonic filter can be applied to minimize the total harmonic distortion of the generator currents. This minimization can reduce the harmonic losses dissipated in the generator's winding and core. As a complement to the electric part of WECS, the grid side converter may use a harmonic filter to reduce the generated harmonics and to meet the requirements that indicated by the grid code [34, 35].

When the transferred voltage of the power inverter and filter is less than the grid voltage, a step-up transformer can be used to connect the filter to the grid side, and finally to electric circuit breaker of the bus-bar. Using power electronic converter at the point of power collection enable to connect system directly to the grid and then the need for step-up transformer can be omitted.

2.2.1.3 Control System

To acquire desired operation as well as stable performance in WECS, the wind turbine system, several auxiliary control systems for both mechanical and electrical components can be used. The control equipment and sensors usually used to monitor various variables and parameters such as the velocity of wind speed and its direction, the voltages and currents of the generator, converters and filters as well as DC-link voltages. These variables have been provided to

adjust the system operating states or variables in the case of the grid voltages and currents are changed to keep the operation at the reference limit [17].

For example, active, passive or pitch stall control should be selected by the master control system when the variation of wind speed is more than the rated speed of the turbine. This control system manages the change of blades angle in way that the turbine output power kept no more than the rated value [22, 36].

Applying a micro-controller, computer, Field Programmable Gate Array (FPGA) or Digital Signal Processor (DSP) used to be provided to the control system for the main tasks that should be performed [37, 38]. Using the recent control strategies, the control process can be faster and performing highly precision calculations (in less than 100 microseconds) and repeatedly.

2.2.2 Operating Voltages of Wind System Configuration

In the North American and European power markets, the definition of WECS operating voltages is summarized recently [39, 40]. These voltages can be more classified according to level margin such as medium voltage (MV) and low voltage (LV) operation. The voltages below 1000 V are classified as LV class, where as voltages approximately $1-34.5$ kV regarded as MV. Various values have been used in LV range, but most standard of them which used for electric generators and converters in different area in electric power system are 575 or 690 V, while applied generators output and converters of MV voltages are within $3-4$ kV [11].

Nowadays the participation of major industrial manufacturing companies in global markets reduce the importance of these regional classifications. Therefore, the commercial wind turbines should be connected to the Point of Common Collection (PCC) by cables or lines using step-up transformers, then the regional voltage will be irrespective.

2.2.3 Grid Code Regulations

The increase of the power penetration of wind turbines and wind farms contribute to significant enhancement in supplying energy of the systems in the existing power plants.

Many specific technical requirements and regulations usually called as Grid Codes have been developed and continuously updated to ensure consumer power quality and the grid stability [41, 42]. The main requirements of grid codes contain the control constraints of active power in order to adjust the grid frequency and control of reactive power to satisfy the grid voltage regulation.

Other valuable variables such as the quality of power, voltage dip, Fault Ride-Through (FRT) detection, harmonic oscillations and overall protective devices are taken into account in grid code requirements. The correct determination of these requirements is crucial for manufacturers and operators of wind turbines.

2.3 Classification of Wind Energy Conversion Systems

Various types of wind turbine-generator categories have predominated the power system application in the last decade. These types are classified and explained in [43] and [44]. There are different winds turbines generator are currently in use, classified according to the combinations between their parts and the output power converted [45, 46].

2.3.1 Type 1: Fixed Speed Wind Turbine Concept

Figure 2.3 shows a fixed speed induction generator used in WECS without power converter interface. In this configuration a starting device and step up transformer are used to connect the generator to the grid [47–49]. This is a primary and oldest technology that developed the wind turbines system. In highly converted power of WECS, the simple types of SCIG consists of 4 or 6 poles in order to operate with the rated frequencies of 50 or 60 Hz.

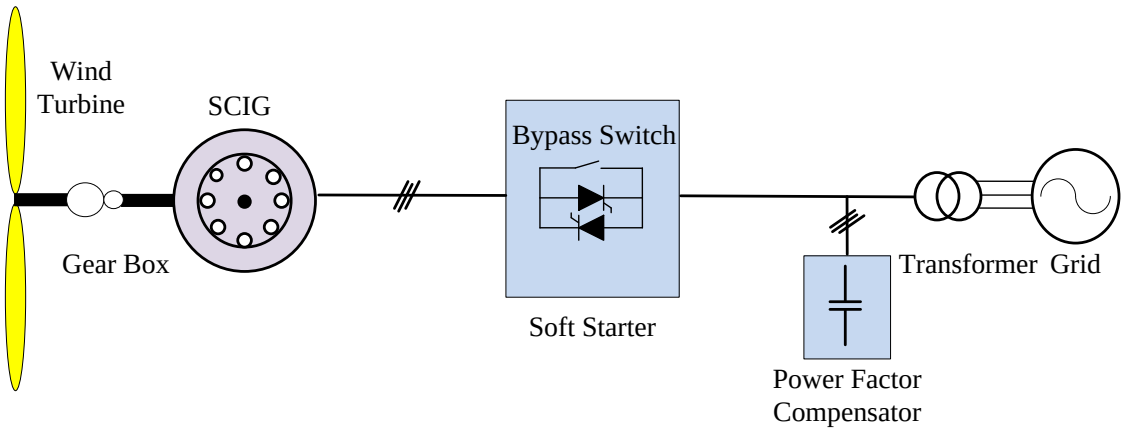

Fig. 2.3 Type 3 grid-connected Fixed speed SCIG WECS

The variation in rotational speed of generator is limited and approximately within 1% of rated speed at different values of wind speeds. Therefore this type of WECS is called fixed-speed [2]. Practically, a gearbox can be used for matching the speed error between the turbine and generator. The starter device can be bypassed after starting by a switch, where the system basically works without need to the converter device.

This type of generator configuration draws a valuable amount of reactive power by the grid. To recover this situation, three-phase banks of capacitors operate as a compensator device are usually applied. The features of this configuration is simple, reliable operation and low initial costs while the main drawbacks can be addressed as: (i) lower efficiency in energy conversion ; (ii) the variations of the wind speed will be transferred to the grid side; and finally (iii) any faults in grid side will cause huge tension on the mechanical parts of the wind turbine. This configuration of WECS is operated with auxiliary devices, like Static Compensator (STATCOM), in order to improve the operation performance and finally converge the grid code requirements [11, 50–53].

2.3.2 Type 2: Variable speed wind turbine with variable rotor resistance

Applying the variable speed of wind turbine generator configuration will lead to increase the efficiency of conversion process, and decrease mechanical tension which may be effected by the wind gusts, and finally decrease the bearings friction and the maintenance requirements, which finally increases the life the system at all. The wind energy system of semi-variable speed are using wound rotor type of IG and partial 10% of rated power conversion is shown in Figure 2.4. The configuration of this type uses the principle of variation of the rotor resistance which affects the characteristic of torque and speed of the generator and acquiring the operation of variable speed wind turbine. The rotor resistance can be adjusted by a power converter which consists the combination of diode-rectifier and chopper circuit. This configuration is usually called Opti-slip control [54]. The range of speed adjustment is limited to be within $\pm 10\%$ of its nominal speed. The operation under variable speed will enable to capture wind energy efficiently, though the existence of power losses in the generator resistance.

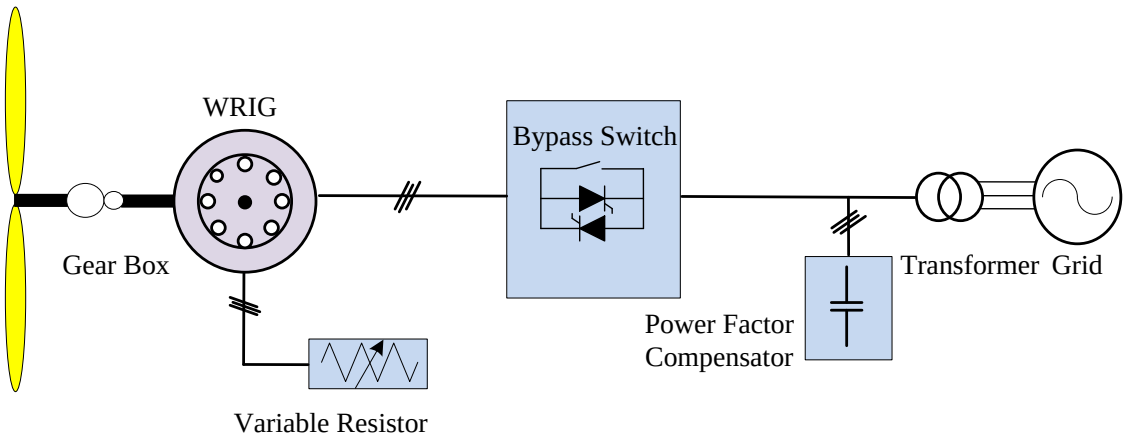

Fig. 2.4 Type 2 grid-connected semi-variable speed WRIG WECS

In this type, it is necessary to use soft starter, gearbox, and compensation devices of reactive power.

2.3.3 Type 3: Doubly-Fed Induction Generator Wind Turbine

This limited-variable speed configuration WECS applying DFIG is shown in Figure 2.5. The principle and operation of this type implies that the generated power is supplied to the grid by two windings, stator and rotor. A part of the converter rated power can be utilized in rotor circuit to recover the slip power, which is around 30% of the generator rated value [55–58].

Similar to those in Types 1 and 2 wind turbines, the gearbox is also used in Type 3 configuration to obtain the required rotation speed of the rotor. At the same time, there is no need to existence the reactive power compensation devices and a soft starter in this type [59]. The power converters are used to allow bidirectional power penetration in the rotor part and increases the range generator speed.

The overall power conversion efficiency can be improved via these features to perform Maximum Power Point Tracking (MPPT) [60, 61], and increase in the speed around 30%, may enhance the dynamic performance and strengthen the robustness against the system

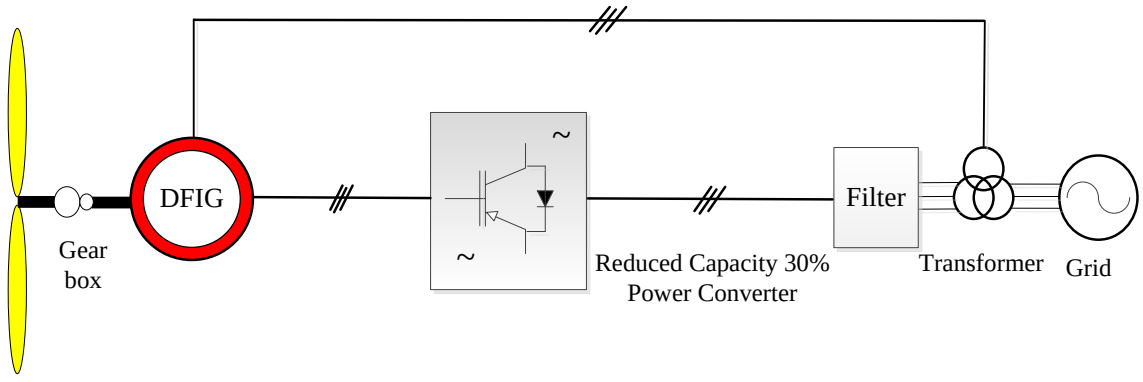

Fig. 2.5 Type 3 grid-connected semi-variable speed DFIG WECS

disturbances which are not available the Types 1 and 2 turbines [62–64]. These features enabled this type of induction machine to be one of the dominating technologies in modern electric market sharing approximately 50% [65]. The capability to FRT is limited because the partial transfer of power. Existing of the gearbox will increase the weight of the system and overall turbine cost as well as demanding continuous maintenance.

Moreover, the brushes and slip rings are needed to connect the power converter to the rotor windings through them. Regular maintenance is fundamental in these types of turbines due to ageing of brushes approximately is 6-12 months, that should be replaced periodically. These main drawbacks restricted these types of turbines being used in offshore wind farms due to highly expensive maintenance cost.

2.3.4 Type 4: Variable Speed Wind Turbine with Full-Scale Converter

Using of full-scale 100% power converters will greatly enhance the performance of WECS as shown in Figure 2.6. The types of SCIG, WRSG and PMSG can be applied in this configuration with a wide range of power rating reach to 8 megawatts. Since the rating of the power converters should be the same as generator rating, therefore the cost, complexity of system configuration and then the size will be increased. For this reason the losses of power converters are higher causing reduction in the efficiency of this type [66–68].

However, in this type of full power conversion, the generator and converters are fully separated from the grid, and generate full rated power during the operation at wide range of rotor speed 0 to 100%. The power converters is also needed to compensate the reactive power and obtain smooth active power [69]. The efficiency of WECS is higher in these turbines than other types [70–72]. The best FRT compliance also can be improved and obtained without external equipment. Although the power converter cost is slightly high, it will be a small fraction; within 7%-12%; of overall equipment cost . By using high number of pole pairs for all types of PMSG, the turbine gearbox can be deleted [11, 73].

This type of WECS is more strong against power system disturbances in comparison with the types 1, 2, and 3 wind systems.

The principle of distributed drive train is applied in developed large scale Type 4 wind system. Although WRSG and SCIG can be applied in this principle, the PMSG showed good operational performance because it removes the slip rings and brushes which provides simple design [31]. The gearbox is capable to drive multiple generators at higher speeds, therefore high power density can be obtained by the distributed drive-train and multiple generators.

Some configuration also shows effective fault tolerant in various operational conditions. The other three converters can still deliver the power to the grid in case of failure of one converter [2]. Applying a multi-winding transformer on the grid-side leads to minimize the circulating currents and reduction in harmonics. Complicated drive-train regarded as the main disadvantage with this configuration, for this reason the designers use multi poles generator to keep the angular frequency within the rated value and eliminate the drive train.

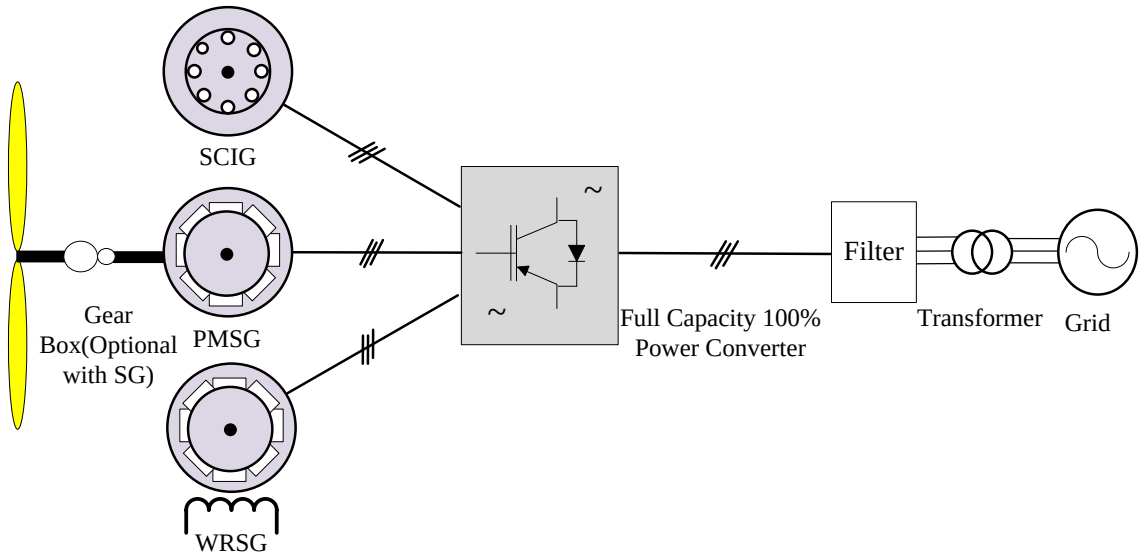

Fig. 2.6 Type 4 grid-connected variable speed WECS

2.3.5 Comparison between WECS types

The Type 3 turbines (DFIG) have been used by seven manufacturers among the top ten companies because it hold the highest market share. Approximately 100 various types of DFIG turbine models are utilized and manufactured by all the wind turbine companies. Few of these companies produce Type 4 turbines, however very little of them are dealing with direct drive solutions. It is shown by review that the best selling and utilization of wind turbines in the electric power markets use Types 3 and 4 technologies. It is expected during coming few years that Type 4 configuration would dominate the electric power market and will have main priority in the future projects which will be held by the manufacturing companies. A brief description of all types of turbines and their manufacturing companies have been explained in detail in [74, 75].

The comparison have been made depends upon electrical issues such as generator; power converters; capacity of power converter; and external reactive power compensation; compliance with the fault ride-through requirement; requirement for soft-starter, and mechanical and control issues such as gearbox and MPPT ability; aerodynamic power control, speed variety achievable; technology situation; and market penetration.

Generally, the Types 3 and 4 turbines are most suitable for large scale power grid connection and their utilizations. In this thesis, the configurations of generators and converters are analysed for the Type 4 of wind turbines in the next chapter.

2.4 Overview of Power Converters

As discussed in the last sections, since last three decades, the power electronics manufacturing and technology has an important participation with the advanced manufactured large scale wind turbines. This technology has been developed rapidly, and the recent manipulated categories are available represented by full-scale converters. Wind turbines as well as wind

farm level use power electronics of the current technology of energy conversion and grid connection. In this section, the power electronics technology is devoted to discuss briefly addressing the general description of power converters, their classification and technical requirements for this converter technology [76].

2.4.1 General Classification of Power Converters

The main objective of the converters is applying technology to operate Types 3 and 4 WECS with variable speed operation, whilst removing starting circuit and reactive power compensation to achieve simple construction. The variable voltage and frequency of the wind generator should be transformed to fixed values in order to enable a regular connection of these wind turbines to the grid.

Most of these converters have been applied commercially in various applications, while some of them have been suggested in research with committed features for future development. According to the power conversion operation, these converter categories are comprehensively classified into direct and indirect converters [11].

The single stage AC/AC converters has been applied as direct conversion process, while indirect one uses two stages of (AC/DC+DC/AC) or three stages of (AC/DC+DC/DC+DC/AC) to processed the power conversion [77].

Generally, electric drives industry depend upon some of these converters and their developments while some other converters have limited development for serving wind power application. The classification also shows different types of converters such as current source converters and direct ac/ac converters. These converters are main contenders to voltage source converters in power system markets [78, 79]. It is noticed that some of typical converters from the electric drive manufacturing market are also developed and studied although they have not been used widely in power factories yet.

2.4.2 Technical Requirements for Power Converters

Generally, the power converters Type 1 wind power generators configurations are applied for the purpose of smoothing the grid connection only. At the moment, when the turbine system is tied to the grid they are disconnected from the circuit. However, Types 3 and 4 configurations utilize these converters to fulfil most of these technical issues and operational requirements. Some important requirements should be taken in to account in wind energy system design have been discussed in some references [80, 81].

Generally, the initial cost of converter forms a small portion (around 7%-12%) of overall cost of wind turbine [73]. This factor is valuable in helping to minimize the Cost Of Energy (COE) and play a vital role in competing with other energy sources. Although it is a small part of the total cost, it can provide huge saving in expenses for a wind energy farm which contains hundreds of wind turbines.

Over the mentioned initial cost, the cost of maintenance which involves components replacement and technicians' expenses should also be minimized to reduce values of COE. Recent studies on wind turbine fault analysis show that electric generators as well as power converters have the highest maintenance priority with an average rate of failure approximately 13%-20% [82, 83].

Furthermore, system efficiency has high importance in cost reduction of high power conversion [84]. Millions of dollars can be saved at the wind farm level; which may contain hundreds of power converters equipment operated with wind turbines; when the efficiency of power converter improved by 1%. To reduce the efficiency, power losses should be reduced by applying high efficient triggering circuit for switching devices, modulation/control schemes, optimal arrangement of switching devices and cooling system.

Power quality can be referred to different parameters and variables of power system. The output voltage profile must be as close as possible to sinusoidal shape waveform which is also indicated by number of dv/dt steps of the voltage waveform. When the number of

steps is increased, the dv/dt ratio will decrease, then the voltage waveform will improve and the need to install output filter is also decreased. Furthermore, the interference with communication system will be reduced as dv/dt reduced [85]. Reduction of Total Harmonic Distortion (THD) of all components of generator and grid variables is important to reduce the oscillations of the generator shaft and to supply undistorted current by the wind system to the grid [11].

In grid connected wind energy system equipped with power converters, the currents must feed with minimum value of THD (approximately less than 5%) to grid, enable reactive power feeding whenever required by the consumers [86]. It is also needed to provide FRT, and acceptable limit of voltage/frequency percentage rather than other factors. These requirements should be obtained through the operation of the power converter, and without requesting help from the external devices such as STATCOM or FACTS or other synchronous generators.

Other parameters such as dimensions and weight can played an important role in wind turbine design. The electric generator and power converters must have high level of density in order to acquire a small size and weight in the nacelle of the turbine. This step regarded as an important issue especially in the offshore wind turbines to reduce the cost and minimize the physical size.

The output of AC converter should be connected to the step-up transformer of and finally to PCC through AC power lines or cables. Modern wind turbines have typical hub heights in the range approximately of 60-150 m, therefore the total cost of lines, cables and associated power losses become significantly high. This factor must be taken into account in in designing and manufacturing to decrease the cost of cable and losses. Ideal power converters must have all the above merits to ensure good performance of the system within rated limits.

Practically, it is difficult to design a power converter taking all mentioned technical merits in to account. Best marketable power converters obviously fulfil most of above regulations

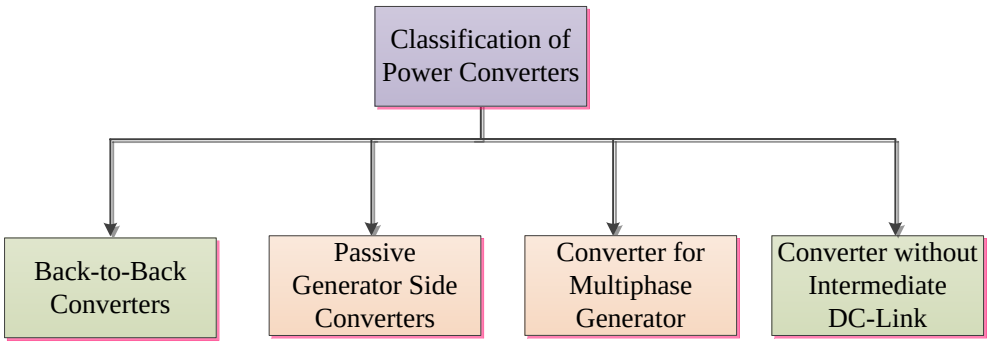

Fig. 2.7 Classification of power converters [11]

for wind turbines. The engineering methodology should imply most crucial requirements of the design while neglecting the other unimportant conditions. To facilitate the schematic diagrams of various types configurations of the WECS in this thesis, the generator side filter is not shown in the design, while the grid side filter is represented by an equivalent block diagram.

In pursuit of acquiring the above mentioned technical requirements, various types of power converters have been developed and utilized by wind turbine manufacturing plants and other suppliers research departments. It is not possible to define all the converters based on one parameter or operational function due to complexity of WECS power converters and their applications.

Generally, the generator-converter configurations can be classified into four different groups as summarized in Figure 2.7 to facilitate easier discussion. These are back-to-back (BTB) converters, electric generator, converter for multiphase generator and converter without intermediate DC link. Power converter types which have been deployed by several wind turbine manufacturers, and also suggested in literature with favourable features, belong to these four distinguished categories.

2.4.3 Back-To-Back Converters

The main conversion process of the electrical energy can be done by the power converter. The BTB converters are identical on both side of the generator and grid, where all parts of power electronic devices such as IDBTs have the same size. The BTB converters have main two groups AC/Dc group and DC/AC group and they are connected through a DC-link. Various types BTB converters which can be used commercially by WECS are summarized in Figure 2.8.

The main task is to perform a conversion of variable voltage/frequency output of the generator to DC, and then DC to AC, taking into consideration fixed values of the grid connected output of voltage/frequency. The power flow is bidirectional, and then the BTB converters can be applied with the both types of induction generators SCIG, DFIG, and in other types synchronous generator PMSG, and WRSG. For the above features, This type of power converters will be concentrated and discussed in this thesis.

These operating voltages that been used in generator and power converters are further classified according to Low Voltage (LV) and Medium Voltage (MV) operation.

The standard LV used by many manufacturers and companies of wind turbine for the LV grid connection are 690 and 575 V. The Voltage Source Rectifier (VSR) and Voltage Source Inverter (VSI) are connected through a DC-link capacitor bank. The VSR and VSI are technically built by LV Insulated Gate Bipolar Transistors (LV-IGBTs) to form the final shape in matrix arrangement [11].

The DC-link part is practically implemented using series or parallel groups of capacitors to obtain the required voltage by the converters and capacitance current limit. At power levels lower than 3 MW in Type 4 turbines the LV converters are simple, efficient and cost effective. As the power rating increased with increase in the number of converter groups and as a result, the size of electric components, total cost, and finally the system complexity will be increased too.

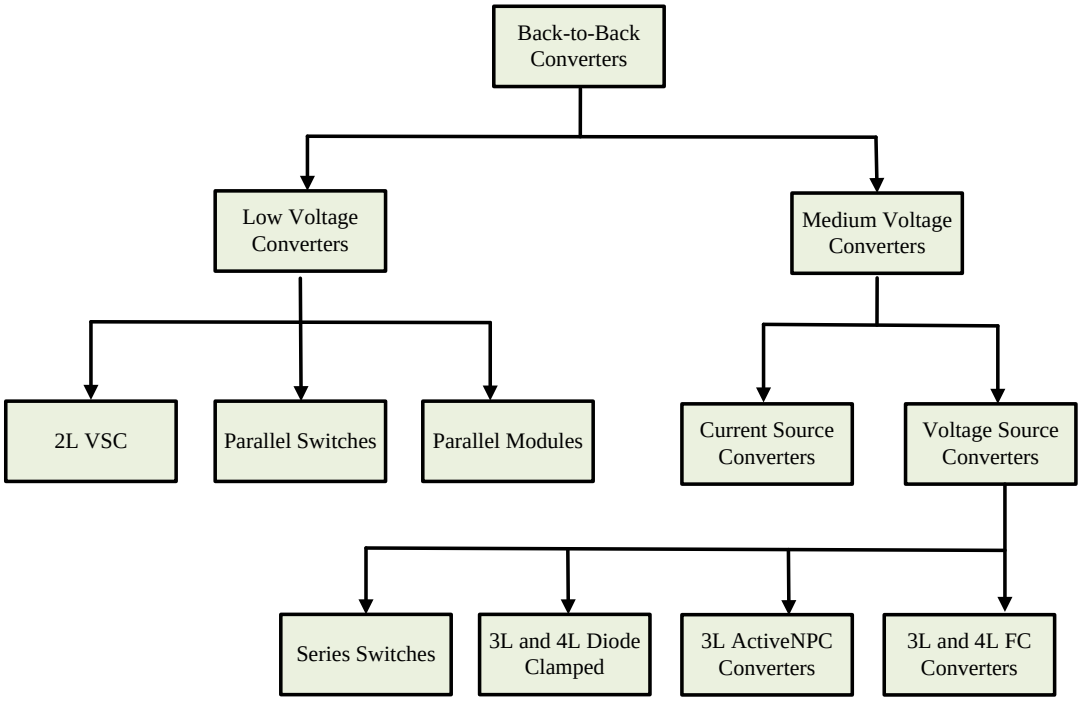

Fig. 2.8 Classification of Back-to-Back converters [11]

Wind turbine manufacturers have low tendency to move from LV to MV technology due to the limited propagation of MV generators and less knowledge acquisition for the MV operation area of turbines, where MV converters is still a mature technology in the electric drives industry [80]. A detailed cost investigation has been presented between the LV and MV operation of wind system using matrix converter. The results show that the energy production cost can be decreased with MV operation by the fraction 2% - 4% [11, 77].

A summary of the LV and MV operation of a 6 MW Type 4 wind turbine are more efficient and applicable in the power market shown in Table 2.1 [87]. It is noticeable that the MV operation of WECS is the most suitable technique for power ratings greater than 3 MW with low cost and effective performance.

Table 2.1 Comparison of LV and MV Operation Wind Turbines

	LV WECS	**MV WECS**
Typical Converter	BTB 2L-VSC	BTB 3L-VSC (NPC)
Typical Power	0.75 – 6 MW	3 – 8 MW
Typical Voltage	690 V	3000 V
Number of Converters	8	1
Number of Switches	96	24
Switching Devices	LV - IGBT	MV – IGBT/IGCT
Clamping Diodes	0	12
Redundancy	High	Low
WECS Efficiency	Medium	High
Converter Complexity	Very High	High
Controller Complexity	Medium - High	Medium
Grid Code Compliance	Good	Excellent
Cable/Transformer/Filter/Nacelle size	High	Medium
Cost of Production	100%	97 – 98 %
Technology Status	Well Established	Well Established
Market penetration	Mature	Available
Example Commercial Products	Inge team FC LV	Inge team FC MV

2.5 Overview of Control Schemes

Several researchers have recently published their works on WECSs and their control schemes. The authors in [88] investigated the dynamics modelling oriented control design for WECS. In [89] authors described various types of wind turbine systems, categories, and classified according to the generators types and rotor speeds. Authors in [90] analysed the stability and reliability of wind turbine system, the power quality, transmission systems and storage, etc. The authors in [47] described a WECS control concept in different working zones. They also described a recent advanced and standard control schemes which consist of multi input and multi output and compared with the traditional controller.

Some studies concentrate on the wind turbine control schemes which use fuzzy logic and neural network [91, 92]. The authors reviewed on controlling process of matching between the wind turbine frequency and wind power saturations. Other surveys are focusing on the

present, past and future trends of wind power control markets using individual Horizontal Axis Wind Turbine (HAWT) [93]. Compared to other types of generators, the authors in [94] showed the optimal power extracting and wind turbine efficiency of synchronous generator compared to DFIG that used in wind system.

Furthermore in [95], reviewed power electronic utilizations in WECS. Some researchers have studied and concentrated on modelling and control based on WECS using PMSG, to show the system integration using grid connected models [96, 97]. Latest survey shows several features in control area that systematically to solve existing problems and develop the output using advanced control technologies for WECS based on different wind turbine generator configurations [98].

In this section, developed types, methods and techniques for a certain number of research articles have been reviewed and discussed.

2.5.1 Wind Turbine Controller Techniques

The most advanced and developed WECS control techniques are classified according to their function and operation as:

1. Proportional Integrator Differentiator controller

Proportional Integrator Differentiator (PID) controller was suggested to increase the efficiency of wind turbine system and improve the performance of operation. This type of controller used also in the modern power converters. This controller placed in control system equipment that manage the switching process of the converters which are situated between wind turbine generator and the point of common collection [99]. However, the PID is utilized to collect the signal of error between the reference value that already specified and the real output power, which can be measured from the load or grid side. In some studies, the authors concentrated on power electronics firing angles of generator side converter and grid side inverter, which are controlled and adjusted to acquire desired values [100, 98].

In addition, some authors proposed a non-linear dynamic wind turbine model with comparative investigation and studies have introduced the effects of combining some optimal techniques with PID controller. However, particle swarm and radial basis function neural network algorithms have much better performance than conventional PID controller [101].

2. Model Predictive Controller

Studies on the use of Model Predictive Controller (MPC) in application to wind turbine control have become more widespread in the last century. Most of the MPC wind turbine studies can be grouped according to the range of operating conditions under which the turbine is simulated. These studies can be more divided into categories by what loads the control system addresses (e.g., drive train [102], tower [103], blades [104], etc.), by whether or not the control uses generator torque, blade pitch, or both for actuation, and whether the blades are pitched individually or with other controllers.

This type of control has also been developed to involve other aspects of the WECS issues as well as individual turbine control. In [105] the use of MPC is analysed in application to the resources dispatching in a power generation side that includes a wind farm configuration; while the author in [106] investigates the use of MPC for integrating battery storage systems with a WECS. Non-linear control issues can be manipulated by the predictive control technique with reasonable limitations. Some researchers discussed the predictive control techniques utilized in wind turbine system and DFIG connected to the power grid [107]. These study claimed that the better design of controller can efficiently follow the speed disturbances of wind turbine in order to keep the injected power constant. Besides that, some studies proposed a new control design that can be preferable to the PI to acquire the dynamics regulation of WECS parameters during optimal operation [108, 109, 98].

Similarly, the authors [110] claimed that those non-linear MPC scheme for a DFIG connected to the power grid is more accurate, easy to use and having good performances

compared to other traditional schemes. In this thesis, the MPC type of control have been discussed and developed.

3. Adaptive Controller

The Model Adaptive Control (MAC) technique is taken into account when it is quite hard to find an unknown parameters of non-linear dynamic model of a wind turbine system. Due to fundamental objective to find non-linear parameters, the adaptive control scheme introduced to operate with WECS. Various studies have been proposed direct adaptive control strategies.

Some studies have focused on two procedures of control techniques: a supervisory control which depends upon crude bounds of the non-linear boundaries of the wind turbine parameters, and a radial system technique depends upon transfer function to design the controller. The tracking error can be reduced to zero by using this technique with taking in to account the dynamics of the WECS [111]. At the same time, the author did not use any method to estimate or track the wind speed.

In similar issue, referring to [112], authors described a direct adaptive control strategy which have concentrated on the optimized tracking of wind speed measurements in order to ensure the following of turbine speed to the required output desired level.

Lyapunov method can be used in self tuning of PID controller which can be applied to control the converters of WECS as described and discussed in [113]. The authors have used this control method that depends up on the training of the impulse response filter to estimate and finally update the values of PID controller during wind energy conversion.

In [114], the Hill Climb Searching (HCS) technique has been used to obtain MPPT of wind turbine speed controller. In this publication, the authors suggest a self-tuning technique associate with changeable efficiencies of the wind subsystem that can be run under stochastic wind speed. The reliability of the wind turbine systems and the cost of the equipment have

been taken into account. The development of HCS to avoid the mechanical sensors using smart sensor-less speed controller was also an important issue in model design [98].

4. Robust Controller

Different review studies [98, 115, 116] discussed this type of controller. The robust controller has been suggested due to unexpected disturbances in wind speed that appeared in power systems. Obtaining maximum power and reduce the load variation can be estimated by applying feedback loop method as mentioned in [117].

In [118], it is presented the effectiveness and influence of H ∞ and H-2 control techniques taking into account stable constraints of WECSs. This study indicate that the H ∞ technique shows a robust performance and has less time response compared to H-2 technique. As a result of this study, the author deduced that H ∞ controller is not suitable for highly disturbance in wind speed. In contrast, the H-2 controller is not applicable for constant wind speed turbine. Even though authors, in reference [119, 120] justify and claim that H ∞ can be applied in variable speed wind system due to some advantages such as simplicity and higher dynamic performance [98].

Many researchers such as [121, 122] developed and simulated a software for regulation of wind turbine using Kalman Filter (KF) techniques for estimation of wind speed. These publications are also proposed anemometer to determine the values of wind speed, in order to smooth gain scheduled controller feedback from wind turbine torque to obtain the maximum operating points. In this suggested technique, the PI controller unable to improve the performance of the gain scheduled controller to the linear state in the case of varying parameter [98].

The study in [123] describes the principles of fractional calculations and also compares features of fractional order control systems with those of classic integer order controllers. In this study, the method uses feature that enable the phase frequency variations around a gain crossover frequency to be insensitive. This will increase the robustness of a fractional

order control system during uncertainties. PMSG wind turbine system is considerable type of WECS that used with this method.

Finally, authors in [124], showed that H ∞ robust controllers used in wide range of operating conditions and obtaining the ability for effective performance. In these techniques the WECSs can be applied by mu-synthesis robust control which adapt DK-iteration method [125]. A little variation will be shown in both system parameters like angles and power in the case of a smaller amount of disturbances.

5. Sliding Mode Controller

Essentially, the sliding mode control schemes show an appropriate environment to manage the non-linear systems using intelligent mechanism [126].

The authors in [127, 128] demonstrate a control design technique for WECS using a DFIG which inject the power to the grid through stator windings and rotor static converter. In more details, they evolved an easy and simple sliding mode controller in which static converter operate as a compensator to the torque of the generator to interpolate the signal between rotor and stator. By this method, it proposed that the system damping will mitigate the essential weakness of generator torque and output power fluctuation. The proposed system will be strongly respond to the constraints of the generator uncertainties and voltage reduction of the power grid [98].

Moreover, the authors in [128], described WECS using appropriate controller to operate under optimum Tip Speed Ratio (TSR) condition and satisfy a maximum power efficiency. The simulation shows the efficient robustness of the control scheme in the case of grid disturbances and uncertainties in the power limit.

Avoiding oscillation issues encourage the authors in [129] to demonstrate suitable compromise between conversion efficiency and torque oscillation smoothing to address above mentioned issues in WECSs. The authors conduct that the controller operates in optimum

tracking area for different operating modes to satisfy maximum power conversion efficiency and damping torque oscillations which provide a good robustness to the system [98].

Another simple method of sliding mode control has been proposed by using a 1.5 MW wind turbine systems with matrix converter calmed by the authors in [130]. The simulations have been used to satisfy the system performance. In this scheme, it is justified the effectiveness and efficiency of the control strategy in terms of power regulations. They proposed a control technique to reduce the oscillation in the generated torque. This design consequently lead to increase the mechanical tension due to strong unbalance torque disturbance.

In [131], authors proposed an energy reliability of WECS by using sliding mode control technique to operate in on-line simulations in order to obtain MPPT. In this publication, the controller show a good performance can be obtained, which are quite satisfying study although that some physical limitations and the need of certain prediction of control signal to improve the performance of the controller [132].

6. Neural Network Controller

Fundamentals of neural network and implementation for a different types of wind turbine have been discussed in [133]. Implementation of Artificial Neural Network (ANN) can be used to track maximum power in various operational conditions for steady state or dynamic state. In addition, the tracking of wind speed is more quickly compared with using external device such as an anemometer as shown in this model. The ANN concept can be applied to compensate the system for a probable drift of wind turbine coefficient. This technique can be implemented as hardware, and in this case, extra cost for a digital controller can be omitted. Furthermore, a new control technique that can be used in WECS has been suggested by the author in [134]. In there publication, authors proposed an ANN in order to forecast the optimum value of wind turbine rotational speed that occur under uncertainty in wind variation to satisfy MPPT. Finally, output results show a good performance which verified via simulations that showing a significant minimization of the system disturbance. Due to

variable wind speed, wind turbine demonstrate valuable non-linear behaviour. For this reason it is quite difficult to build the system model to identify these issues [98].

Safety and protected system can be achieved and finally more power can be captured in the case of uncertain wind speed. Moreover, authors in [135] recommended an ANN depends upon Jordan recurrent concept wich can be trained on line. The system consists of four input signals such as output power, rotor or wind speed, and optimal power in order to estimate the reference to track the rotor speed. Moreover, they supposed that the feedback of ANN returned signal can be collected via the output, and then back to dissemination as an input signal. The difference between the maximum power and measured power can be applied for updating the network weights and finally generate reference rotor speed. It is concluded from these points that the ANN mechanism is satisfactorily applied to WECSs based on PMSGs.

In the same way, the WECS model based on Markov schemes approaches have been designed by the authors in [136] using ANN techniques in order to optimize the output power of the wind system. It is shown by this publication that the control scheme has been operated using central control environment. It is shown that the suggested method reduced the rotor speed fluctuations, besides the improvement of wind turbine system.

7. Fuzzy Logic Controller

Applying an intelligent control techniques for WECSs have taken the attention of the researchers. This brief survey is focusing on the latest publications talking about the FLC development and utilization in wind energy market. The authors in [137] described a principles of the optimal power capturing from the wind using FLC techniques in order to track the turbine speed using the cyclo-converter configuration. The meteorological data acquisitions has been used to test the system control scheme by simulation.

Optimum power extracting and pitch angle control using FLC that applied in designing of uncertain wind speed has been described in [138]. The main aim of this controller is to replace the linearity of FLC to acquire the speed control improvement and extract maximum power.

The output results of the proposed design which uses a real 800 kW wind turbine showed that the maximum power is obviously captured during a wide range of speed operation.

A closed loop fuzzy control used together with fuzzy observer scheme to give a practical solution to the main issues related to the process of power conversion and regulation of the constraints as proposed in [139]. The configuration of Takagi-Sugeno fuzzy logic has been applied with non-linear system model in order to improve the performance of operation and show the impact of applying fuzzy controller in wind turbine. Moreover, this technique is more accurate, simple and easy to use compared to the conventional controller. The disturbance in the system which usually occurs in WECS due to the uncertain values of wind speed can be reduce using this proposed controller based on Linear Matrix Inequality approaches [98].

Furthermore, a fuzzy controller using H ∞ can be designed by applying bilinear matrix inequalities as in [140]. In this type of control technique, the two-step method of linear matrix inequalities can be reduced. These steps can be evaluated by convex optimization principle. Consequently, authors refused this principle that appeared in their publication before [139]. However, in order to mitigate the effect of over-rated variation of wind speed, a new techniques have been used in [141, 142] to design a FLC for under and over the rated values of wind speed. The main control design operated by using two input variables to capture the optimal value of wind power.

These inputs can be signals like error between TSR of measured speed and TSR of actual speed, the error derivative, and one output can be used like the value of generator voltage. The exact same dynamic structure can be used to design the second controller that performs the stabilization of output power. Therefore, the error will be between the estimated and measured output power while the output will be the value (in degrees) of pitch angle of turbine blades. In these papers, the authors designed these control schemes to acquire MPPT following slightest disturbances of rotor speed and output power. As conclusion, it is noticed

that these studies have demonstrated the tracking process of maximum power using FLC to satisfy the operational performance through simulation and experiments where no need to detect the value of wind speed.

Different designs, techniques and applications such as pitch angle control, maximum energy extraction, 3-phase grid current and voltage and DC-link voltage control schemes for various types of generators have been proposed in [143–145].

8. Optimal Controller

Many researchers proposed good ideas for capturing the optimal power of uncertain wind variation, but these approaches were not supportive enough for the optimal control schemes for WECSs [146, 147]. Then, the authors in [71] have suggested an optimal control algorithm for the MPPT using PMSG wind turbine with fixed blades angle. In this control scheme, the authors have made a combination of predicted maximum DC output power versus DC voltage characteristics with the frequency of PMSG to run the system at level of maximum power, in order to omit other techniques to track the wind speed to keep operation within optimal power level. Fast Fourier Transform has been used in this scheme to acquire the maximum power. The authors in [148] have presented developed method using an efficient conventional PI controller in order to maximize gains of PI controller and improve the error tracking quality .

Later, a simple sensor less control technique using variable speed PMSG have been proposed for WECS [149]. In this publication, the control design technique is distinguished compared to other studies where the authors justify that the the power at the maximum level at uncertain wind speed can be captured by using this control strategy in the case of grid connected system. Using the above concept of control scheme, PMSGs have been combined to provide a proper connection of 3-phase source inverter mode and switch mode to obtain maximum power extraction [98].

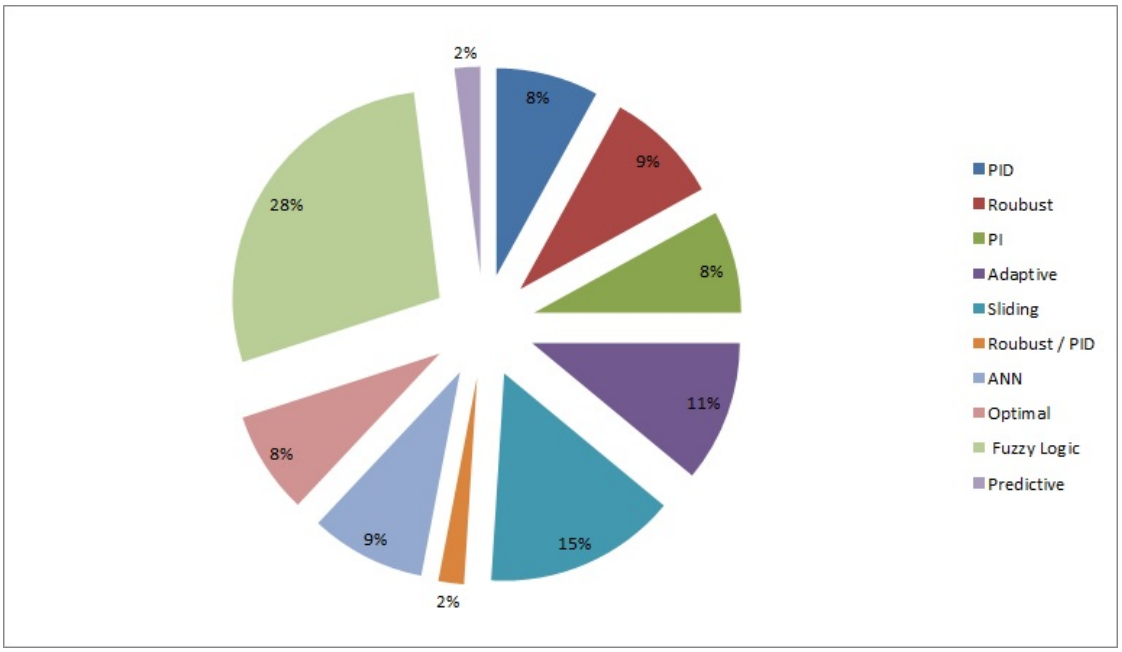

Fig. 2.9 Development of control techniques and the percentage of their researches [98]

Latest thoughts have been proposed to improve MPPT algorithm for PMSG of wind energy system in [150]. Using this algorithm of MPPT, synchronous machine speed controller is combined with the power rectifier control and finally boost converter control. This method can be used to control the speed and current to obtain optimal operational conditions. Various types of control techniques and the percentages of the relevant researches that contribute are shown in Figure 2.9. It is shown that PI controller has the major interest by the studying all situations and applications while the predictive and robust controllers have minimum interest in the fields of researches.

2.5.2 Developed Configurations Studies of Control Systems

One of the earliest studies [151] is also one of the most sophisticated control scheme which applies Non-Linear MPC (NMPC), uses a neural network to adaptively adjust the model parameters, and simulates the turbine response in conditions that encompass rated and above rated operation. More recently, authors in [152] demonstrate a NMPC for collective pitch

and generator torque control in all operating conditions. Tower loads have been termed in the cost function by punishing the tower top velocity. This controller operates in all operating regions and utilizes constraints to control rotor speed and tip-speed-ratio.

Utilisation of plug-in hybrid-electric vehicles as a storage method for balancing wind farm power production is studied in [153, 154] imply the MPC at the supervisory level to manage a hybrid wind-solar stand-alone system; and finally [155] uses a fast set-membership technique for NMPC to satisfy and actually design controls for a prototype high altitude kite WECS.

In less relevant applications to the Horizontal Axis Wind Turbine (HAWT), there are also abundant existing MPC studies in the literature. In[156], authors use only a single linear model serves as a basis for the MPC algorithm which is demonstrated in all load conditions; the present mechanical power of turbine and rotor speed are both determining the MPC cost function which is reduced as well as the control actuations available to the MPC algorithm. In their study, the goal was to show an MPC architecture that operates with all load conditions of the wind turbine involving to actuation constraints. It is noticeable that this control algorithm performance was not independent to other controllers in terms of structural load mitigation. On the other hand the intelligent control system such as FLC and ANN and their combinations have been proposed to mitigate the errors and overshoot or reduce the settling time of the main controlled signals like currents, voltages, active power or the signal of mechanical equipment such as rotor speed and pitch angle.

In addition, it explicitly estimates a preview of rotor effective wind speed based on a specific pattern of specific measurements, and uses this information in the NMPC algorithm. The study reports significant reductions in tower loads and speed fluctuation in both instantaneous wind variation and in turbulent wind variation generated using TurbSim [157]. Different type of controllers and control strategies have been proposed in [98, 158–161].

The work in this thesis is divided into several stages. The first stage addresses the modelling and design of a traditional control scheme for currents and speed in machine side converter control, and the grid side converter control for the grid current control and DC link voltage control. The next stage is investigation of this modelling which is focusing on capturing maximum power in case of variable wind speed in time that the output voltage and frequency of the grid are still constant and keep them within the limit margin of the grid code during wind speed variation.

Developed control schemes using fuzzy logic system have been proposed in the machine side converter control to show the impact of this controller on the generator speed variation. Then, the final stage to develop an advanced control scheme using MPC control with FLC to form the FPC to achieve the benefits of non linearity of the system and reduction in overshoot of rotor speed of the generator in case of sudden change in wind speed.

2.6 Summary

Fundamentals, principles and applications of WECS been discussed in this chapter.The main configurations, types of converters that used in the systems and the the types of controllers of these equipment were introduced and discussed in this chapter.

Chapter 3

Modelling and Control of Wind System

The whole system of a grid connected wind turbine has been described in this chapter. The main parts contains several equipments. The mechanical modellings of the WECS and their specific function in the energy conversion process from wind energy into electrical energy has been discussed showing all components such as PMSG, converters which transfer the electric power from AC to DC to AC with different categorises and finally the modelling of the grid. To show the principle and operation of the traditional control schemes, the classical control scheme using PI controllers has been simulated and results have been previewed for different values of wind speeds.

3.1 Introduction

Since the wind turbine manufacturing and development began in 1980 until today, wind energy and its application is shown as a new technology and has become an attractive invention in the power generation market. Various wind turbine concepts and designed models have been evolved during this period of time. The Wind Energy Conversion System (WECS) has different mechanical and electrical components collected and operated together

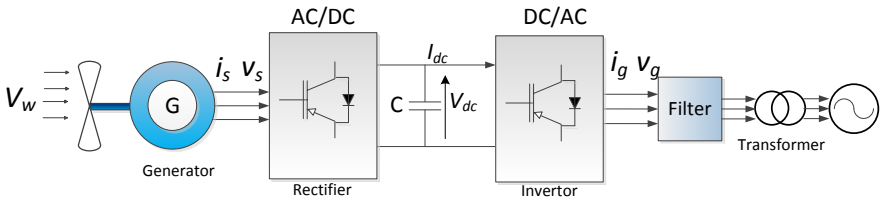

Fig. 3.1 Schematic diagram of grid connected WECS model

and controlled to harvest the wind mechanical power and convert it into useful electrical power within rated voltage and frequency [162, 163]

In this chapter, all components will be presented and detailed in real values to satisfy overall description of the system during all operational cases. The whole system of a grid connected WECS consists of several components, which contribute to the operation of the conversion process of electric energy from wind energy into electrical energy. Figure 3.1 shows the main structure of wind turbine connected to generator which convert the power through a traditional Type 4 , back to back converter and finally to the grid through filter [162].

Firstly, the aerodynamics of the wind turbine will be expressed and formulated in detail. Simulation model will be developed to generate the wind turbine mechanical characteristics. Secondly; the electrical and mechanical models of the generator configuration will be presented, explained and followed by the power electronic converter interface design and control connected to the grid. In some cases the harmonics of the output currents distort the signal profile then the filter of R-L, L-C or L-C-L should be used to mitigate the Total Harmonic Distortion (THD) and finally reduce the power dissipation and losses.

It is also noticeable that the output voltage of the grid side should be the same of the grid. Otherwise, the transformer should be connected to convert the low voltage to high voltage to synchronise the vector quantities of the system voltages.

3.2 Mechanical Modelling of WECS

3.2.1 Wind Turbine Model

Wind energy is converted to mechanical power by a wind turbine and then to electrical energy by an electric generator. The kinetic energy which has been stored by the air is proportional to the unit area perpendicular to the direction of wind speed per unit mass is converted to mechanical energy. Assuming the front end of the wind stream is uniform, that is, all the particles have the same speed at the time. From Newton's Law, the kinetic energy exists in the wind stream can be expressed as follows [164]:

$$E_{kin} = \frac{1}{2} m v_w^2 \tag{3.1}$$

where E_{kin} is the kinetic energy stored in the wind, m mass of the air and v_w is the wind speed (m/s). By substitution the mass by the density times the volume, and the volume is the speed times the area and time. Therefore, determination of the mass in a circular interfacing area between the wind stream and the turbine blades with area A , can be derived:

$$m = \rho v = \rho v_w A t = \rho v_w \pi R^2 t \tag{3.2}$$

where ρ is the air density values from 1.1 to 1.3 (kg/m^3), t is the time, R is the radius of the circular area swiped by the turbine blades.

By substituting equation (3.2) into equation (3.1) yields:

$$E_{kin} = \frac{1}{2} \rho v_w^3 \pi R^2 t \tag{3.3}$$

Then, the stream power of the wind (P_{wind}) can be expressed as [165]:

$$P_{wind} = \frac{1}{2}\rho\pi R^2 v_w^3 \tag{3.4}$$

The power captured by a wind turbine from an air stream flowing through an area A is equal to:

$$P_m = \frac{1}{2}\rho A C_p v_w^3 \tag{3.5}$$

where P_m is the wind power (watts or J/s) ,and A is the area swept out by turbine blades (m^2) . where R is the radius of the area swept out by blades turbine and ω_m is the mechanical speed of the generator in rad/s. The power coefficient (C_p) can then be expressed as a function of the Tip Speed Ratio (TSR)denoted by (λ) and pitch angle β in equation (3.6)[166]:

$$C_p(\lambda,\beta) = C_1(\frac{C_2}{\gamma} - C_3\beta - C_4)e^{\frac{-C_5}{\gamma}} + C_6\lambda \tag{3.6}$$

and

$$\gamma = \frac{1}{(\lambda + 0.08\beta) - (0.035\beta^2 + 1)} \tag{3.7}$$

where β is the pitch angle of the blade in degrees. The coefficients parameters of equation (3.6) are empirical constants and can be estimated for a WT as: C_1 = 0.5176, C_2 = 116, C_3 = 0.4, C_4 = 5, C_5 = 21, and C_6 = 0.0068. The Tip Speed Ratio (TSR) can be defined as follows:

$$\lambda = \frac{\omega_m R}{v_w} \tag{3.8}$$

In ideal case, the power coefficient C_p reaches a maximum value that will be within the range 59.26 % according to Betz's limit. This means that the extracted power is practically from the wind is always less than this value [167]. In other words, the extracted power from the wind is always less than 50 %. The value less than the theoretical limit is caused by the inefficient conversion of power that lead to different types of losses, which depend on the

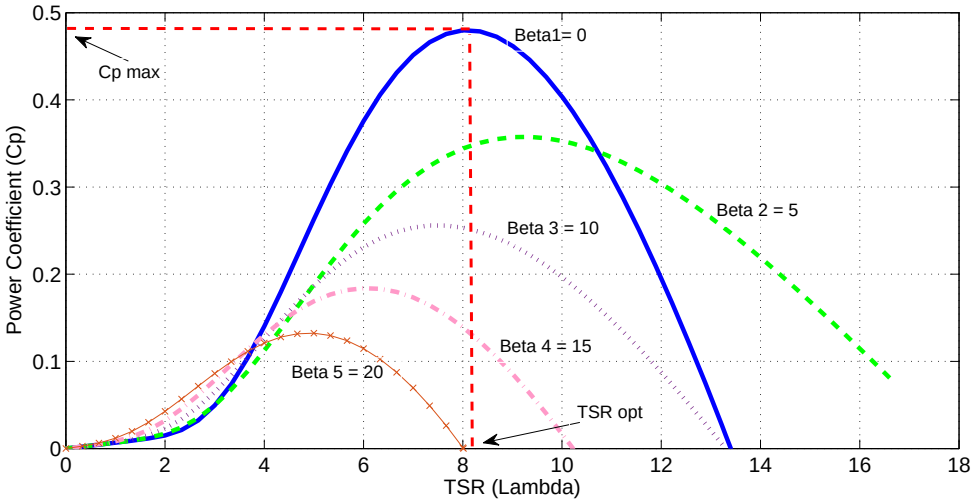

Fig. 3.2 Variation of power cofficient with TSR

construction of the generator rotor with regard to weight, stiffness, number and structure of blades of the turbine.

The relationship of the performance power coefficient, C_p of a wind turbine and the TSR shows that the maximum values of C_p in all operational situations occur at optimum values of TSR. By adjusting these values in the control circuit it is possible to obtain the Maximum Power Point Tracking MPPT for any variation of wind speed. Figure 3.2 shows the relationship between the power coefficient C_p and optimum values of TSR for different values of pitch angle β. The output mechanical power varies with the angular velocity ω_m , for variable values of the wind speed according to the synchronous machine characteristics. A significant aim of this research is to achieve optimum values of ω_m that satisfy the maximum output mechanical power of the wind. Therefore the above important relationships of C_p and λ should be taken in to account in order to obtain optimum design as shown in Figure 3.2. The dynamic equation of the wind turbine is given in equation (3.9):

$$J\frac{d\omega_m}{dt} = T_e - T_m - F\omega_m \tag{3.9}$$

where J is the total moment of inertia of wind turbine and generator, F is the friction of viscosity coefficient and T_m is the input mechanical torque to the turbine.

3.3 Electrical Modelling of WECS

Electrical components of WECS can be modelled as a static or dynamic components according to their operations of the system.

3.3.1 PMSG Model

Electrical generator is the main device converting wind energy into electric power. However, permanent magnet synchronous machines (PMSM) are generally manufactured for high capacity up to a rated power of about (8 MWs) and (10 MW in research), which settles a new development in wind power generation. There characteristics show more efficiently than the conventional synchronous machine due to less mechanical equipment of gear box and reduction in electrical losses due to operation without excitation circuit.

Permanent magnet machine consists of fixed flux due to permanent magnet. Although the cost of a synchronous generator is more expensive for a same size of Induction Generator (IG), there are different advantages that enable us to use it in large scale generation. One of these advantages that it does not required reactive magnetizing current in order to operate correctly, whereas, the magnetic field can be generated from permanent magnet of the rotor. Another feature that leads to reduce the cost where the generator used for wind turbine application can be directly driven without gearbox with appropriate number of poles. Thus, despite of the cost and complexity, synchronous generator is regarded as desirable tool for wind turbine generator, especially for low wind speed where the number of poles can be high to achieve agreeable frequencyn [168].

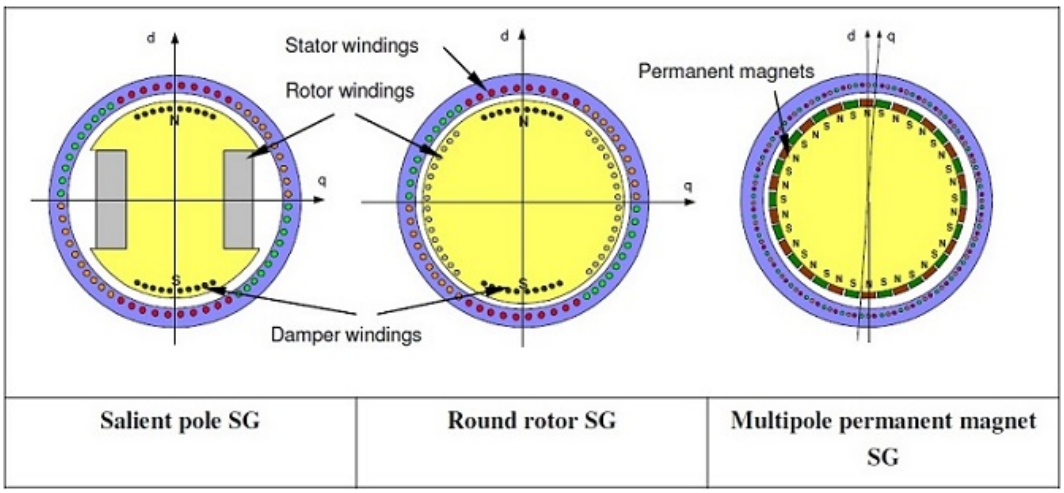

Fig. 3.3 Cross section of different synchronous generator types [162]

Nevertheless, synchronous generator is much more complex than induction generator. The output voltages of PMSG can be represented in the reference frame rotating synchronously where the q-axis is shifted by 90 degrees ahead of the perpendicular d-axis with respect to the direction of rotation [169].

Three various models of synchronous generators (SG) are shown in the Figure 3.3:

- **Salient pole SG:** In this model, the windings of the rotor are situated and represented as a coil around the pole shoe. This new structure leads to a different magnetic resistance (reluctance) in the rotor oriented d and q axis, and consequently a different machine reactances x_d and x_q ($x_d > x_q$). A damper winding is also usually used and situated in the pole shoe. These components can be 8 or 16 poles and a respective speed of 750 or 375 rpm. The famous utilization of this type of synchronous generator is more commonly used in hydro-electric power stations, and rotating with lower speed compared to round rotor synchronous generators [170].

- **Round rotor SG:** The windings of the rotor are regularly spread in the rotor slots. This configuration leads to an equal reactance in d and q axis ($x_d = x_q$). In practice, 2-pole or 4-pole round rotor SGs are used in thermal power plants or diesel fuel which

operating at very high speed are commonly used and have a rotor speed as (3000 rpm, 1500 rpm) [171].

- **Multipole permanent magnet SG:** To operate the wind turbine with low speeds, e.g. at 20 rpm, increase the number of poles in PMSG wind turbines is a good way to obtain a required operational speed. The permanent magnets provide the magnetic rotor field instead of electrical DC excitation Figure 3.3 shows a design with surface mounting of permanent magnets in the machine body. The reactances in d and q axis differ by only a few percent due to the equal distribution of the surface mounted magnets and a permeability of the magnet material μ_m approximately as big as the free space permeability ($\mu_m \simeq \mu_o$) [172, 173].

  For this manipulation in designing, this model of surface mounted PMSGs can be considered as round rotor machines ($x_d = x_q$). Due to the multi-pole PMSG is a converter connected low speed application (compared to high dynamic drives), the damper winding is not necessary.

3.3.1.1 Steady State Generator Model

The phasor diagram of the synchronous generator can be plotted for any arbitrary operational point. If the stator windings resistance R_s is neglected the equivalent circuit can be simplified as shown in Figure 3.5. The voltage E is induced by permanent magnets and finally the stator current I_s and stator voltage U_s will be appeared.

3.3.1.2 Dynamic Model of the PMSG

The output voltages of PMSG can be represented in the synchronous rotating reference frame where the q-axis is 90 degrees ahead of the d-axis with respect to the direction of rotation. The phasor diagram of abc voltage and dq voltage is shown in Figure 3.4. The d-q stator

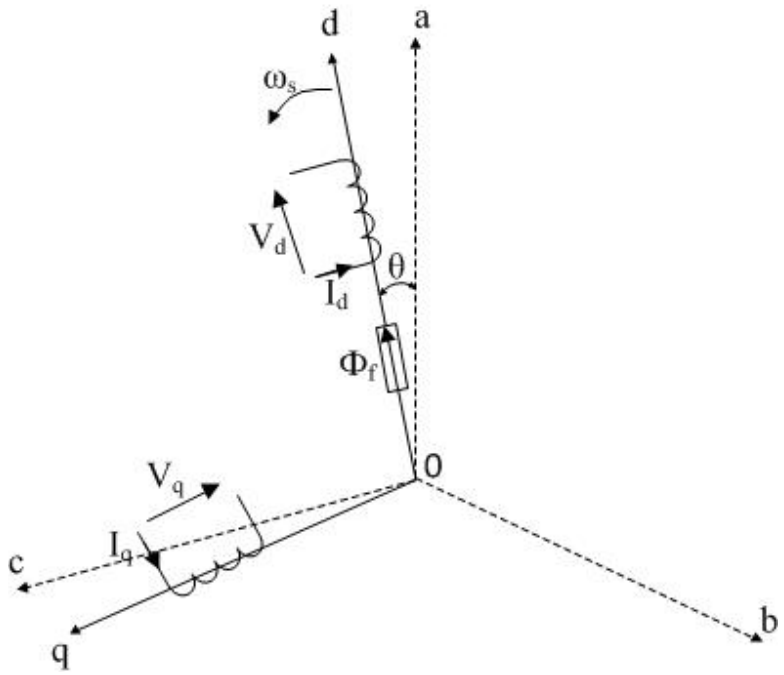

Fig. 3.4 abc-dq axis.

voltages equations of this generator are shown in equations (3.10) and (3.11) respectively.

$$v_d = R_d i_d + L_d \frac{di_d}{dt} - \omega_e \psi_q \tag{3.10}$$

$$v_q = R_q i_q + L_q \frac{di_q}{dt} + \omega_e \psi_d \tag{3.11}$$

$$\psi_q = L_q i_q \tag{3.12}$$

$$\psi_d = L_d i_d + \psi_{PM} \tag{3.13}$$

where L_d and L_q are the inductances of the rotor on the d and q axes, R_d and R_q are the resistance of the rotor on the d and q axis, i_d and i_q are the generator currents on the d and q axis, ψ_{PM} is the flux of the permanent magnet and ω_e is the electrical angular speed of the PMSG which is defined as:

$$\omega_e = p_n \omega_m \tag{3.14}$$

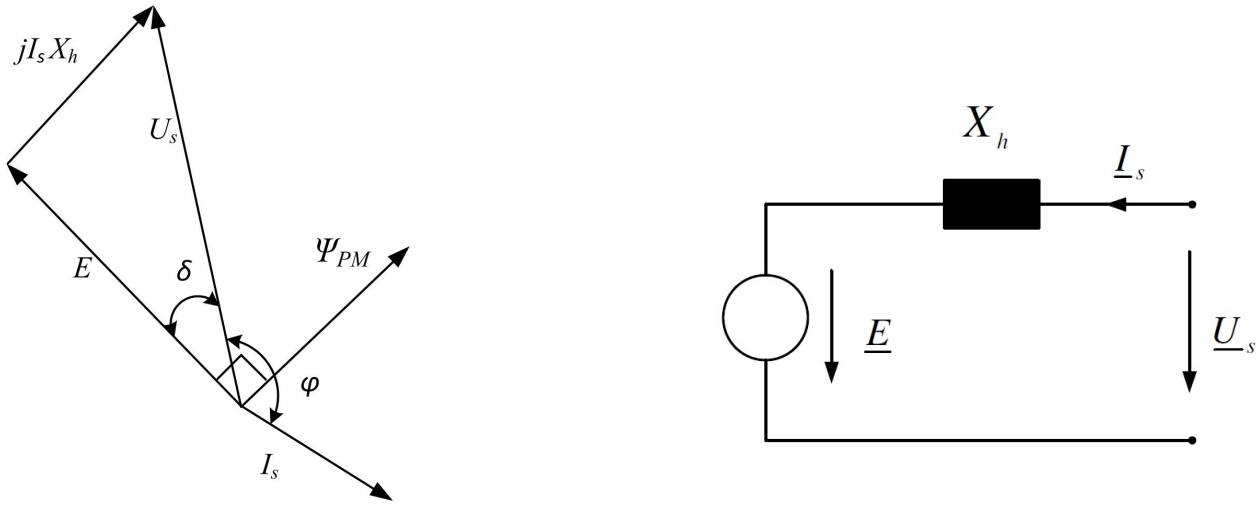

Fig. 3.5 Phasor diagram and equivalent circuit of PMSG

where p_n is the number of pole pairs.

For p_n number of pole pairs in the machine, the electromagnetic torque can be expressed as:

$$T_e = \frac{3}{2} p_n \left[\left(L_{sd} - L_{sq} \right) i_{sd} i_{sq} + \psi_{PM} i_{sq} \right] \tag{3.15}$$

If a surface-mounted PMSG is considered, equation (3.15) for T_e can be further simplified since $L_d = L_q$:

$$T_e = \frac{3}{2} p_n \psi_{PM} i_{sq} \tag{3.16}$$

By controlling the value of i_{sq}, electromagnetic torque can be changed. The values of this torque followed the mechanical torque and then mechanical power which satisfy MPPT. Thus, i_{sq} is called the torque producing current component. The modelling of the PMSG is completed by the equation of motion given by:

$$\frac{d\omega_m}{dt} = \frac{1}{J} \left[T_e - T_m - F \omega_m \right] \tag{3.17}$$

It is obvious that the PMSG model is a second order system, which has a constant parameter such as rotor flux in the design and modelling of the machine[174][175]. Active and

reactive powers of the synchronous generator can be expressed in equations (3.18) and (3.19) respectively:

$$P_{gen} = \frac{3}{2}[v_{sd}i_{sd} + v_{sq}i_{sq}] \tag{3.18}$$

$$Q_{gen} = \frac{3}{2}[v_{sq}i_{sd} - v_{sd}i_{sq}] \tag{3.19}$$

As the generator is fully converted the power to the grid through Back-to-Back converter, the reactive power which obtained before will be exchanged with the generator side converter reactive power and not with the grid, thus the net reactive power supplied to the grid will be zero and the machine will inject the active power only. As multi-pole synchronous generators are low speed machines and generally could be connected to the grid within a fully decoupled converter system, therefore there is no need to exist damper winding in core of the generator . Furthermore, due to the permanent magnet, there is no need to apply field windings in PMSG which can be apply to induce or damp the transient currents. Hence, in case of any disturbance the PMSG would not contribute to damping in all cases of operation. However, the damping power injected to the grid could be generated from the WECS by independent equipment control of the active and the reactive power which can be built separately [176].

3.3.2 Voltage Source Rectifier Model

In modern variable speed electric machine drives, Voltage Source Converters (VSC) are an important device in conversion process. The main task of this equipment is to convert the electrical power form AC to DC or in vice versa. The VSC has different advantages such as ease of control with open loop V/Hz control, compact size, low cost and provide higher power factor as well as lower power losses [177, 178]. These specifications make the designers to use VSC in industry more than Current Source Converter (CSC)which is also widely used in power electronic conversion [179, 180]. The passive bridge type of diode rectifier is shown in Figure 3.6 represents a simple,cheap and easiest rectification tool of low

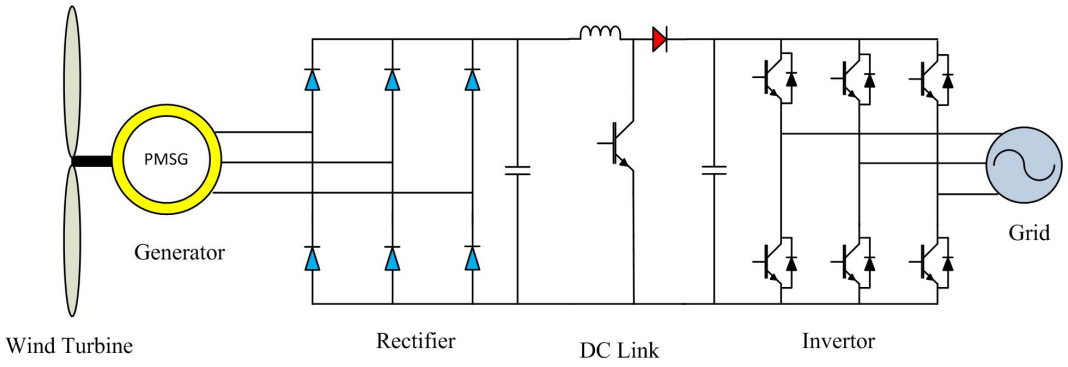

Fig. 3.6 AC to DC diode rectifier

losses. However, it is obvious that the DC voltage and then the stator voltage will depend upon the speed. Therefore, a low DC voltage at low speeds can be obtained.

Furthermore, the diode rectifier is uncontrolled device therefore it does not have the ability to supply reactive power to the generator. This leads to that the stator current and voltage will be in phase along the operation.

Increasing of stater current due to increase in torque and load angle, leads to drop in the stator voltage, which in turn leads to a decreasing DC-link voltage [181, 182]. Therefore, the converter shown in Figure 3.6 (which called step-up converter) in the DC-link must balance the effect of the drop in the DC link voltage. Since the excitation of the PMSG is fixed and constant, it is only appropriate for one point of operation. The reactive power cannot be provided or consumed by the diode rectifier when it is used, this lead to insufficient utilization of PMSG when the operational point is changed [183]. Therefore, the best performance of low speed PMSG ca be obtained with fully controllable of the inverters, such as using the PWM control technique for IGBT voltage source rectifier and inverter. Additional reactive power can then be supplied or absorbed by the converter where a very high efficiency of the system can be achieved. However, IGBT converters are more expensive and need more protection against sudden change in currents and voltages. This type of converter as described in chapter 2 is called Back-to-Back converter.

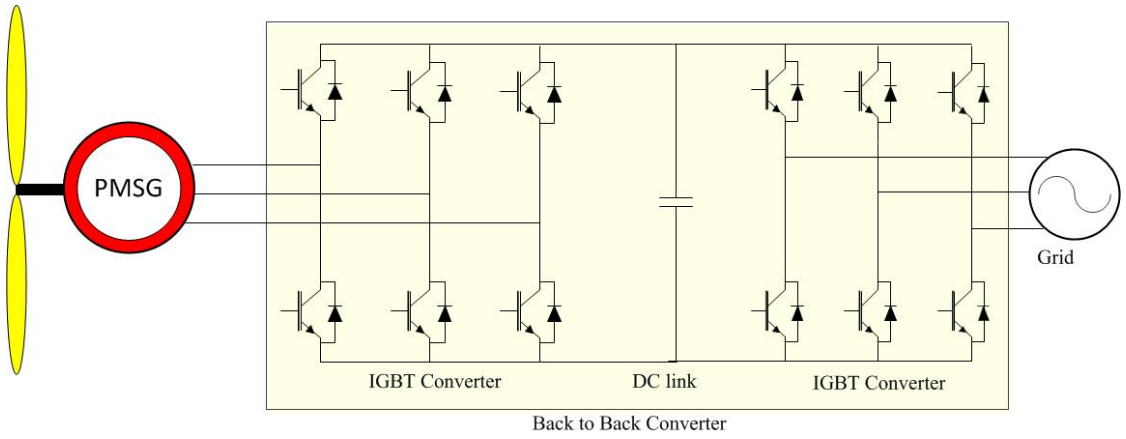

Fig. 3.7 Back to Back IGBT converters

3.3.3 Back-To-Back Converter Model

The power flow of the grid side converter can be controlled in order to keep the DC voltage constant, while the function of the the generator side controller is set to obtain the Maximum Power capturing from the wind [184]. De-coupling capacitor between the grid inverter and the generator inverter has several advantages. These advantages give some protection to the system from over voltages and offers also separate control of the rectifier and inverter, enable the compensation of asymmetry on both generator side and grid side independently [185, 186]. The schematic diagram of WECS with Back-to-Back converter connected to the grid is shown in Figure 3.7. In some applications, a boost inductance in the DC link circuit is exist. This inductance increases time delay of capacitor charging, but in the same time, the good effect reduces the demands on the performance of the grid side harmonic filter. On the other hand, the combination of inductor and capacitor is also provides some protection of the converter against abnormal conditions on the grid [187].

3.3.4 Grid Model

The mathematical model of the grid will be explained in this section [188]. The grid is represented as an ideal symmetrical three-phase voltage source shown in Figure 3.8. The

three phase voltages of the symmetrical system v_a,v_b and $v_c$are defined as:

$$v_a = V_m cos(\omega.t) \tag{3.20}$$

$$v_b = V_m cos(\omega.t - \frac{2\pi}{3}) \tag{3.21}$$

$$v_c = V_m cos(\omega.t - \frac{4\pi}{3}) \tag{3.22}$$

where V_m is the amplitude of the phase voltage and ω is the angular frequency. The three phase currents of the symmetrical system are defined as:

$$i_a = I_m cos(\omega.t + \varphi) \tag{3.23}$$

$$i_b = I_m cos(\omega.t - \frac{2\pi}{3} + \varphi) \tag{3.24}$$

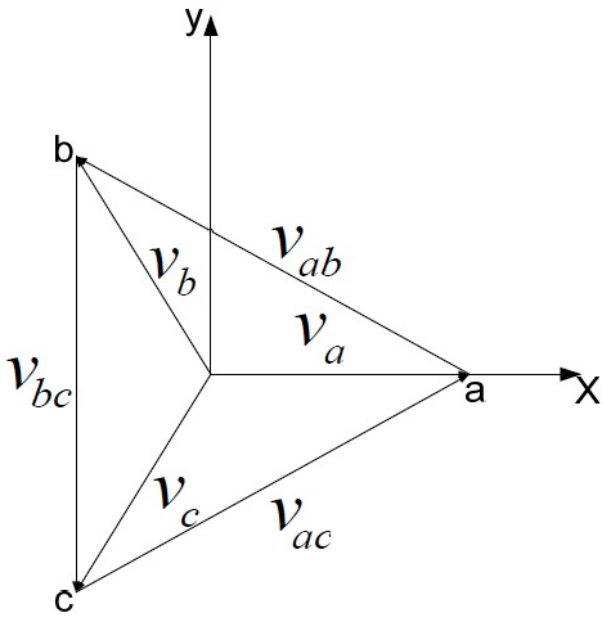

Fig. 3.8 Representation of the symmetrical three-phase voltage

$$i_c = I_m cos(\omega.t - \frac{4\pi}{3} + \varphi) \tag{3.25}$$

where I_m is the amplitude of the phase current and φ is the phase between the voltage and the current. From symmetry, the line-to-line voltages can be also defined as:

$$v_{ab} = v_a - v_b \tag{3.26}$$

$$v_{bc} = v_b - v_c \tag{3.27}$$

$$v_{ca} = v_c - v_a \tag{3.28}$$

The total neutral current i_N is:

$$i_N = i_a + i_b + i_c \tag{3.29}$$

In balance case where the neutral currents is zero ($i_N = 0$) then the equations (3.30) and (3.31) should be satisfied:

$$i_a + i_b + i_c = 0 \tag{3.30}$$

$$v_a + v_b + v_c = 0 \tag{3.31}$$

Apparent power in (VA) can be represented as:

$$S = v.i^* \tag{3.32}$$

The power flow of the grid side converter should be controlled in order to maintain the DC-link voltage within constant limit, while the control of the generator side is set to suit to capture the maximum power converted by the wind.

3.4 Control System Schemes

A control technique for the PMSG-side converter aims to control either flux or torque separately (through the control of generator phase currents), which can be achieved directly by using Vector Control. Different types of vector control can be achieved for PMSG side such as Direct Torque Control (DTC) or indirectly by using Field Oriented Control (FOC), and Direct Power Control (DPC) or Voltage Oriented Control (VOC) for the grid side. This section presents the design of the FOC and VOC strategies for a the proposed model of PMSG.

FOC scheme is implemented in the synchronous rotating reference frame for an easier control by which spatial orientation of the PM flux inside the machine can be controlled. Figure 3.9 shows the schematic diagrame of FOC sckeme used in MSC. One of the famous control scheme is vector control which use field oriented control FOC to achieve an acceptable limit of accuracy and speed. Vector control is based on the use of the dq-axis reference frame, whose direct axis is fixed to the position of rotor flux vector. Consequently, considering a constant magnet flux, the electromagnetic torque is directly proportional to the q-axis stator current component (equation 3.16). Therefore, the maximum torque per ampere in a surfaced mounted PMSG is obtained with $i_{sd} = 0$.

3.4.1 Reference Frames for Control Schemes

The control of any electrical machine should be performed normally in a reference frame, which rotates with one of the state space vectors of the generator in order to obtain steady state control signals instead of sinusoidal signals. In addition to that, a phaser diagram of the generator is displayed in order to illustrate the alignment of the machine vectors to the reference frames. Various types of control strategies can be applied to the frequency converters have been discussed in [189].

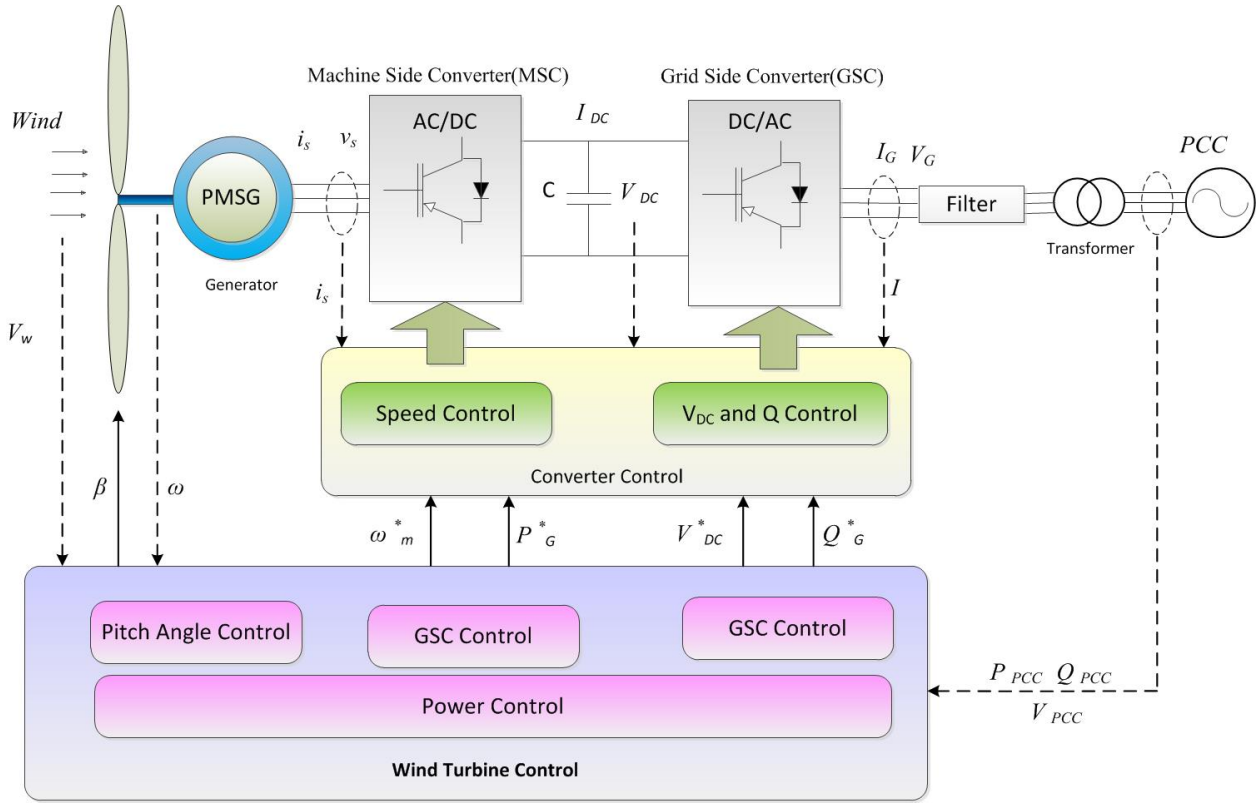

Fig. 3.9 Schematic Diagram of PMSG Control Scheme

3.4.2 Control Schemes of Variable Speed Generator

The control methods of PMSGs can be divided into scalar and vector control. Generally, the classification of the variable frequency control is shown in Figure 3.10. The scalar control techniques are depends upon the steady state representation of the model, where the magnitude and frequency of voltage and currents as well as the flux linkage space vectors can be controlled.

The most famous scalar control method of PMSM is Volt/Hertz (V/Hz) control. The V/Hz control is the simplest method, but with little-performances. On the other hand, vector control is based on a relation valid for dynamic states where the position of the voltage, current and flux space vectors as well as magnitude and frequency are controlled. This variety make the control concept can be implemented in several control methods. There are two

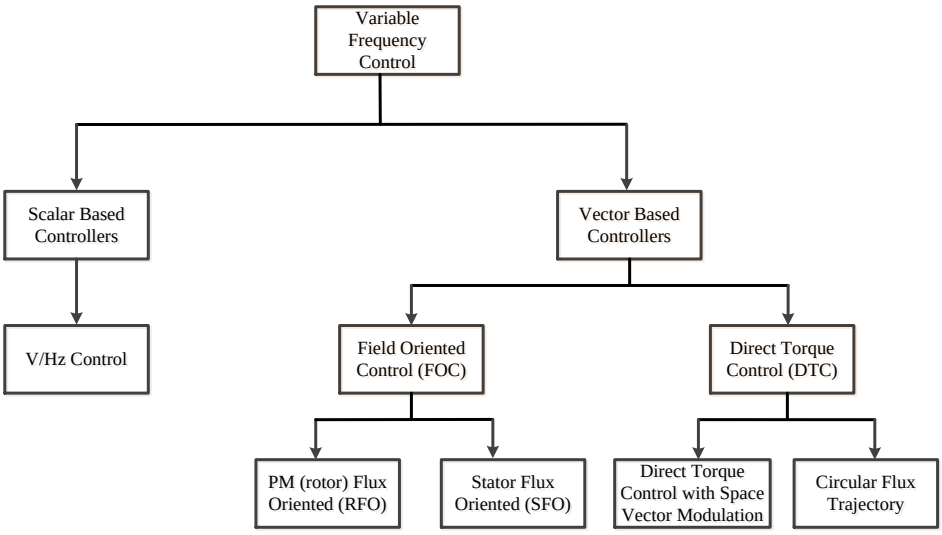

Fig. 3.10 Classification of Control Schemes of PMSG

types of vector control: Field Oriented Control (FOC) and Direct Torque Control (DTC). The early development of FOC was in 1970s, and by which the operation gave the PMSG high level performance. In this method the machine voltage equations are transformed into a coordinate system that rotates in synchronism with the permanent magnet flux [190].

The flux and torque can be controlled separately and indirectly by FOC using separately and indirectly using current control loop. The the shaft speed, obtained by an encoder organize the control process of FOC which is used as a feedback in the control strategy. This type of control schemes show several advantages such as: accurate speed control,good torque response and acquires full torque standstill [191].

In the mid 1980s, searchers developed DTC as a simpler and good performance control system a new vector control. This control method allows control the torque and flux directly without inner control loops, which corresponds very well method to the on/off operation of VSI semiconductor power devices. The main merits of DTC that its simple structure technique and has a good dynamic behaviour. On the other hand, the main disadvantages of

DTC are: high torque pulsation and fast sampling time requirements and variable switching frequency. In this thesis, FOC will be used due to discussed advantages.

3.4.3 Machine Side Converter Control

The FOC scheme is presented with the dq-axis current controllers in the inner loops and the speed controller in the outer loop as shown in Figure 3.11. This type of control uses a Proportional Integral (PI) controller to adjust the error of signals where the steady state errors of PI controllers are zero due to the integrator term [192, 15]. The implemented controls are performed in continuous time domain and PI's in design. For implementing this category the acquisition devices of the three phase stator currents (i_a, i_b and i_c), the DC link voltage V_{dc} and the rotor position θ_m are required.

Bases on the sum of the three phase balanced currents is always equal to zero, therefore to simplify the design, it is sufficient to use only two current sensors because . The permanent magnet flux of generator is fixed onto the direct axis of the rotor, therefore the position of ψ_m is easily obtained by the measurement of rotor speed ω_m. With the aid of encoding device ω_m can be calculating by integration of θ_m. The stator reference frame currents can be measured using Clarke's transformation that transforms the form of the abc reference frame into two dimensional i_α and i_β. The feedback loop currents i_{sd} and i_{sq} can be obtained using Park coordinate transformation which applied to dimensional currents after knowing the rotor position θ_m. The stator current reference in d axis i^*_{sd} is maintained at zero, for producing maximum torque at minimum speed of the generator. The outputs of the two PI current controllers are added to coupling term of the network to obtain the dq axis reference voltages $v^*_{s\alpha}$ and $v^*_{s\beta}$ which form together with V_{dc} the command values of the the input voltage of the Space Vector Modulation (SVM).

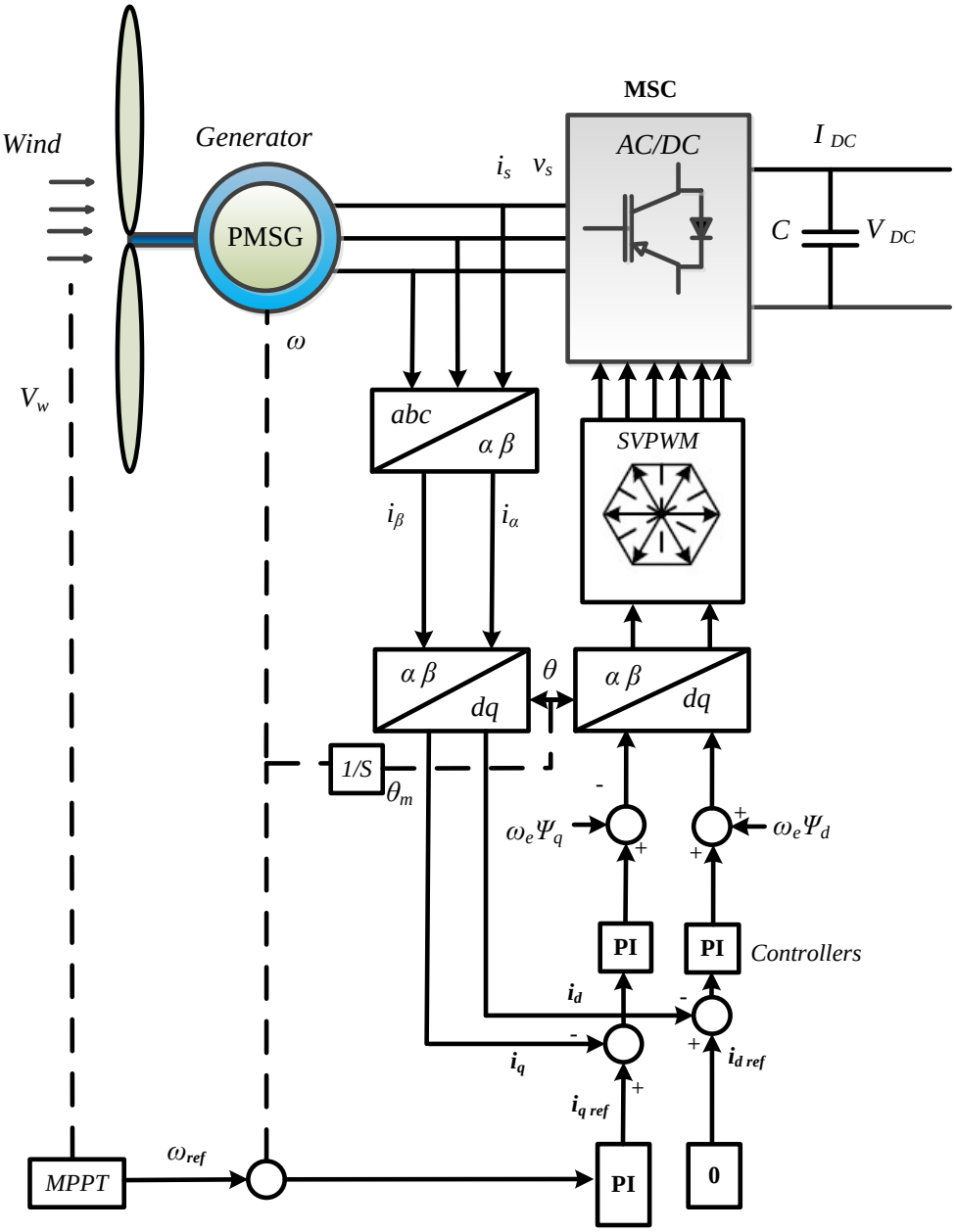

Fig. 3.11 Field Oriented Control Schematic Diagram

Since all quantities have to be kept within acceptable limits; the output voltage and frequency have to be constant. Then the control system has been designed to perform this aim in both the machine side and the grid side to satisfy the requirement [193].

In MSC control circuit, there are two loops that perform this scheme, inner loop and outer loop. The aim of inner loop is to control the d axis and q axis currents while the outer loop to control the generator speed. The outer loop controls the speed of the generator with the set value that satisfy the condition of MPPT of the power captured from the wind.

3.4.3.1 Current Control Loop

This PI controller has a proportional parameter K_P and integrator parameter K_I, which have to be tuned in a proper way to obtain the optimum operation and response [66, 194]. The commanded q reference current i_{sq}^* is determined by speed controller and the output of PI controller is:

$$i_{sq}^* = K_{P\omega} + K_{I\omega} \int e_\omega \, dt \tag{3.33}$$

where $K_{P\omega}$ and $K_{I\omega}$ are the proportional and integral parameters of the PI controller of the outer loop, while e_ω is the error between the reference rotor speed and measured rotor speed of the machine as shown in equation (3.34):

$$e_\omega = \omega_m^* - \omega_m \tag{3.34}$$

The reference value of d axis current i_{sd}^* is equal to zero in order as mentioned before. According to q axis reference current, the d axis and $q$axis controlled voltages of the inner loop can be determined by other two PI controllers as shown in equations (3.35) and (3.36):

$$V_{sd}^* = K_{Pi} e_d + K_{Ii} \int e_d \, dt - \omega_r L_q i_q \tag{3.35}$$

$$V_{sq}^* = K_{Pi} e_q + K_{Ii} \int e_q \, dt + \omega_r (L_d i_d + \psi_m) \tag{3.36}$$

where V_{sd}^*, V_{sq}^* are the reference voltages of dq axis voltages, and K_{Pi} and K_{Ii} are the gain of the proportional and integral parameters of the current loop PI controller respectively, while

e_d and e_q are the error of dq current component as shown in equations (3.37), and (3.38):

$$e_d = i_{sq}^* - i_d \tag{3.37}$$

$$e_q = i_{sq}^* - i_q \tag{3.38}$$

Generally, in the time domain, the equation for the PI controller, applied to an error signal $e(t)$ can be expressed in equation (3.39) :

$$u(t) = K_P.e(t) + K_I.\int e(t)\,dt \tag{3.39}$$

where $u(t)$ is the output signal, and K_P, K_I are the proportionality constant and the integration constant respectively. In the time domain the PI controller is the ratio between the output signal and error signal, called transfer function, as shown in equation (3.40):

$$G(s) = \frac{U(s)}{E(s)} = K_P + \frac{K_I}{s} \tag{3.40}$$

$$= K_p(\frac{s + \frac{1}{T_i}}{s}) \tag{3.41}$$

and the ratio between K_P and K_I is called integrator time, denoted as T_i in equation (3.41):

$$T_i = \frac{K_p}{K_I} \tag{3.42}$$

The voltage equations for the PMSG are mentioned in equations (3.43) and (3.44) respectively. Using PI controller, the dq-axis voltages are cross coupled by the terms $-\omega_e L_q i_q$ and $-\omega_e(L_d i_d + \psi_{PM})$ respectively. Due to these terms voltage disturbances may appear in the system and the i_d and i_q currents should be controlled together. Adding decoupling terms

to the current controllers, not only simplifies the control model but improves the accuracy of the control.

The system after eliminating the cross-coupling terms can be represented in the following equations (3.43) and (3.44):

$$v_d = R_d i_d + L_d \frac{di_d}{dt} \tag{3.43}$$

$$v_q = R_q i_q + L_q \frac{di_q}{dt} \tag{3.44}$$

Considering ($s = d/dt$) the following transfer functions for the plant are obtained (with $Id(s)$ as input and $Vd(s)$ as output in the system):

$$G_d(s) = \frac{I_d(s)}{U_d(s)} = \frac{1}{R_d + L_d s} \tag{3.45}$$

$$G_q(s) = \frac{I_q(s)}{U_q(s)} = \frac{1}{R_q + L_q s} \tag{3.46}$$

Assuming the generator has surface mounted magnets on the rotor, the d and q-axis inductances have the same values, thus the two transfer functions $Gd(s)$ and $Gq(s)$ are identical. All control blocks can be implemented in Simulink control environment using Single Input Single Output (SISO) tools.

The q-axis current controller is designed using the block diagram to find the gain parameters. Figure 3.13. presents the control architecture for a PI control loop taken from SISOtool for the plant and feedback of delay time T_d. After performing the decoupling on voltage equations, the current loop can be minimised and arranged as shown in Figure 3.14. The process of defining the SISOtool in block is going forward and finally the control circuit will be ready to simulate. In the same manner, the control circuit of the d- axis can be implemented in SISOtool of Simulation and all parameters will be known. Finally, the controlled voltages will be transferred to *abc* voltages by Park inverse transformation to get

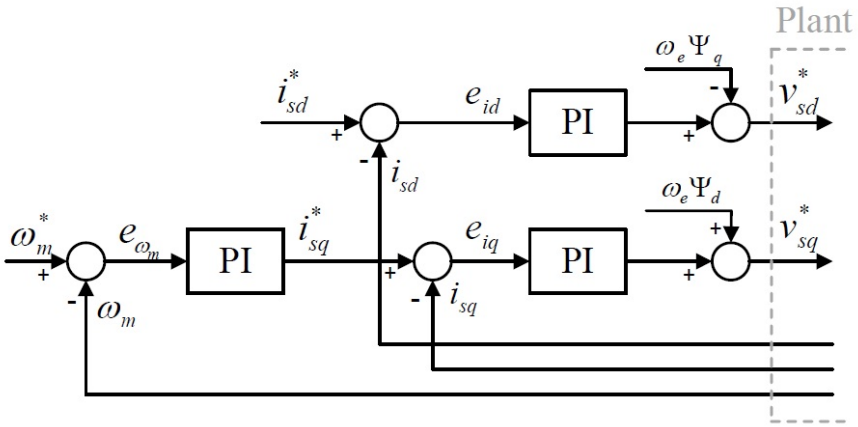

Fig. 3.12 Synchronous reference frame control loops

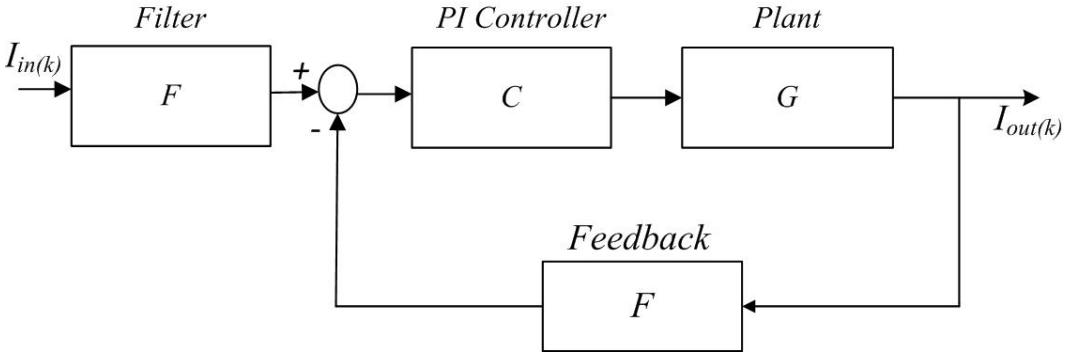

Fig. 3.13 Control architecture provided by SISO tool

the values of switches of Insulated Gate Bipolar Transistor (IGBT)[195].

3.4.3.2 Speed Control Loop

The speed controller represents the outer loop in a FOC strategy. This loop gets its feedback from the rotor position sensor. The mechanical equation of the generator, showing the relation between mechanical speed ω_m, mechanical torque T_m and electromagnetic torque T_e and can be expressed in swing equation (3.17) that mentioned in subsection 3.3.1. The equation can be arranged as the plant transfer function is derived from equation (3.9) assuming soft

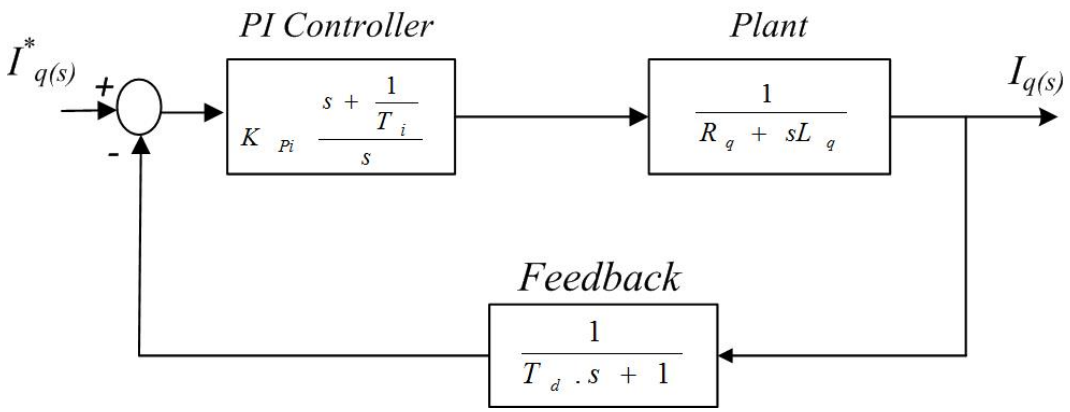

Fig. 3.14 q-axis current loop

rotating without friction ($F = 0$) as follows:

$$G_\omega(s) = \frac{\omega_m(s)}{T_e(s)} = \frac{1}{J.s} \tag{3.47}$$

The transfer function of the PI speed controller is:

$$C_\omega(s) = K_{P\omega}\left(1 + \frac{1}{T_{i\omega}s}\right) = K_{P\omega}\left(\frac{s + \frac{1}{T_{i\omega}}}{s}\right) \tag{3.48}$$

where $K_{P\omega}$ is the proportional gain and $T_{i\omega}$ is the integrator time constant of the controller.

Applying the design that mentioned in current loop control and shown in Figure 3.13 the control parameters are:

- $C(s)$ is the compensator block, which the PI controller needed to be designed using equation (3.49).
- $D_i(s)$ is the inner current loop transfer function which the transfer function of current open loop.
- $G(s)$ is the mechanical plant block

- $H(s)$ is the first order transfer function, which represents the delay introduced by the speed sensor and can be determined by:

$$H_{\omega}(s) = \frac{1}{T_d.s+1} \tag{3.49}$$

These transfer functions, after being defined in Matlab Workspace, were imported into SISOtool and then the design of the speed PI is made. The procedure for tuning of the PI parameters was the same as for the current controller.

3.4.4 Grid Side Converter Control

There are various control strategies can be used to do the control of the grid side converter. The main target of these schemes are focusing on the same issue: the active and reactive powers delivered to the grid, the control of the DC-link voltage and grid synchronization to ensure high quality of the injected power [196]. According to the derivation of grid side converter models, the d and q axis voltage V_{gd} and V_{gq} of the grid side converter from original

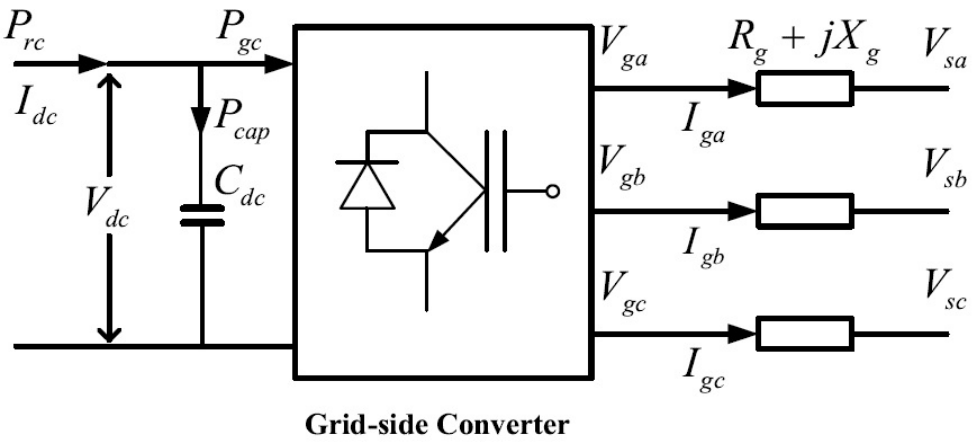

Fig. 3.15 Schematic diagram of grid side converter configuration

three phases V_{ga}, V_{gb} and V_{gc} shown in Figure by equations (3.50) and (3.51):

$$V_{gd} = V_{gd} + R_g I_{gd} + L_g \frac{dI_{gd}}{dt} - \omega_s L_g I_{gq} \tag{3.50}$$

$$V_{gq} = V_{gq} + R_g I_{gq} + L_g \frac{dI_{gq}}{dt} + \omega_s L_g I_{gd} \tag{3.51}$$

where I_{gd} and I_{gq} are the d and q axis currents of grid side converter. R_g and L_g are the resistance and reactance of the grid side converter, ω_s is the rotational speed of the grid side converter.

3.4.4.1 Grid Current Control Loop

In equations (3.50) and (3.51), the terms $L_g \frac{dI_{gd}}{dt}$ and $L_g \frac{dI_{gq}}{dt}$ are replaced by the controlled voltages V^*_{gd} and V^*_{gq} using PI controllers expressed by :

$$V^*_{gd} = K_{Pi} e_{gd} + K_{Ii} \int e_{dg}\, dt \tag{3.52}$$

$$V^*_{gq} = K_{Pi} e_{gq} + K_{Ii} \int e_{gq}\, dt \tag{3.53}$$

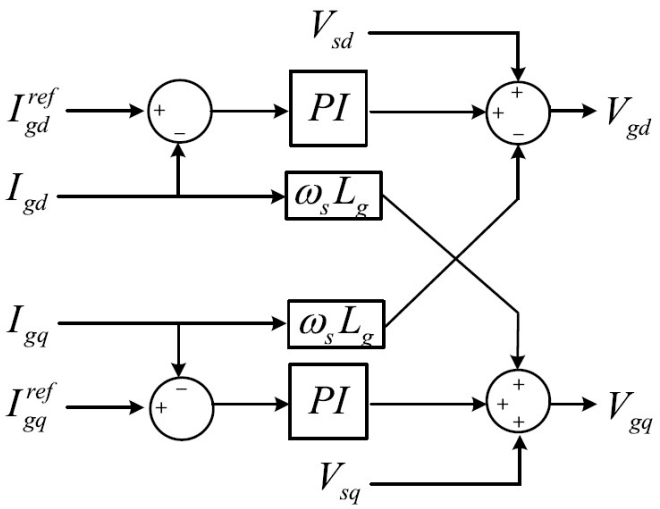

Fig. 3.16 Current control of grid side converter

where V_{gd}^{*}, V_{gq}^{*} are the reference voltages of dq axis grid voltage, and K_{Pi} and K_{Ii} are the a proportional and integral parameters gain of the current loop PI controller respectively, while e_{gd} and e_{gq} are the error of dq current component error as shown in equations (3.54), and (3.55):

$$e_{gd} = I_{gd}^{ref} - I_{gd} \tag{3.54}$$

$$e_{gq} = I_{gq}^{ref} - I_{gq} \tag{3.55}$$

Based on equations (3.52) and (3.53), the decoupled current controller is shown in Figure 3.16. The voltages V_{gd} and V_{gq} are regulated as modulation index for generation the signal for the PWM of grid side converter [197, 198].

3.4.4.2 DC Voltage Control Loop

The derivation of DC link voltage and its reference value are sent to d- axis PI controller to specify the reference value of the current I_{gd}^{ref} as shown in Figure 3.17 and expressed by equation (3.56):

$$I_{gd}^{ref} = K_{Pdc}\, e_{dc} + K_{Idc} \int e_{dc}\, dt \tag{3.56}$$

where K_{Pdc} and K_{Idc} are proportional and integral parameters of the PI controller and e_{dc} is the error of measured and reference values of the DC voltage as in equation (3.57):

$$e_{dc} = V_{dc}^{ref} - V_{dc} \tag{3.57}$$

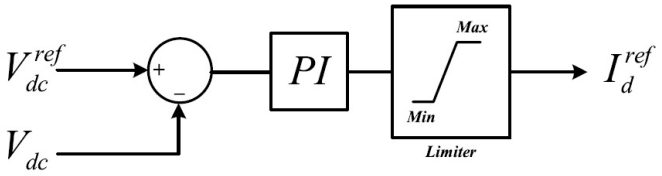

Fig. 3.17 DC voltage loop control

The q-axis current reference I_{gq}^{ref} is usually predefined as zero while the grid side voltage control can be used to control the DC link voltage to maintain it at the rated level for DC/AC power conversion during normal and disturbances due to variable wind speed.

3.4.5 Phase Locked Loop

To achieve a synchronized quantities of amplitude, phase and frequency of the inverted voltage which regarded as a variable and critical information for the operation of the grid-connected inverter systems, the synchronization process is required.

Synchronization method which can be used to synchronize the magnitude and angle of reference current of the VSI with the grid voltage. In this equipment and its utilization, fast and accurate detection of the amplitude, phase angle and frequency of the inverted voltage of VSI is basically to assure the correct generation of the reference signals and follow the requirements of the grid connected system. On the other hand, grid connected WECS have been controlled to work as close as the unity power factor in order to satisfy minimum power dissipation and fellow the standards of grid code[199]. Two basic synchronization methods can be used for this purpose: Filtered Zero Cross Detection (ZCD) and Phase Locked Loop (PLL).

The detection of the zero crossing of the grid voltage can be achieved by the first method while the PLL provide a feedback control system that adjusts the phase of a generated signals automatically to correspond the input signal phase. The function of PLL is acquisition process to obtain the power factor as close as possible to 1. This process seek to synchronize the angle of inverter current, θ_{inv}, with the grid voltage angle, θ_{grid}. The angle θ_{inv} used to determine the reference current which is compared to the actual value of the inverter output current. From three phase systems representation, the space vector voltage v_{abc} can be represented by two orthogonal voltages v_d and v_q and should be easily obtained to satisfy the

algorithm of PLL. The main idea in the PLL is altering the frequency of inverter current, ω_m, in case of phase shift between the grid voltage and the inverter current.

The process depends upon the lagging and leading angle between currents and voltages. When the inverter current lags the grid voltage the PLL will decrease ω_m until the inverter current be in phase with the grid voltage. In case of leading inverter current, then the grid voltage ω_m will be increased until they are in phase again. The most common PLL technique applied to three phase grid connected systems is based on an algorithm implemented in synchronous reference frame dq-axis.

3.4.6 Pitch Angle Control

The pitch control is basically used for controlling the amount of generated power of the wind turbine. Its function is to maintain the output power of the turbine constant when it exceeded above the rated values, by varying the pitch angle of the rotor blades. There are two main methods to generate the pitch angle: one is from the difference between measured electrical power and power reference, and the other is to obtain the pitch from the difference between measured mechanical speed and reference speed. These two signals give the error which can be input in the pitch controller.

Various strategies can be used to achieve the the best values of pitch angle to maintain the output power within the limit using different controller such as P or PI controllers, fuzzy logic control [200]. The pitch controller has been used in this thesis is in the form of a PI controller. The selection of pitch control technique is illustrated in Figure 3.18, where the difference between the rated power P_{rated} and actual power P_e shows the error signal that will be controlled by the PI controller.

For a better understanding of the pitch angle control mechanism the following power characteristic for a typical large scale wind turbine will be explained. Four different regions shown in the power curve as function of the wind speed as shown in Figure 3.19. In regions

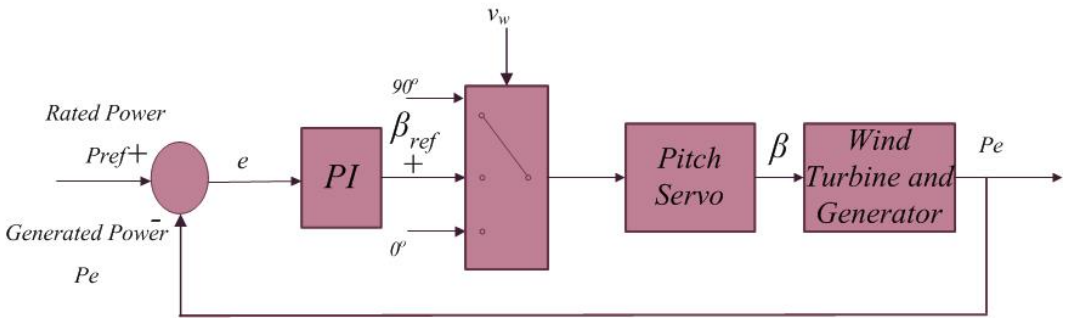

Fig. 3.18 Schematic diagram of the pitch angle control method

I and IV, when the wind is below cut-in wind $v_{w(cut-in)}$ and above cut-out wind $v_{w(cut-out)}$ the pitch angle is kept at 90 degrees to stop the rotor from rotating. In region II, for wind speeds between $Vt_{cut-out}$ and $v_{w(rated)}$ the pitch angle is fixed at 0 degrees for maximum aerodynamics of the rotor, and then maximum power capture from the wind kinetic energy. In region III for wind speeds between $v_{w(rated)}$ and $v_{w(cut-out)}$ the pitch angle β is varied (decreased with an actuator constant rate limiter of 10 degrees/sec) for keeping the power generated at its rated value.

3.5 Simulations and Results

Generally, the simulations have been done for the classical controller using Matlab programming environment. Implementation and built blocks are used in the Matlab/Simulink 14 which is built in the same program.

In this simulations the variation of different values of wind speed will be an input to the system during the chosen time interval, while the output will be the values of 3-phase voltages and currents injected to the system. The initial conditions of simulation are taken in to account in order to operate the system in a stable manner. In classical control scheme, PI controller have been used to design both control schemes of MSC and GSC. The simulation have been implemented for the schematic diagram shown in Figure 3.11.

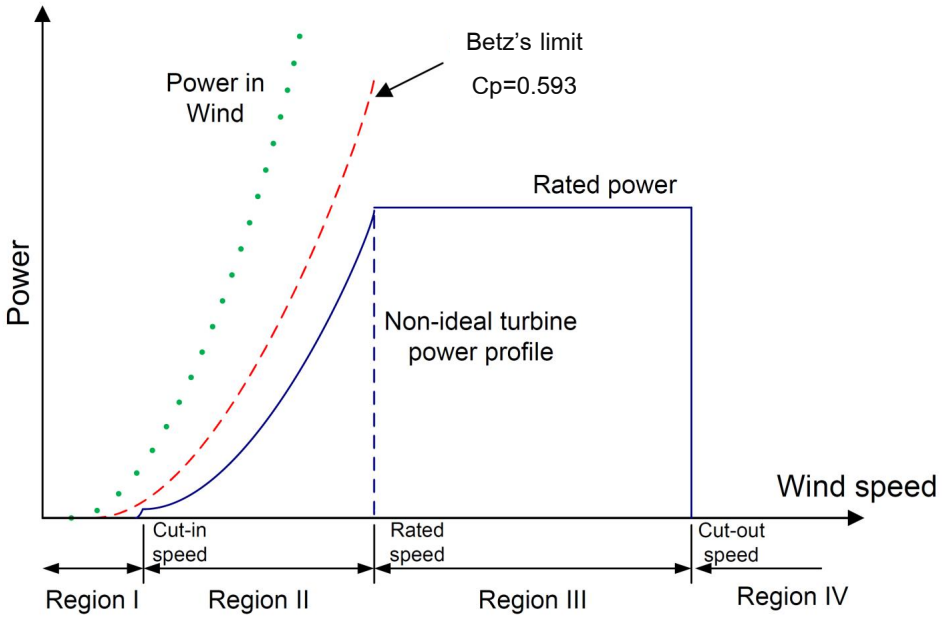

Fig. 3.19 Power Output fo a Wind Turbine Generator[201]

The parameters of WECS have been taken from [202, 203]:

(a) Wind turbine: blade radius $R_o = 39$ m, inertia $J_{eq} = 10,000\ kg.m^2$, air density $\rho = 1.205\ kg/m3$, rated wind speed $V_{w-rated} = 11.4\ m/s$, cut-in speed $V_{w,cut-in} = 5m/s$, and cut-out speed $V_{w,cut-out} = 24m/s$.

(b) Parameters of generator: rated power $P_{g-rated} = 2MW$, number of poles pair $p = 11$, stator resistance $Ra = 50\ \mu\Omega$, d-axis inductance $L_d = 0.0055\ H$ q-axis inductance $L_q = 0.00375\ H$, field flux $\psi = 135.25\ V.s/rad$, rotational damping $D = 0$.

(c) Parameters of power converter: PWM carrier frequency $fp = 10kHz$, rated DC-link voltage $V_{dc-rated} = 7.1kV$, DC-link capacitor $C = 15,000\mu F$.

(d) Parameters of Control schemes: MSC: speed loop controller $K_p = 33$, $K_I = 100$, current loop $K_p = 100$, $K_I = 5$. GSC: DC voltage loop controller $K_p = 2$, $K_I = 70$, current loop $K_p = 100$, $K_I = 10$.

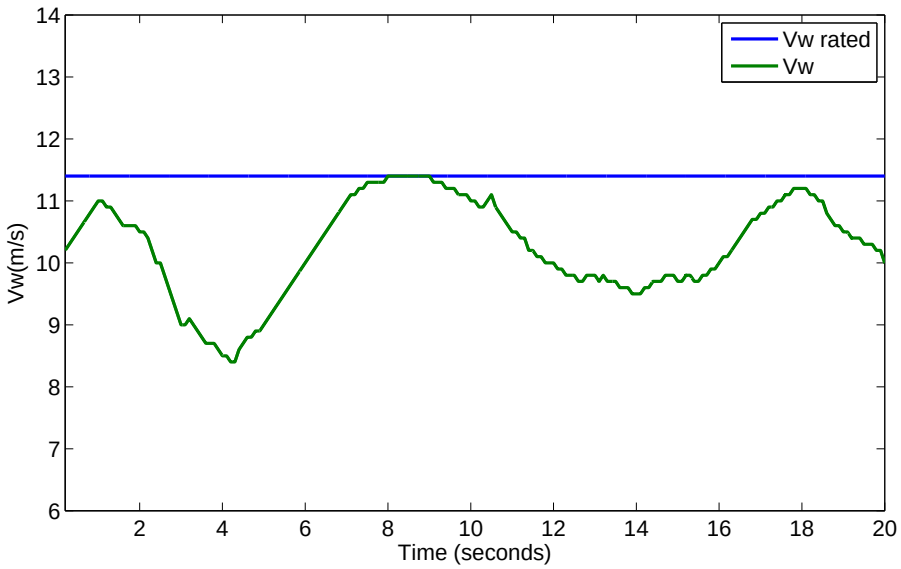

Fig. 3.20 Wind speed variation with time

3.5.1 Wind Turbine Control Simulations

In this work, the modelling of single machine, 3-phase horizontal axis wind turbine direct train can be connected to PMSG to feed AC power to the DC link and then converted to the grid through 3 phases IGBT inverter. The movement of wind turbine cases a mechanical output power and torque with mechanical rotor speed. The variation of wind speed and mechanical rotor speed are shown in Figures 3.20 and 3.21 respectively.

To achieve MPPT, the values of TSR should be within the optimum value in time that the power coefficient should be maximum. These values are shown in Figures 3.22 and 3.23 respectively.

3.5.2 Generator Current Control Simulations

Machine side converter control schematic diagram is shown in Figure 3.11. The variation of the 3-phase currents have been changed due to change of the input torque which is consequent

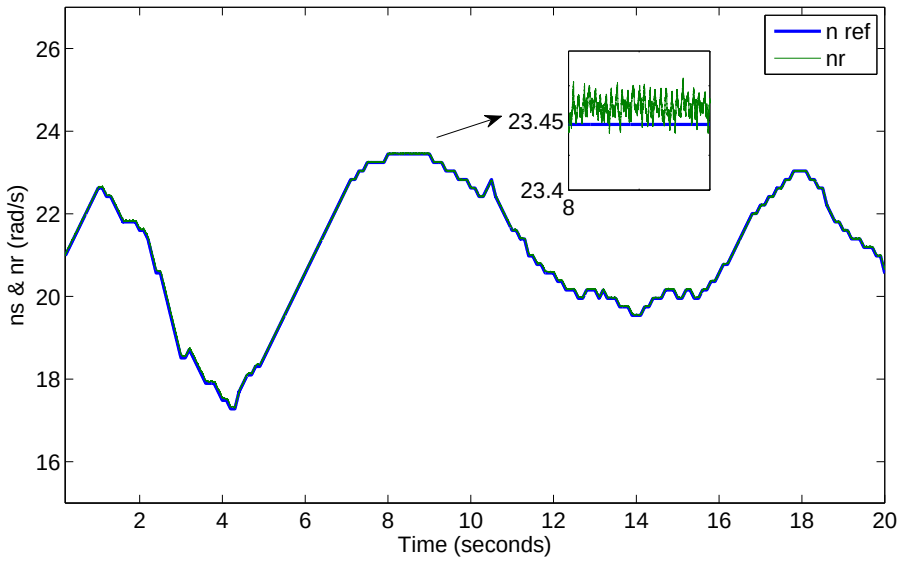

Fig. 3.21 Rotational rotor speed and reference speed with time

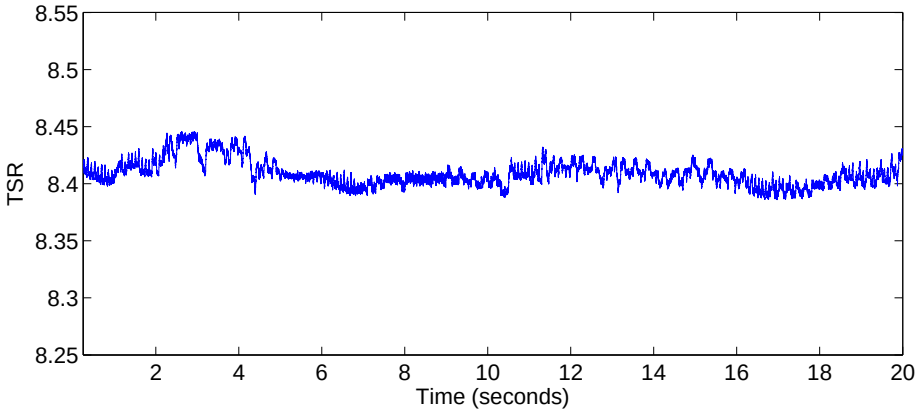

Fig. 3.22 Tip Speed Ratio TSR

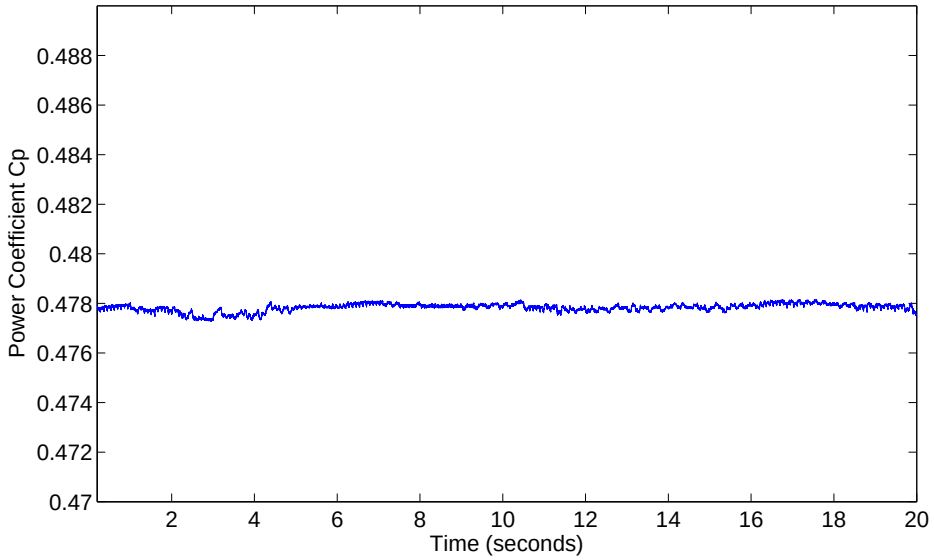

Fig. 3.23 Variation of power coefficient with time

to the wind speed variation. The 3-phase output currents of the generates are shown in Figures 3.24.

3.5.3 Grid Current Control Simulations

Grid side control schematic diagram is shown in Figure 3.15. The aim of the grid side control is to keep the DC link voltage of Back-to-back converter constant during the wind variation where the set point is ($V_{DC} = 7.1kV$). This DC voltage is shown in Figure 3.25. It is obvious that the DC voltage will be varied within acceptable limit during the simulation to keep the output voltage consequently constant. Grid side 3-phase currents with time are shown in Figure 3.26 and 3-phase grid voltages with time are shown in Figure 3.31.

It is noticeable that the current increased while the wind speed increase to inject more active power to the grid. The variation of wind speed usually causes a small fluctuation in DC voltage which leads to a fluctuation in current frequency profile as shown in Figure 3.30 where the grid voltage frequency will be constant.

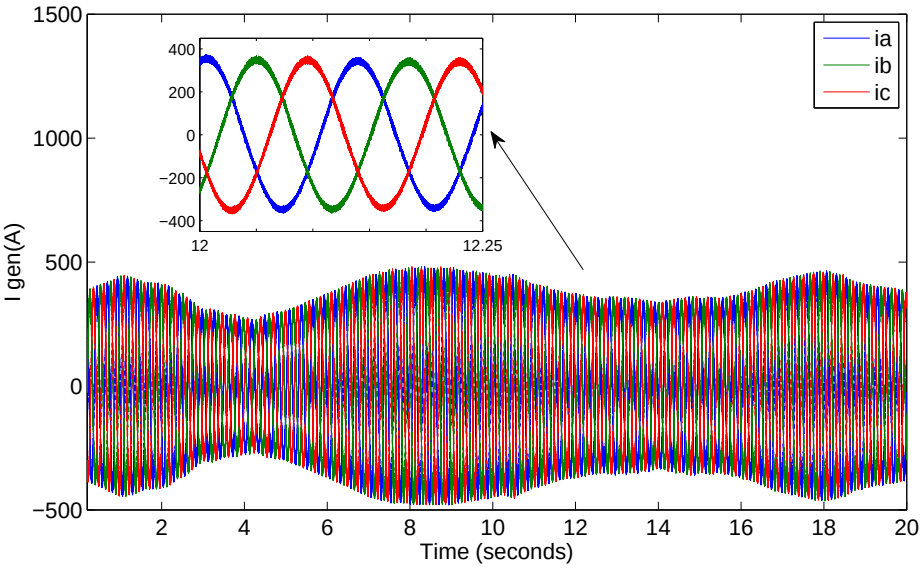

Fig. 3.24 Generated 3-phase current with respect to time

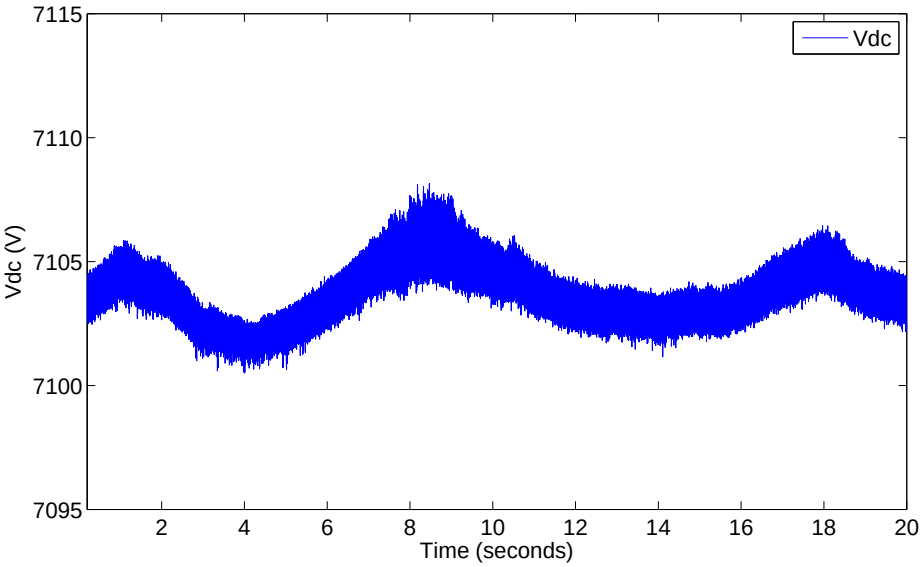

Fig. 3.25 DC link voltages during wind variation with time

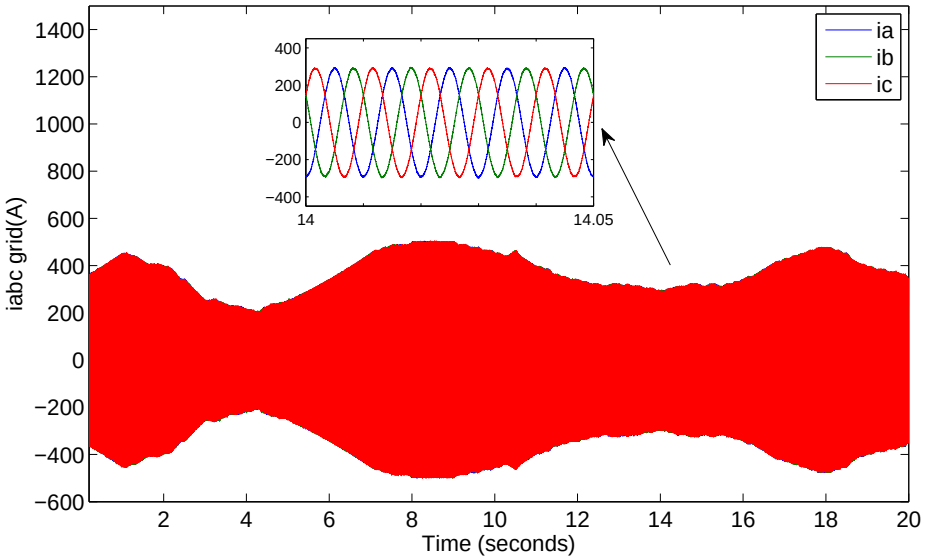

Fig. 3.26 Grid side 3-phase Current 50 Hz with respect to time

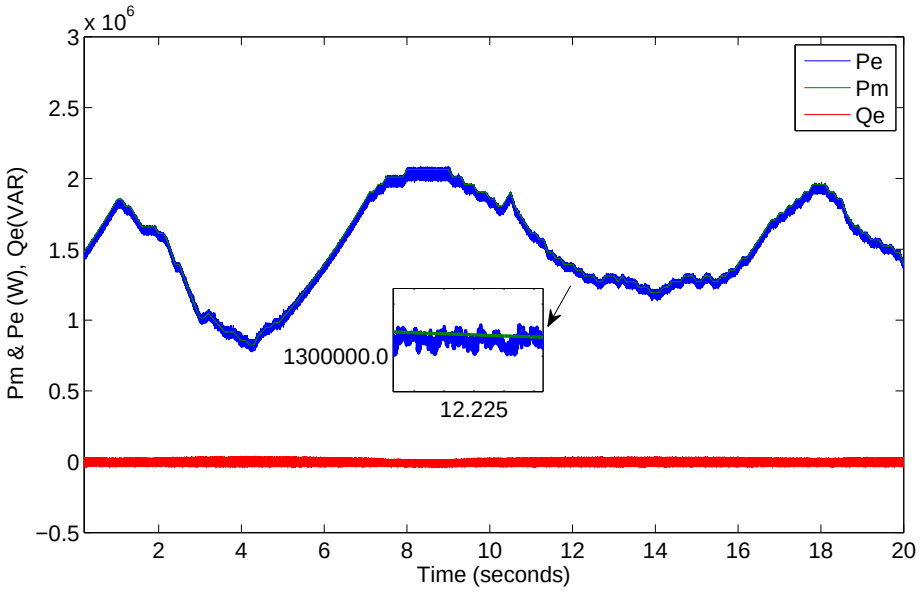

Fig. 3.27 Grid side 3-phase active, reactive and mechanical power with time

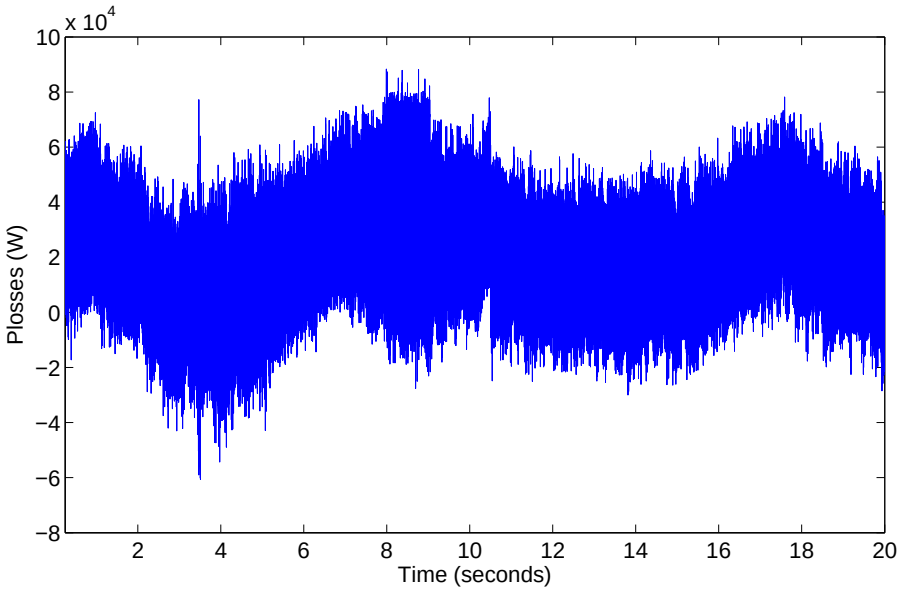

Fig. 3.28 3-phase active power losses with time

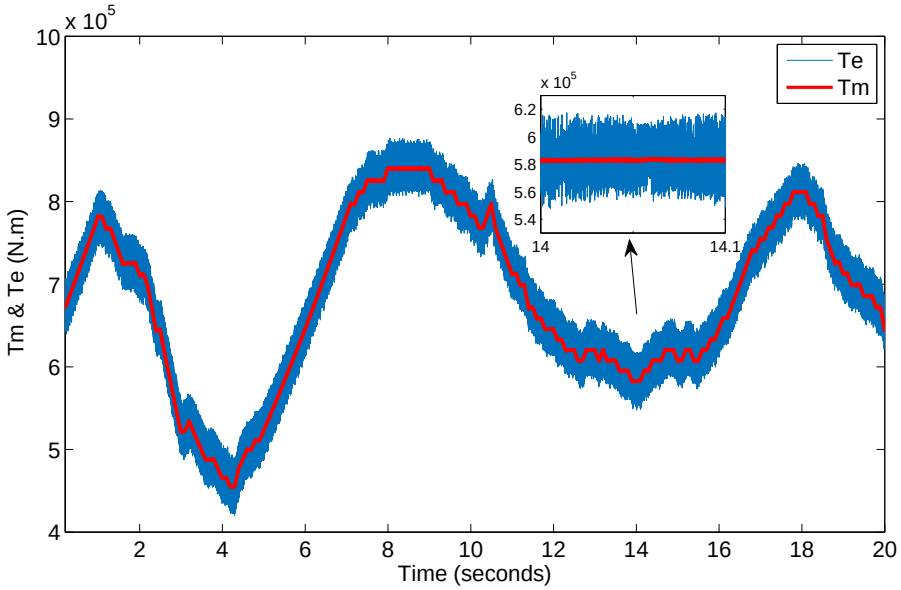

Fig. 3.29 mechanical and electromagnetic torque variation

3.6 Summary

In this chapter, a modelling of WECS, Type 4 has been proposed using a traditional control such as PI controller is also discussed. The main control system depends up on two controllers

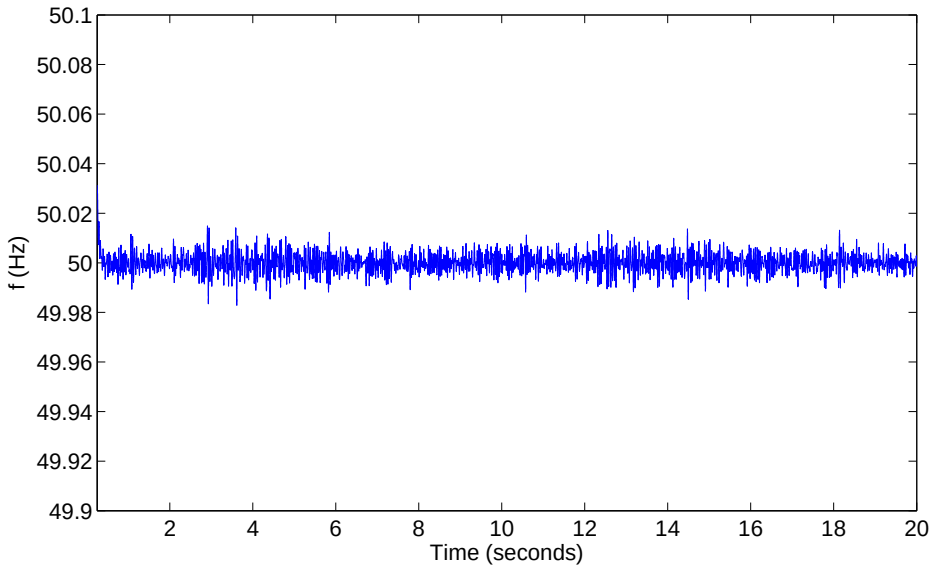

Fig. 3.30 Grid side Frequency Variation

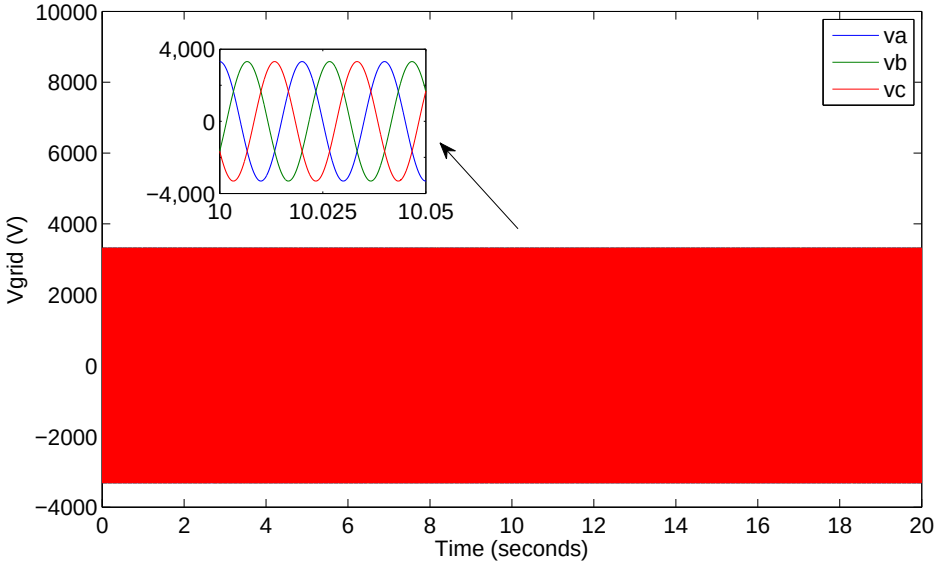

Fig. 3.31 3-phase Grid voltage

for MSC and GSC respectively. The function of the first controller is to achieve the MPPT in MSC during variable wind speed while the second controller is working in order to keep the

DC link voltage constant during simulation to keep the output voltage and frequency within acceptable limits. All simulations have been done in MATLAB/Simulink 14.

Chapter 4

Advanced Control Schemes of Wind System

In this chapter, the state-of-the-art of advanced control schemes which can be used in variable speed synchronous machine have been discussed. The description contains the modelling and application of digital control technique such as hysteresis control, PI/PID control, intelligent control, predictive control and hybrid control. The operating principle of these techniques is analysed briefly and summarised of Various classes of the predictive control techniques are discussed along with their merits and demerits of these type has been discussed at all, with focussing on both intelligent and predictive control as a new techniques that have been used in last decades.

4.1 Introduction

Many semiconductor devices have been developed to obtain the ideal characteristics of a switch of power conversion process [204–207]. The first generation of simple model configure diode rectifiers of semiconductor devices with uncontrolled commutation and called natural commutation control process. The second generation semiconductor devices,

the gating terminals will be controlled according to desired input information by turning on and off of gate switches. Consequently, many power devices have been designed such as thyristor which is regarded as one of the latest developments in this categories.

Control techniques have been developed since 1960s, depend up on operational amplifiers and passive components to adjust the firing angles of thyristors to keep the output voltage within desired values [208]. With thyristors, the turn-on instant can be controlled, but the turn-off instant is uncontrollable and is dependent on the line frequency. In an effort to achieve controllable turn-off, Insulated Gate Bipolar Transistors (IGBTs) have been developed [204]. A prime model of using IGBT to acquire controllable performance is a buck converter whose output voltage can be adjusted by changing the value of the duty cycle [177].

In this type of converters, analogue control circuits have been applied in the past, where a single-phase pulse width modulator or other linear controller such as hysteresis controller can be used to form the gates signals. Although the analogue control techniques are simple and easy in use, several drawbacks have been noticed such as a large number of components, reduced system reliability and poor computational capability.

To eliminate those drawbacks typically of analogue systems and achieve a high performance operation, digital control systems made a big revolution especially in the industrial world virtually which involve powerful calculations, complex strategies and sophisticated mathematical algorithms [37]. Introduction of Digital Signal Processors (DSPs) by Texas Instruments in 1983 was a giant leap to which applied later in the digital control systems. One example of the earlier DSPs is a 16-bit processor and operational power of 10 million instructions per second [177].

Recently the technological progresses in semiconductor devices have produced in different types switching devices such as the power Metal-Oxide Semiconductor Field Effect Transistor (MOSFET), MOSFET-Controlled Thyristor (MCT), Gate Turn-Off thyristor (GTO), Insulated Gate Commutated Thyristor (IGCT), Emitter Turn-Off thyristor (ETO), Insulated

Gate Bipolar Transistor (IGBT), Reverse Blocking (RB) IGBT, Static Induction Thyristor (SIT), Silicon-Controlled Rectifier (SCR), Injection-Enhanced Gate Transistor (IEGT), Gate Commutated Thyristor (GCT) and Symmetrical Gate Commutated Thyristor (SGCT).

Digital control techniques has also developed industrially allowing the user to improve sophisticated control algorithms to perform more complicated mathematical tasks. Controllers such as: micro-controllers, DSP, Field Programmable Gate Array (FPGA), rapid prototyping systems are examples of modern Real-Time digital control. These platforms have a good features like low cost, more reliability and high computational power. For this reasons they have been utilized widely in the controlling process of different types of power electronic converters [209].

Genetic Algorithms (GA), Fuzzy Logic Control (FLC), Expert Systems (ES), and Artificial Neutral Network (ANN) belong to the family of intelligent control techniques. As demonstrated in this thesis, FLC scheme is used instead of PI controller to acquire the above features.

The current reference tracking error and its derivative are used as the input to the fuzzy controller. In this technique, the robustness of the system performance during the variations of the machine parameter can be improved by using the fuzzy technique. In this case, the knowing the exact converter model is not important. FLC works within the non-linear control techniques, and positively it is evaluated as the best among other controllers [210–212].

This controller has the membership functions which implies the knowledge, experience and intuition of the converter operator/designer. To reduce the dependence upon the implication knowledge, some novel control schemes have been suggested by the designers in order to satisfy this purpose and achieve better performance of the output as well. These novel control schemes contain: Fuzzy and PID, Neural networks and PID, Fuzzy and Neural Networks, Fuzzy and Genetic Algorithm, Fuzzy and Adaptive Control, Fuzzy and Predictive Control and finally Fuzzy and Sliding Mode Control. Application of FLC and Model Reference

Control will be discussed in this chapter, and the other model of Fuzzy Predictive Control will be discussed in the next chapter.

4.2 Fuzzy Logic Controller

In this section, a principle design and operation of the advanced control schemes is presented. The proposed approach, addressed as Fuzzy Logic Control (FLC) scheme is based on logical situation and decision will be discussed in the following section.

4.2.1 Fuzzy Logic System

As traditional PI controllers are linear feedback controllers, then they cannot improve and respond to fast variations of the process. In addition, PI controlled system is less responsive to real and relatively fast change in wind speed. As a result, modern robust controllers become more and more necessary in order to follow grid code requirements and adhere to engineering recommendations.

Non-linear behaviour of the power system leads to the non-linearised problems, then the control of the wind turbine-generator system will be difficult by using the conventional control scheme such as PI controller. Although PI controller is simple , cheap and easy to use with low maintenance, it has some drawbacks such as irregularity of operation during disturbances or the change in system parameters in operation due to warming or friction impact. Advanced control schemes have overcomes some of these drawbacks with good performance and highly level of efficient operation. A recently developed approaches use the intelligent control systems such as FLC to satisfy proper behaviour and operation of the system [13]. The fuzzy controller can be expressed as a rule based to non-linear control method. This controller presents some advantages as compared to the traditional controller.

Variable gains can be obtained depending on the errors in order to tackle the problems which are affected by an uncertainty of the system.

From these figures, the conventional PI controllers are replaced by the fuzzy controllers. In this thesis, FOC scheme for MSC control has been designed with direct FLC is used and compared with respect to the output values of PI controller. Traditional control scheme has used a PI controller in both inner circuit to control the currents of direct axis i_d and the quadrature axis i_q and while in this control scheme the FLC will be used in stead, where the output should be the value of i^*_{sq} for the outer loop and V^*_d and V^*_q for the inner control loops.

The PI controller which used in the outer circuit to control the generator speed is also can be replaced by FLC in complete design. At present, different types of controllers have been developed and have enhanced the wind system in order to achieve several advantages such as, reduction in system losses, size and cost and give a high performance of output voltages and currents during non-linearity of the system [66]. One of the advanced control system have been used with intelligent controller such as FLC which is used to overcome the uncertainty of the system in case of sudden change disturbance or variation in system parameters.

This section presents the analysis and design of FLC and its behaviour during variable wind speed compared traditional PI controller. As a result, modern robust controllers become more and more necessary in order to follow grid code requirements and adhere to engineering recommendations. A recently developed approaches use the intelligent control systems as FLC to satisfy the the proper behaviour and operation of the system [13].

4.3 Analysis of Fuzzy Logic Controller

The FOC scheme for MSC control shown in Figure 3.11 uses PI controllers to achieve the control process in inner and outer loops as described above. In the proposed control scheme, PI controllers are replaced by three FLCs for the same loops to control the speed and currents. The schematic diagram of FLC system that is used in MSC shown in Figure 4.1. The two

inputs variables are the error (e) and change of error (Δe). The behaviour of a FLC depends on the shape of membership functions and the rule base [213]. FLC system approach is capable to improve the tracking of the operation when compared to conventional control systems for both grid or load connected cases of linear or non-linear loads.

In simulations of this chapter, the design of FLC controller depends upon the the error input will be explained in the following sections. The structure of the FLC scheme consists of three main function: fuzzification which depends upon the input membership function, inference engine which depends upon the rule base and defuzzification which depends upon the output membership function. The inputs variables of FLC are selected as a signals that should be varied with the change of outputs. The behaviour of a FLC depends on the shape of membership functions of the rule base [213].

4.3.1 Fuzzification

The membership function values are assigned to the linguistic variables using fuzzy subsets named: Negative Big (NB), Negative Small (NS), Zero (Z), Positive Small (PS) and Positive Big (PB). The signals (e) and (Δe) are selected as an inputs to FLC in all cases as shown in Figure 4.1 , while $I^*_{(k)}$ is the outputs of the FLC for the outer control loop.

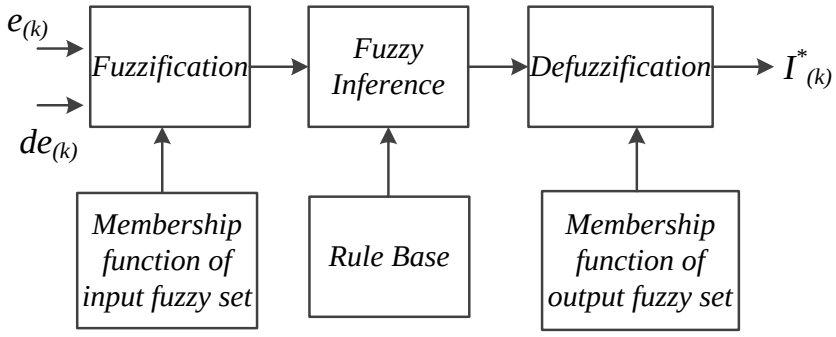

Fig. 4.1 Structure of Fuzzy Logic Controller

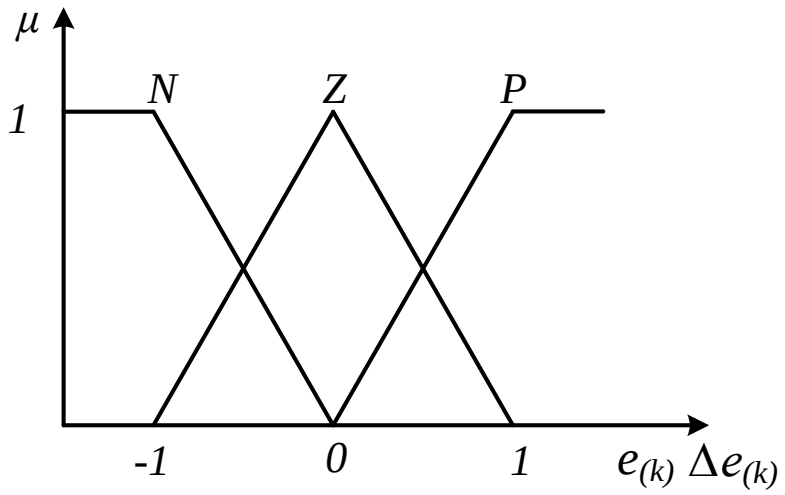

Fig. 4.2 Membership Function of FLC for the input variables

In the inner control loop of MSC, the signal (e) is the error between the reference current signals and actual current signal of the system for both d-axis and q-axis circuits, while Δe is the change in error in the sampling period of time. In the outer control loop of MSC, the signal (e) is the error between the angular speed signals and actual angular speed signal of the system for q-axis circuit only with Δe is the change in error, while q-axis circuit reference current will be fixed on zero value.

In the first stage, the crisp variables of errors are converted into fuzzy variables using the triangle shape as shown in Figure 4.2, and each fuzzy variable is a member of the subsets with a degree of membership varying between 0 and 1.

Table 4.1 Rule base table of the Fuzzy Controller

$e/\Delta e$	**N**	**Z**	**P**
N	N	N	Z
Z	N	Z	P
P	Z	P	P

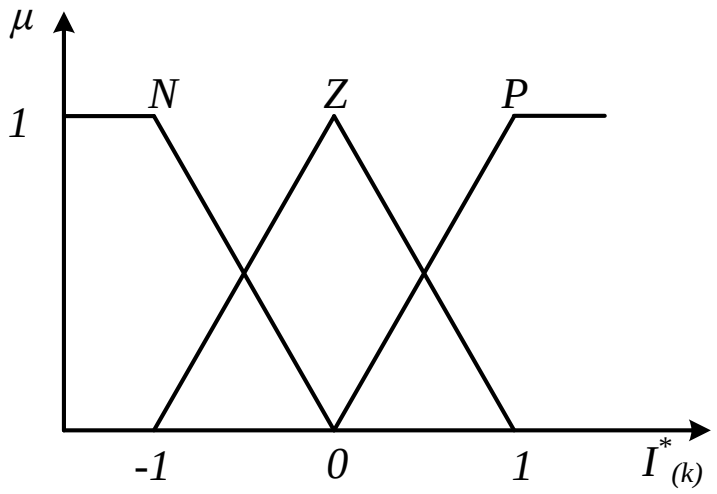

Fig. 4.3 Membership Function of FLC for the output variable

4.3.2 Inference Engine

The fuzzified inputs are fed to the interface engine which mainly consists of fuzzy rule base and fuzzy implication sub-blocks. At this stage the rule base is applied to obtain the output fuzzy set using the fuzzy implication method. There are different methods that can be used for this process such as max-min implication technique. The rules-base of the proposed system are shown in Table 4.1.

4.3.3 Defuzzification

In the defuzzification process, the inference engine output variables are converted into a crisp values as shown in Figure 4.3. The output reference current is represented by $I^*_{(k)}$.

Different algorithms have been developed to perform this function such as the centroid defuzzification algorithm, in which the crisp value can be determined as the centre of gravity of the membership function. The estimation of the spread of each partition is generally a compromise between the equally spaced triangles of the output values. Inputs and outputs

normally differ from the range of membership functions, therefore the fuzzy logic outputs can be changed by multiplying the signal controller of input and output variables by gain factors in order to match these variables with the normalized intervals [214, 215].

4.4 Application of Fuzzy Logic in Control Scheme

Fuzzy logic controller can be used in different types of control scheme that control the input signal to process based on the output signal.

4.4.1 Direct Fuzzy Logic Controller

For the machine side control circuit, the controllers (1 and 2) can be replaced by FLC in stead of PI controller as shown in Figure 4.4.

The cascaded control loops have been used to control the currents and speed of the machine. This can be divided into internal loop for currents and external loop for speed. The external speed loop can be controlled by conventional methods to adjust the rotor speed. Alternatively, an FLC internal loop will controls the currents in the dq synchronous reference axis. Maximum torque at the minimum current can be obtained by adjusting the d- axis stator current reference i_{sd}^{*} to zero. The q- axis stator current reference i_{sq}^{*} is computed via the PI external speed controller. In order to obtain the values of controlled voltage, the equations (4.1) and (4.2) can be represented by applying the FLC control circuit in d- axis and q- axis respectively.

$$v_d = R_d i_d + L_d \frac{di_d}{dt} \tag{4.1}$$

$$v_q = R_q i_q + L_q \frac{di_q}{dt} \tag{4.2}$$

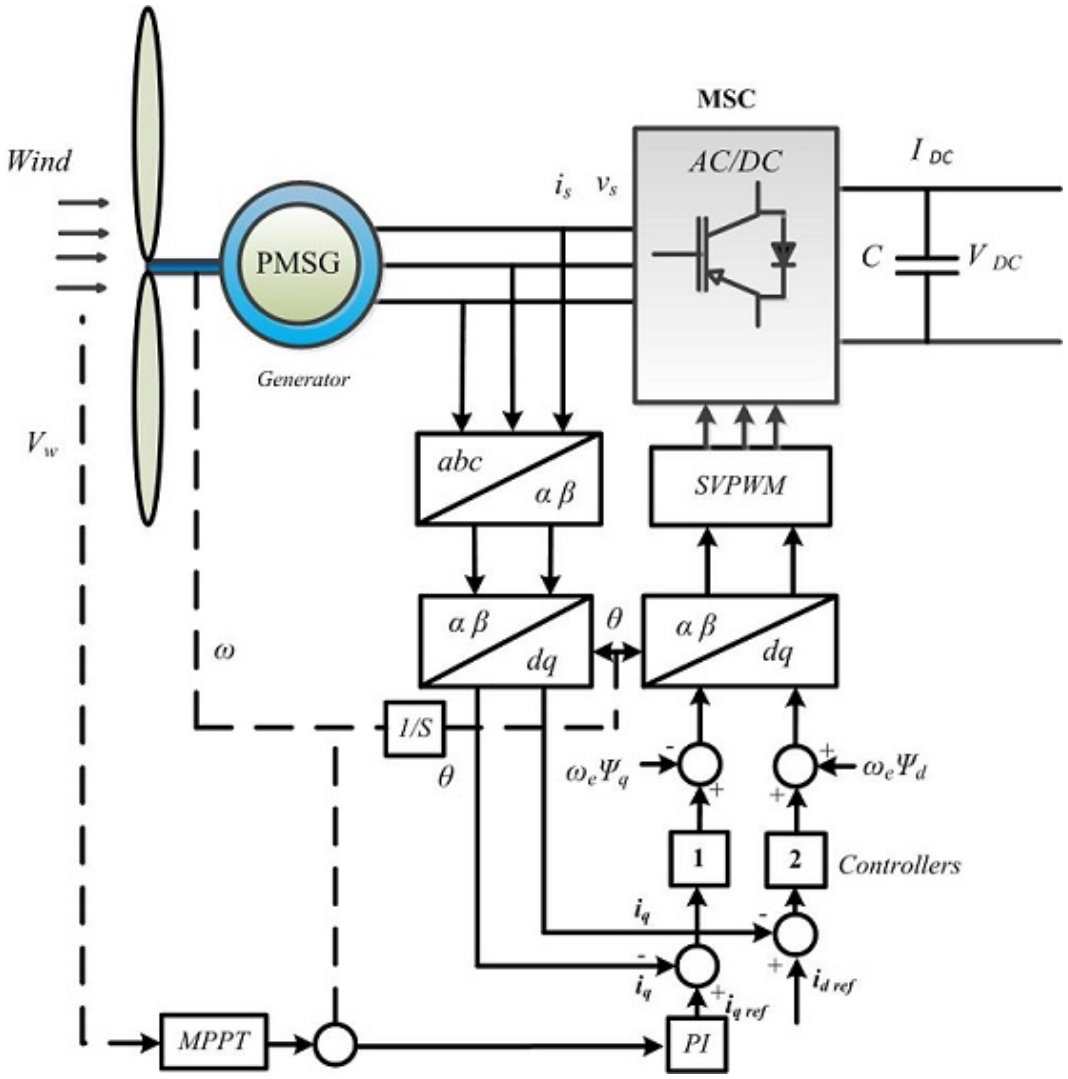

Fig. 4.4 FOC scheme using FLC for current variable

The PI controller of proportional gain $K_{P\omega}$ and integral gain $K_{I\omega}$ can be used for speed control. The block diagram of the outer loop of speed controller has been constructed as a conventional PI control system [216].

4.4.2 Model Reference Fuzzy Controller

The traditional control schemes depend upon the mathematical model representation parameters of the controlled plant which are time varying due to temperature rise and changes in

generator drive operating conditions. Therefore, it is desirable to design a robust controller for the system to reduce parameter dependency. Various control algorithms developed require the system states, thus they are not easy to implement [217]. To overcome this problem and to enhance the flexibility of changing control algorithm, a FLC is used to implement the combination with model reference. When the model is uncertain then the intelligent control schemes such as FLC show a better performance. It has been discussed before that the FLC requires expertise knowledge of the process operation of the plant to set the FLC parameters and it works as good as the expertise involved in the design.

To reduce the dependence of the controller on the quality of the expert knowledge, the speed controller can be added to the model following error managing fuzzy adaptive control mechanism in order to compensate this deficiency and reduce the effect of the plant parameters variations. Model reference is an efficient technique to mitigate the effect of parameter variations. The control input signal can be designed to drive the controlled plant for tracking the generated response by the main model [218].

Fuzzy control systems based on model reference can be combined as novel control scheme called a Model Reference Fuzzy Control (MRFC) which has been introduced and discussed by some researchers for various applications. The reference model can be used to appoint the desired performance that fulfils design requirements [219]. The proposed novel controller designed to enable the plant output to be varied to track the reference model output. When parameters external disturbance occur or the system parameters changed, an augmented signal will be setting up automatically by the FLC adaptive mechanism that depends upon the error between model output and the reference output as an input to the controller.

The main components of the system are the reference model, direct fuzzy logic controller (FLC) and model reference signal. In some model design, FLC used with PI controller to give more smoothing to the output signals. The loop of fuzzy logic adaptation can be added

in parallel to the loop of fuzzy control feedback. Normally, the assumption has been made that the following model is linear and the fuzzy controller adaptation loop should be operated in idle case to show the desired performance characteristics of the overall system [215]. The design of classical adaptive control system is applied based on the mathematical modelling and adaptive control based on the gradient algorithm method [220]. When the parameters varied, an adaptive signal generated by adaptation mechanism will be corrected the output of the fuzzy logic controller to keep the desired model following the control output and improve the model performance [221].

Figure 4.5 shows the schematic diagram of MRFC which simulated in this thesis. This method is explained as learning a more global control function with high speed convergence. The reference signal is affected by changing the references values of the fuzzy sets according to the membership function that have been represented in FLC membership functions [222].

The error of the proposed scheme and the changing of error can be measured between the speed of generator and the reference model output which can be applied to a fuzzy logic control. The output signal will force the system to behave like the model by improving the knowledge base of the fuzzy controller or by adding the reference signal to the output of fuzzy controller [223]. The output variables which obtained by the suggested fuzzy logic adaptation technique is used to generate a corrected values of ΔI_q and finally this correction term will added to the FLC output to obtain the set values of currents.

4.5 Simulation and Results

Matlab/Simulink programming environment has been used to demonstrate the effectiveness of the conventional and advanced control system using PI controller, FLC and MRFC respectively.

In most residential areas, offices and some industrial plants, small size wind turbines are more applicable. In addition, the control schemes of small turbines are easy to use

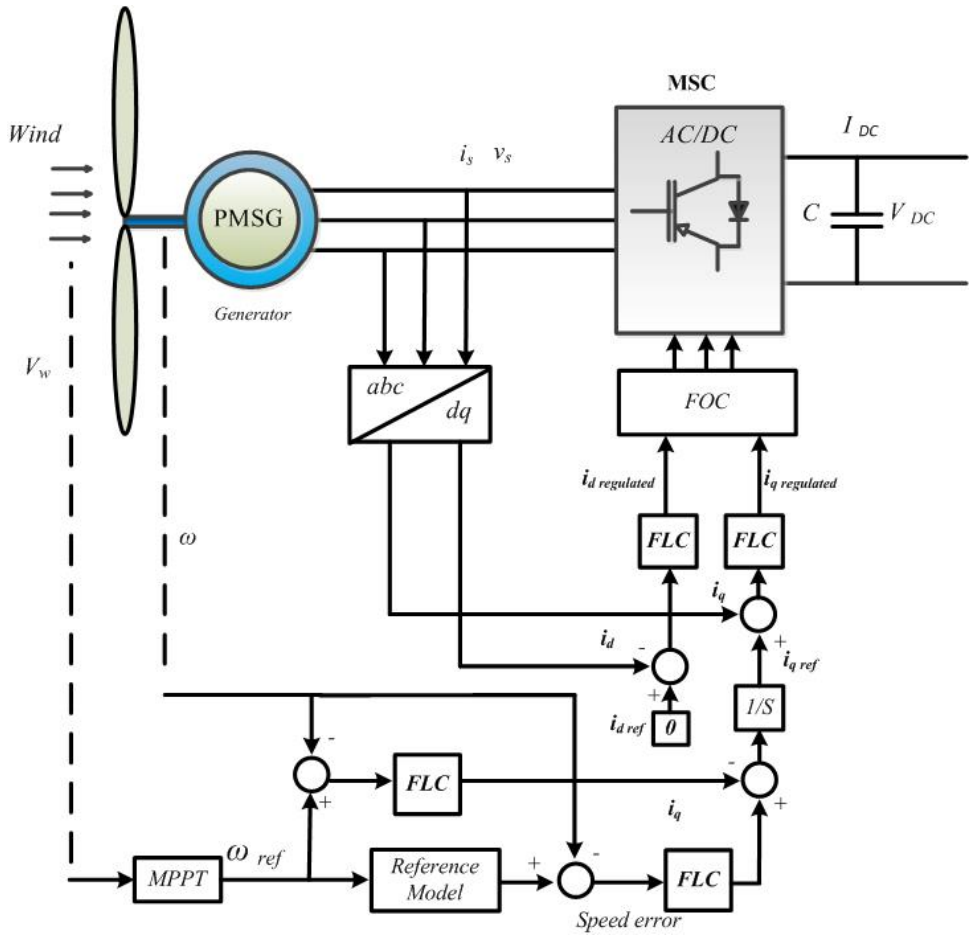

Fig. 4.5 MRFC scheme using FLC with model reference for current variable

and applying the traditional PI controllers. However, most controllers are designed for the purpose of battery charging requirements as well as supplying power to the consumers taking in to account limited range of wind speed variation. To achieve maximum power capturing from the wind and constant output voltage during step change in wind speed, the variation in rotor sped and electromagnetic torque should be controlled to follow the change in wind speed, therefore FLC and MRFC have been used in small size machine and subjected to step change in wind speed to show the behaviour of these controllers compared to the traditional PI controller.

In the MSC, the rotor speed, current and torque have been obtained in all cases for these controller. The parameters of whole system are:

(a) Wind turbine: blade radius $R_o = 2\ m$, inertia $J_{eq} = 10\ kg.m^2$, air density $\rho = 1.2$ $kg/m3$, rated wind speed $V_{w-rated} = 12\ m/s$, cut-in speed $V_{w,cut-in} = 5\ m/s$, and cut-out speed $V_{w,cut-out} = 24\ m/s$.

(b) Parameters of generator: rated power $P_{g-rated} = 6KW$, number of poles pair $p = 4$, stator resistance $Rs = 0.6\ \Omega$, d-axis inductance $L_d = 1.4\ mH$, q-axis inductance $L_q = 2.8$ mH, field flux $\psi = 0.12\ V.s/rad$, rotational damping $D = 0$.

(c) Parameters of power converter: PWM carrier frequency $fp = 5kHz$, rated DC-link voltage $V_{dc-rated} = 300V$, DC-link capacitor $C = 2,000\mu F$.

The simulation results show the effects of controllers during different values of wind speed. The initial conditions of simulation are taken into account in order to operate the system in a stable manner. In MSC the set value of i_d is equal to zero to achieve maximum torque at the minimum current. The DC-link capacitor should be charged to the rated value of DC voltage such that (Vdc = 300V). Figure 4.6 shows the simulation of wind speed with respect to time.

4.5.1 Simulation Using PI Controller

As a result of the variation of wind speed, the rotor speed will be varied when the wind speed changes, then the output generator current also be changed as shown in Figure 4.7. The variation d-axis and q-axis currents are shown in Figure 4.8. This figure shows that the values of q- axis current varied with variation of wind speed whereas d- axis current kept at zero level. The variation in rotor speed will follow the reference speed for as shown in Figure 4.9.

Input mechanical torque and output electromagnetic torque are shown in Figure 4.10. It is notice that there is a difference between two torques due to the friction term ($F\omega_m$) of the swing equation of the machine.

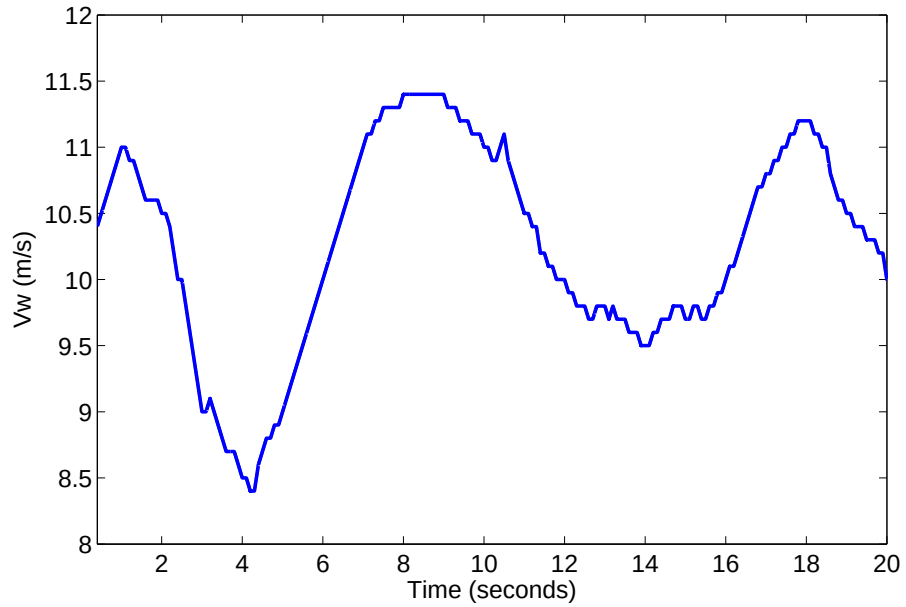

Fig. 4.6 Wind speed variation with respect to time

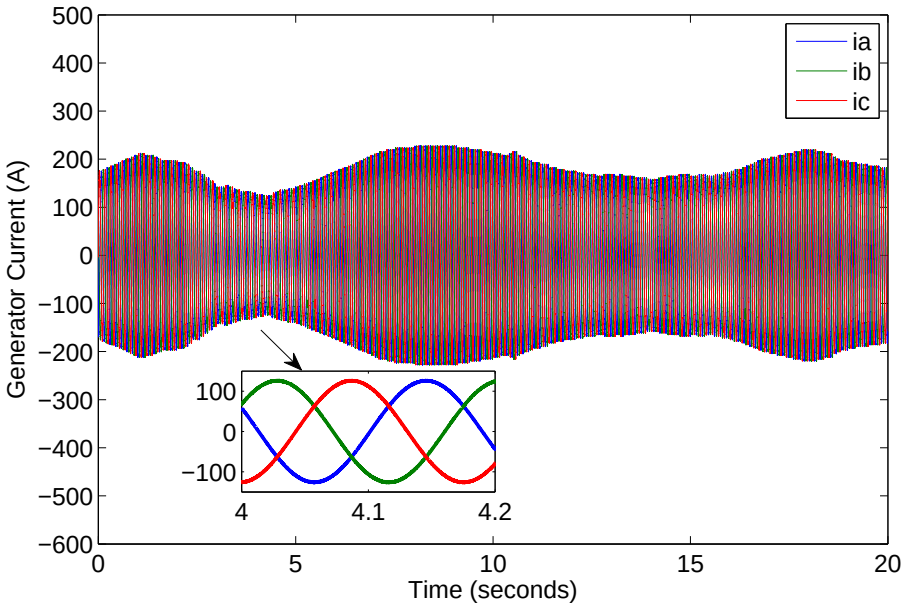

Fig. 4.7 3-phase generator currents applying PI

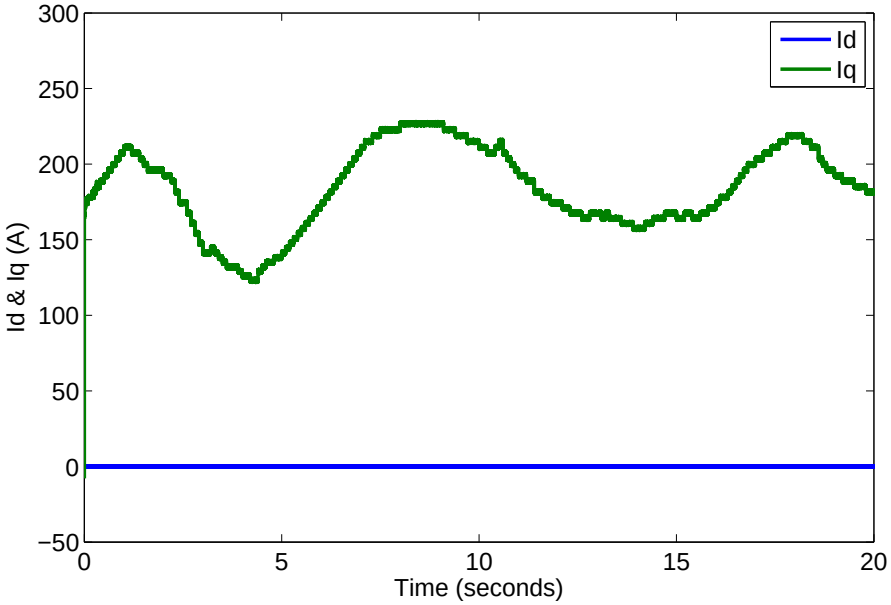

Fig. 4.8 Direct and quadrature axis currents variation applying PI

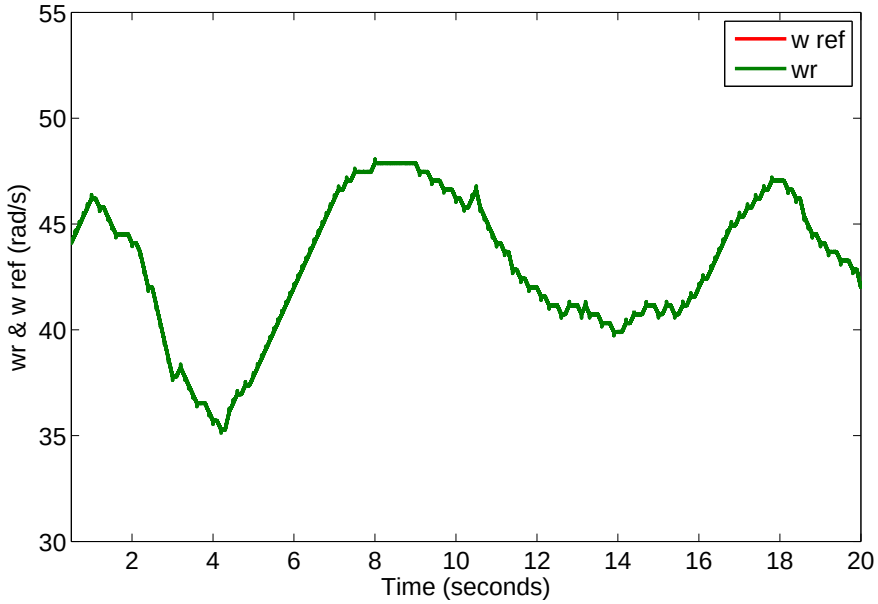

Fig. 4.9 Variation of reference and rotor speeds applying PI

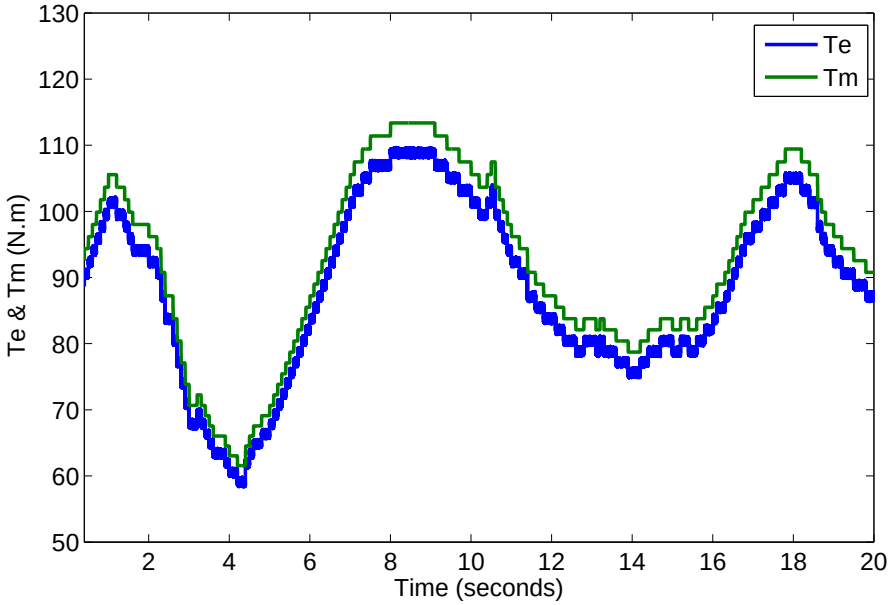

Fig. 4.10 Variation of mechanical and electromagnetic torques applying PI

4.5.2 Simulation Using FLC

The simulation has been used for the design shown in Figure 4.4. FLC model has been test for the same values of variable wind speed as shown in Figure 4.6. Three phase generator current is shown in Figure 4.11 and the d-axis and q-axis currents are shown in Figure 4.12 It is obvious that the values of q- axis current varied with variation of wind speed whereas d- axis kept at zero level. The changed of rotor speed will follow the reference speed for for any variation of wind speed as shown in Figure 4.13. Finally the mechanical torque ans electromagnetic torque are shown in Figure 4.14.

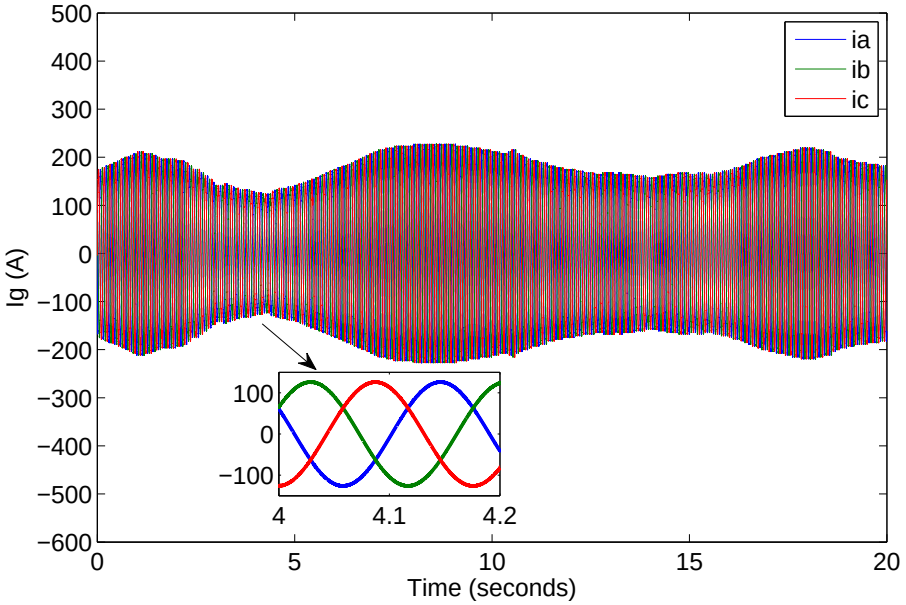

Fig. 4.11 3-phase Generator current variation using FLC

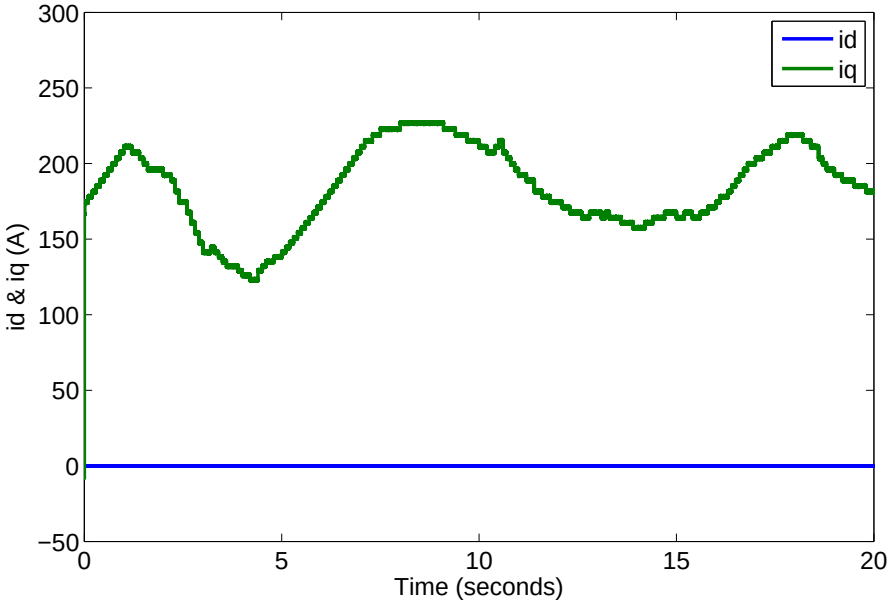

Fig. 4.12 Direct and quadrature axis currents variation using FLC

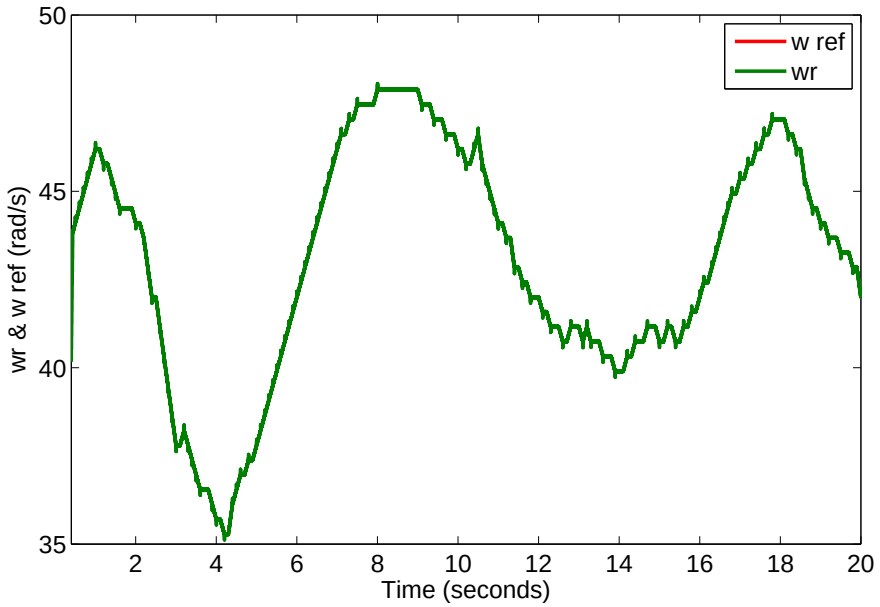

Fig. 4.13 Variation of reference and rotor speeds using FLC

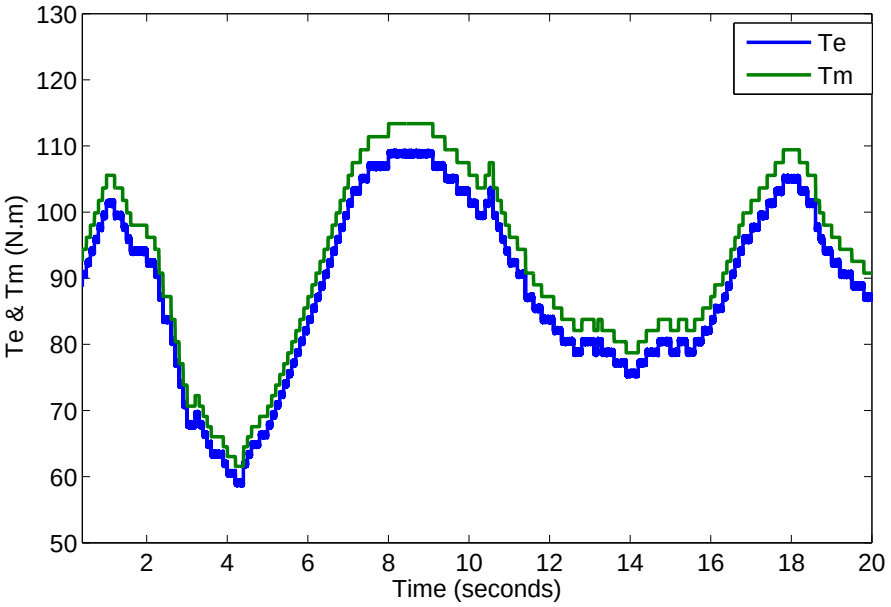

Fig. 4.14 Variation of mechanical and electromagnetic torques using FLC

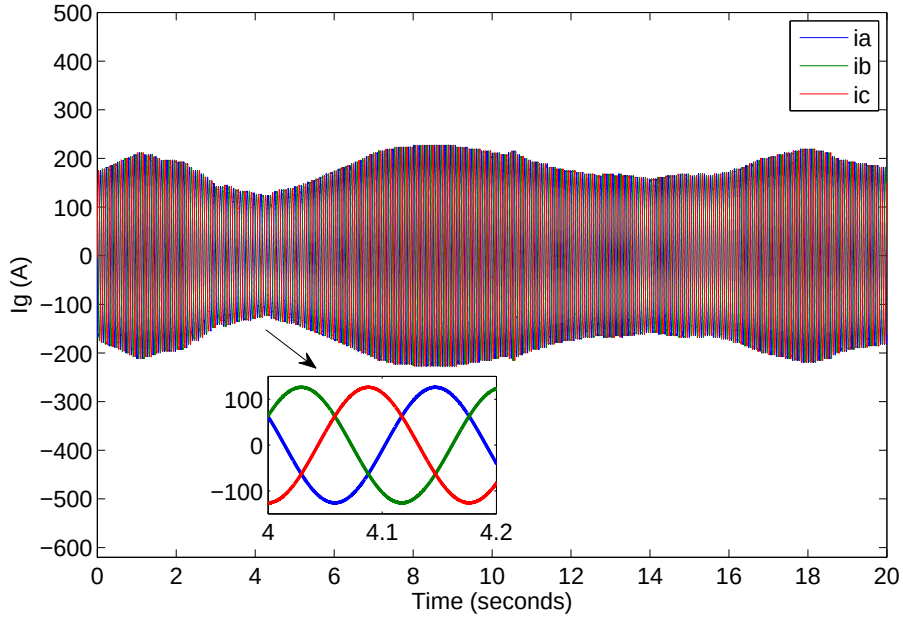

Fig. 4.15 3-phases Generator currents variation using MRFC

4.5.3 Simulation Using MRFC

The simulation has been used for the design shown in Figure 4.5. The MRFC scheme has been test for the same values of variable wind speed as shown in Figure 4.7. Three phases generator currents is shown in Figure 4.15 while the d-axis and q-axis currents are shown in Figure 4.12. It is obvious that the values of q- axis current varied with variation of wind speed. The variation in rotor speed will follow the reference speed for the proposed controller as shown in Figure 4.13. Finally the mechanical torque ans electromagnetic torque are shown in Figure 4.14.

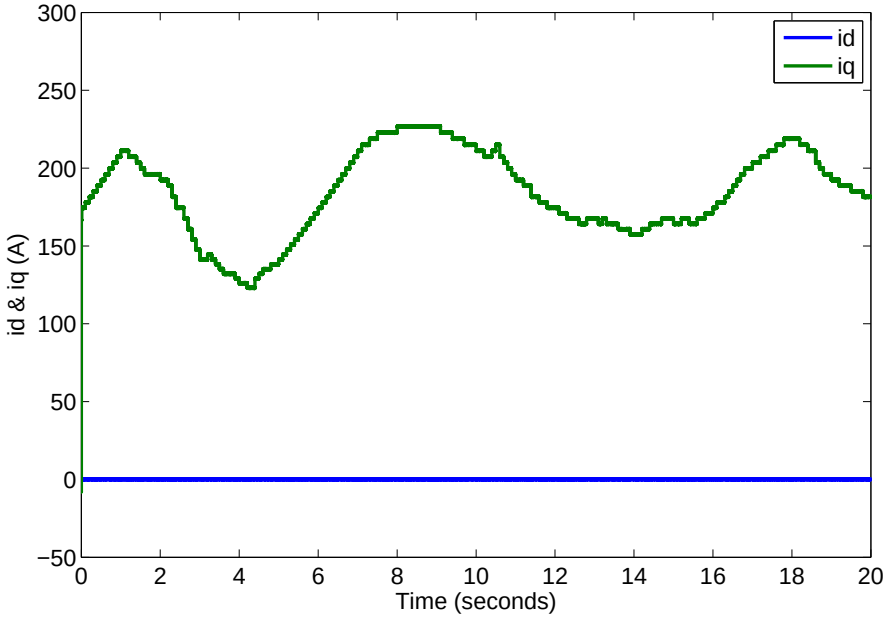

Fig. 4.16 Direct and quadrature axis currents variation using MRFC

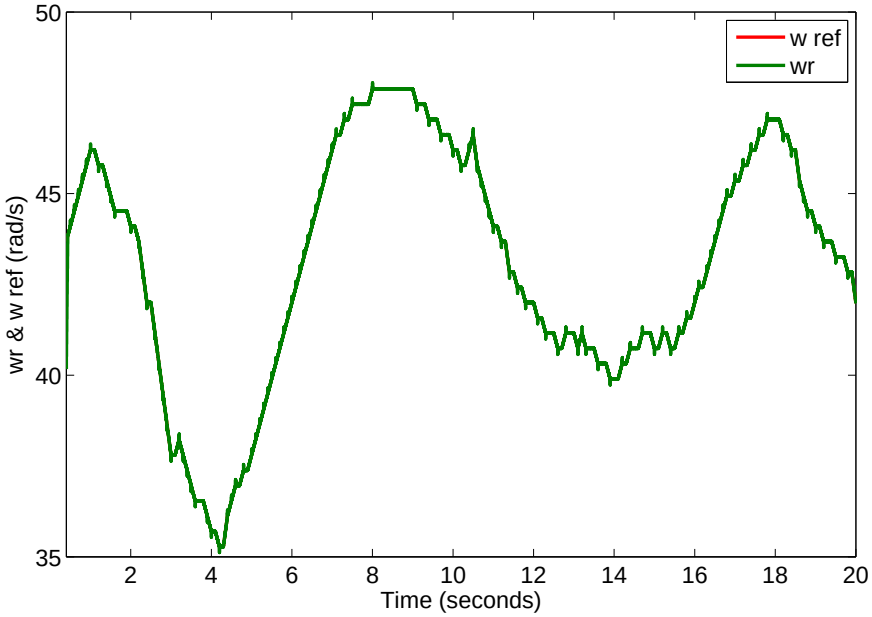

Fig. 4.17 Variation of reference and rotor speeds applying MRFC

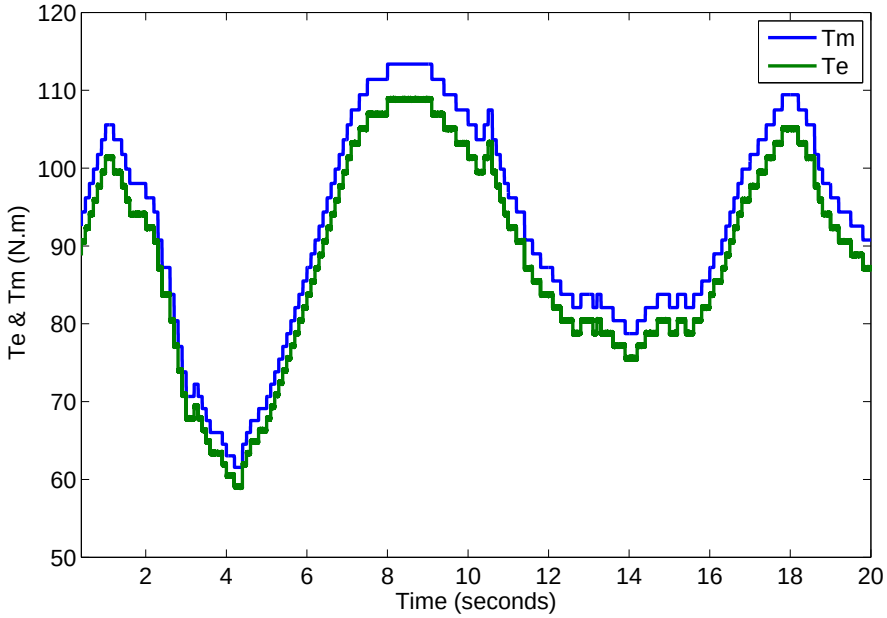

Fig. 4.18 Variation of mechanical and electromechanical torques using MRFC

4.5.4 Comparison Between Controllers

From realistic values of wind speed simulation results, it is shown that the power capturing from the wind is better in case of MRFC compared to FLC and PI controller.

Consequently, the power coefficients are shown in Figure 5.21 of PI controller, FLC and MRFC. It is shown also that the rotor speed error is high in case of PI controller and reduced by using FLC and will be minimum using MRFC.

Compared to PI controller, the difference between of the set value of C_{pref} and actual controlled value of C_p can be expressed:

$$\Delta C_p = C_{pref} - C_p \tag{4.3}$$

It is noticed that the error of power coefficient in case of MRFC is minimum and equal to $3.525e\_5$ compared to FLC which increased in by $3.746e\_5$ and better than PI controller which is $4.136e\_5$. In the same manner, the rotor speed error can be calculated. It is shown

Table 4.2 Standard deviation in variations of the power coefficient and rotor speed

	Delta Cp	**Delta wr**
PI	4.136 e-5	0.0723
FPC	3.746 e-5	0.0654
MRFC	3.525 e-5	0.0614

also that the error of rotor speed in case of MRFC is minimum and equal to 0.0614 compared to FLC which increased in by 0.0654 and better than PI controller which is 0.0723. In the same manner, the rotor speed error can be calculated. The standard deviation of ΔC_p and $\Delta\omega_r$ for all controllers is tabulated in Table 4.2.

From step change simulation results, it is shown that the overshoot of the rotor speeds appears using both PI controller and reduced by using FLC and will be minimum using MRFC. Also it is clear from the results that the oscillation in the rotor speed is reduced when comparing the FLC to the PI controller and reduced by using MRFC.

From the simulation, the absolute errors of rotor speeds for each values are determined. The results show that the steady state error between the original rotor speed and the measured one is (0.015) using PI, then reduced to (0.01) by using FLC and will be minimum as (0.005) by using MRFC. It is shown that the FLC has lower overshoot and errors and minimum in case of MRFC, however, it is noticed that the settling time will be (2.5 ms) and remains constant during the simulations. These results are tabulated in Table 4.3. As a comparison between the three controllers, step change and steady state in rotor speed of the generator is shown in Figure 4.19 and Figure 4.20 for all controllers. It is noticed that the fluctuation in rotor speed will be reduced in case of FLC and more reduction appeared in case of MRFC.

Table 4.3 Calculation of change response for rated rotor speed for different controllers

	Overshoot %	**Settling Time (ms)**	**Error %**
PI	30.7	2.5	1.5
FLC	12.6	2.5	1
MRFC	3.5	2.5	0.5

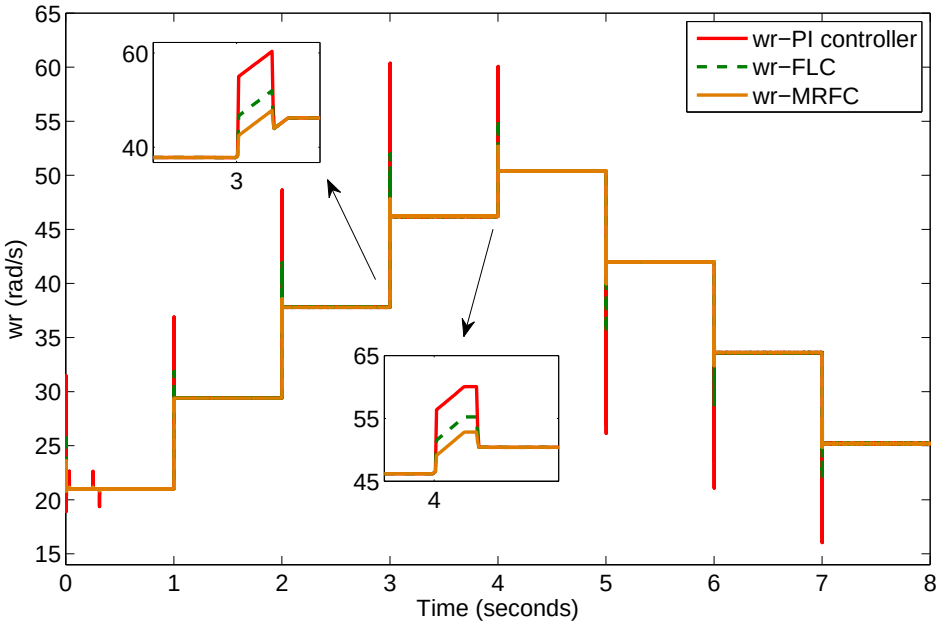

Fig. 4.19 Variation of rotor speed for in case of step change for all controllers

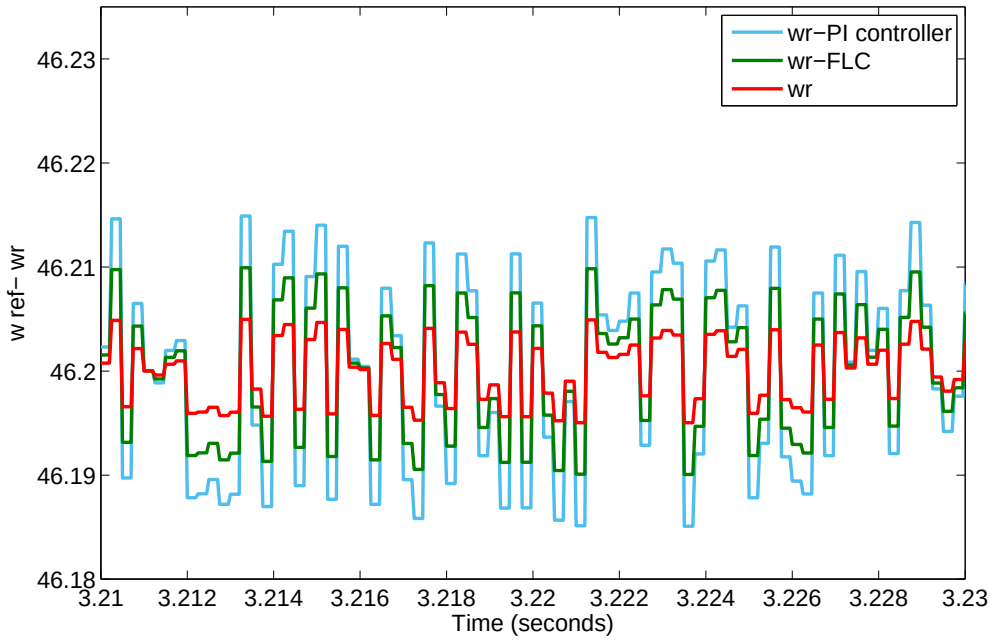

Fig. 4.20 Variation of rotor speed for steady state for all controllers

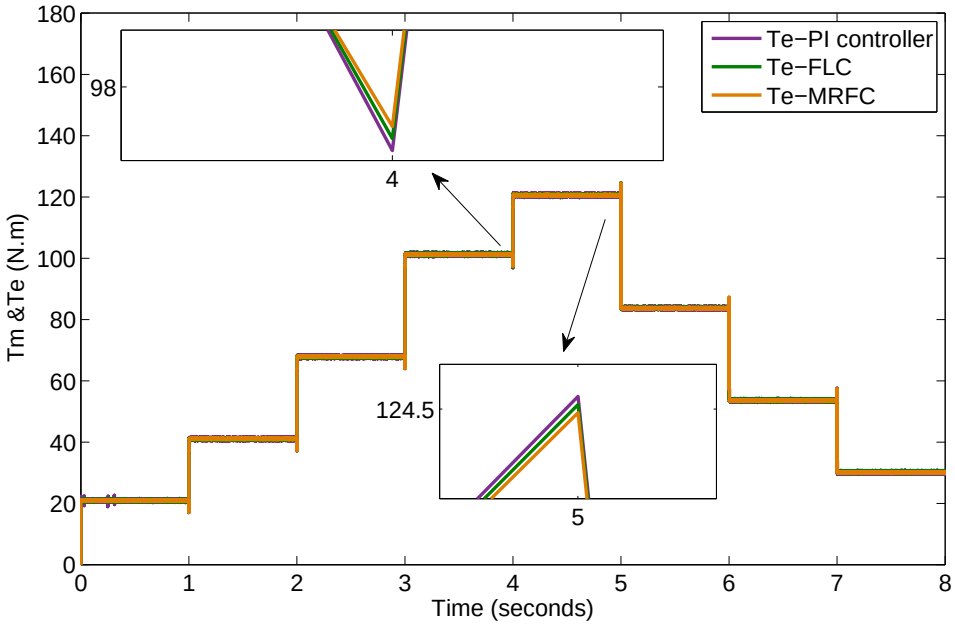

Fig. 4.21 Variation of electromechanical torques in case of step change for all controllers

For the reference rotor speed $\omega_r^* = 46.2\ rad/s$, the values of overshoot, settling time and errors for PI, FLC and MRFC are shown in Table 4.3.

From the torque graphs in Figures 4.10, 4.14 and 4.18 respectively, it is shown that the mechanical and electromagnetic torques are unchanged in certain wind speed for the three types of controllers. For example, at rated wind speed (Vw = 12 m/s) the mechanical torque will be (Tm = 125.63 N.m) and electromagnetic torque (Te = 120.6 N.m) and will be the same in all types of controllers. It is also notice that the settling time = 2.5 ms in all time intervals. These variables are changed due to the improvement of control signals by the relevant controllers as shown in Table 4.4.

An other comparison between the three controllers, the electromagnetic torque of the generator in cases of step change and steady state of wind speed are shown in Figure 4.21 and Figure 4.22 for all controllers. Reduction in the torque is shown in case of FLC compared to PI, and reduced rapidly in case of MRFC.

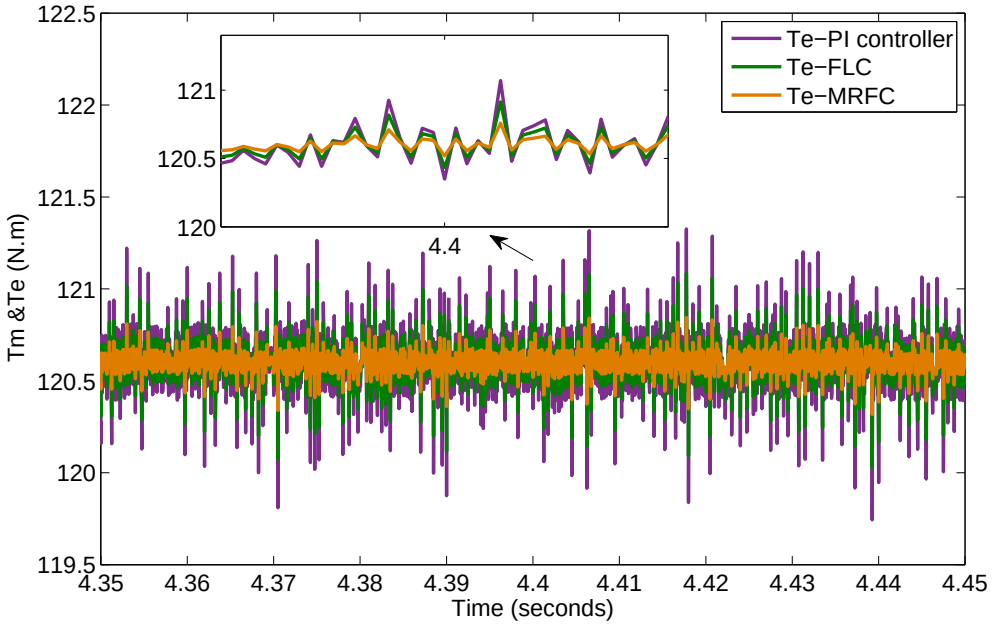

Fig. 4.22 Variation of electromechanical torques in case of steady state for all controllers

Table 4.4 Calculation of torque variation

	Overshoot %	**Settling Time (ms)**	**Error %**	THD %
PI	3.31	2.5	0.75	2.73
FLC	3.25	2.5	0.35	2.75
MRFC	3.19	2.5	0.15	2.43

Finally, the quadrature axis current indicates to the power transferred from the machine to DC link, and can be compared in cases of three controllers as shown in Figure 4.23. The comparison shows the low distortion in current of MRFC compared to other controllers.

It is noticed that the torque error, overshoot and current THD % have minimum values in case of MRFC than other controllers. In FLC, the torque error will be improved with overshoot while the current THD % is approximately the same as PI controller.

The simulation shows that the MRFC scheme as presented in this chapter has a robust performance with regard to wind variation and significantly reduces the overshoot and error in rotor speed when compared to a conventional PI controller and FLC. Reduction in overshoot

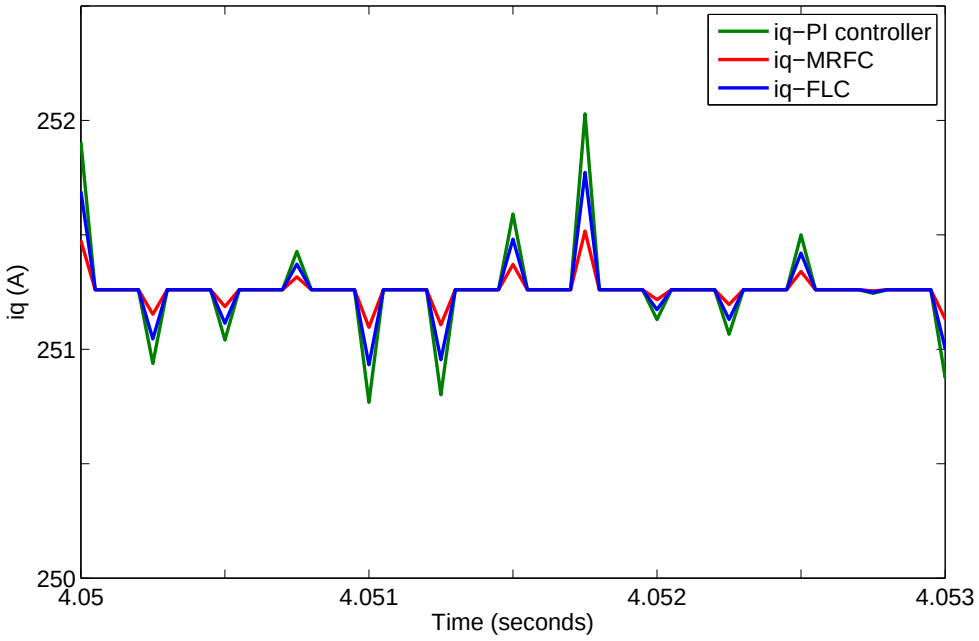

Fig. 4.23 Variation of steady state quadrature axis current for all controllers

and error of rotor speed leads to an increase in the lifetime of the mechanical parts and provides more generator stability in cases of variable wind speeds.

4.6 Summary

This control scheme has been applied to provide FOC for MSC control section. Different types of control schemes have been used in this thesis, traditional control schemes using PI controller and advanced control scheme using direct FLC and adaptive control scheme using Fuzzy MRAC.

The FOC scheme is divided into two loops in MSC, inner and outer loops. The outer loop adjusts the rotor speed to achieve MPPT in order to obtain high efficiency in power capturing from the wind, whilst the inner loop of the scheme controls the dq- axis currents to adjust the control signals of converter voltage as well. The simulation shows that the FLC scheme

as presented in in above sections has a robust performance with regard to wind variation and reduce the overshoot in rotor speed compared to a conventional PI controller. This reduction in overshoot gives more mechanical stability to the generator in case of variable wind speed.

On the other hand the hybrid control scheme uses Fuzzy MRAC has been used in the same model to reduce the dependency of the controller on the plant parameters. The simulation shows a good reduction in overshoot in rotor speed compared to the traditional controller and direct FLC.

Chapter 5

Fuzzy Predictive Control Schemes

Fuzzy Predictive Control scheme is studied in this chapter. Section 5.1 provides a short introduction to beginning of this the fuzzy predictive control. Section 5.2 shows the description of Model predictive Control scheme that can be used as a new modelling in both MSC and GSC control. The suggested analysis is described in Section 5.3. Simulations and results of the evaluation of the proposed approach are reported in section 5.5. Summary of this chapter is given in Section 5.6.

5.1 Introduction

As the manufacturing and wind energy markets have developed, modern robust controllers become more and more necessary in order to follow the grid code requirements and adhere to engineering recommendations. So different types of controllers have been developed and enhanced the wind system in order to achieve several advantages such as, reduction in system losses, size and cost. Combination of FLC with other controllers such as predictive one will form a hybrid control system.

5.2 Model Predictive Controller

A recently developed approach is Model Predictive Control (MPC) that has been introduced as an alternative controller in the power system industry due to a range of advantages [224, 225]. MPC is one of the most effective control techniques for controlling multi-variable systems with limitations. It is also widely used and technically implemented for advanced control schemes in industry for many products and applications [226]. MPC appeared in the 1970s, and since that time it has been developed to convoy the technological evolution and still being widely studied in recent years using different algorithms and approaches to satisfy the purpose [227]. Very good mathematical models to predict the behaviour of the variables under control is growing nowadays leads to growing interest in the use of MPC in this field in both electrical and mechanical systems. As well as this, recent developments of microprocessors which can perform the large amount of calculations needed for different algorithms with high speed performance and reduction in cost enable the designers to implement it in complex devices such as MPC. In general, MPC is a collection of various control methods which use the model of the process to forecast future system dynamics and determine the control inputs according to predicted future state of the system behaviour.

5.2.1 Control Strategy of MPC

MPC is an attractive technique that can influence nonlinear control problems in the system with their constraints quite well [163]. Originally, MPCs have been studied and applied in the process industry and research, where it has been in use for decades [228]. Nowadays, predictive control is being considered in other areas of application, such as control system, power electronics technologies and drives [208], [229, 230, 10]. Predictive control has been demonstrated a wide class of controllers that main characteristic is applying the model of the system for the prediction of the future attitude of the some variables over a specific prediction interval [231].

MPC control strategy uses these information to obtain the mechanism sequence for the system control by optimizing a calculated cost function [232]. It should be noticed that the algorithm is executed for every sampling period and only the first optimized value can be applied to the system at instant k. The cost function can have any form but usually can be defined as:

$$g = \sum_{i=1}^{n} \lambda_i (x_i^* - x_i^p)^2 \tag{5.1}$$

where x_i^* is the reference command and x_i^p is the predicted value for variable x_i, λ_i is a weighting factor and index i indicate to the controlled variables. By this easy way, it is capable to imply variable control objectives such as (multi-variable case) constrains and non-linearities.

5.2.2 MPC Control Principle

The flow chart execution of MPC is shown in Figure 5.1 where an IGBT converter is used to convert DC power to AD grid. The converter presents J different switching states for calculated variables. The control objective pursuits that variable x has to follow the reference x^*. The MPC algorithm has the following basic steps [233]:

1. Measurements and/or estimation of the controlled variables.

2. Computational process of the optimal switching state (computed in the previous sampling interval).

3. Prediction process to know the behaviour of variable x in the next sampling interval x^p for each switching state of the converter, (using the mathematical model).

4. Determination of the cost function, or error between the set and predicted values, for each prediction for instance: $g = |x^* - x^p|$.

5. Minimization of the cost function by selecting the switching state that satisfy minimum value, S_{opt} and re-save it to be used in the converter at the next sampling period.

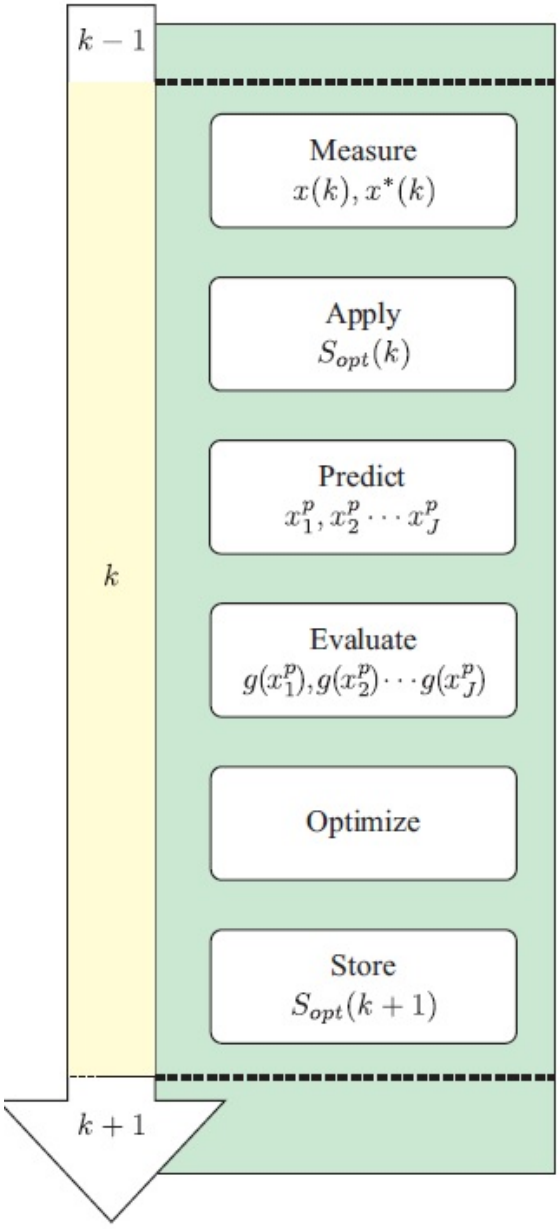

Fig. 5.1 Timing diagram of the execution of the MPC algorithm

5.3 Analysis of Fuzzy Predictive Control

As well as the development in prediction algorithms of variables fulfill the requred calculations, Combination with the smart intelligent control has been proposed to obtain good robustness to the sudden change and uncertainty of these variables [234]. FPC can be formed by a combination of FLC with MPC to obtain hybrid control scheme [235]. The following sections describe the the theoretical analysis of this proposed model and its operation in all parts of the system.

First of all, the design of FOC has been used to design a PI controller as a traditional control scheme in inner and outer circuit of MSC control. As the traditional PI controllers are fixed gain feedback controllers, then they cannot compensate the parameters of K_P and K_I variations in the process. In addition, PI controlled system is less responsive to real and relatively fast change in wind speed.

As a result, modern robust controllers become more and more necessary in order to follow grid code requirements and adhere to engineering recommendations. A recently developed approaches use the intelligent control systems such as FLC to satisfy the proper behaviour and operation of the system [13]. FLC system technique is capable to improve the tracking performance as compared to traditional control system for both grid or load connected in cases of linear or non-linear load.

To obtain fast response of the output signal, the combination of FLC system controller with MPC forms a hybrid control system called Fuzzy Predictive Control (FPC) where minimization of overshoot and settling time can be achieved [236].

The schematic diagram of FLC system that used is shown in Figure 5.2. From the principles that have been discussed in Chapter 4, input and output variables are determined. The two inputs variables of the system are the error e and change of error Δe. The behaviour of a FLC depends on the shape of membership functions of the rule base [213].

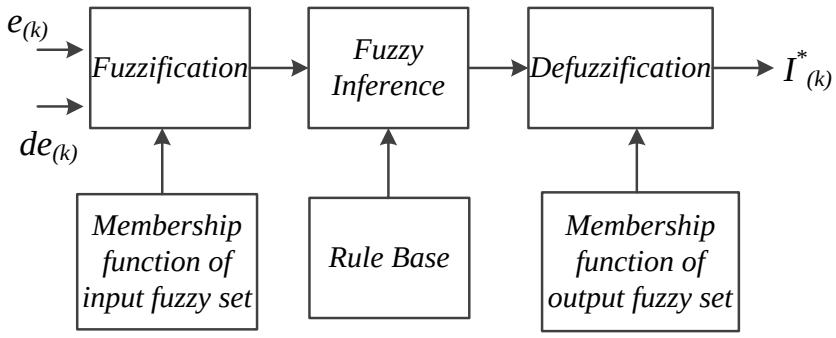

Fig. 5.2 Structure of Fuzzy Logic Controller

In this section, the design of FPC scheme depends upon the output of the FLC. Therefore, the output should be the reference value of i_q that will be an input to MPC.

The membership function values are assigned to the linguistic variables using seven fuzzy subset called: Negative Big (NB), Negative Small (NS), Zero(Z), Positive Small (PS) and Positive Big (PB).

The signals e and Δe are selected as an inputs to FLC in all cases as shown in Figure 5.3, while the output values of $i_{sq}(k)$ is the outputs of the the FLC as shown in Figure 5.4. In MSC, the signal e is the error between the reference current signals i^*_{sd} and i^*_{sq} and actual current signal of the system for both d and q circuits as mentioned in equations (5.18) and (5.19) respectively, Δe is the change in error in a sampling period of time.

In the same manner described in Chapter 4, the fuzzified inputs are fed to the interface engine which is mainly consists of fuzzy rule base and fuzzy implication sub blocks. In this

Table 5.1 Rule base table of the Fuzzy Controller

e \de	**NB**	**NS**	**Z**	**PS**	**PB**
NB	*NB*	*NB*	*NS*	*NS*	*Z*
NS	*NB*	*NS*	*NS*	*Z*	*PS*
Z	*NS*	*NS*	*Z*	*PS*	*PS*
PS	*NS*	*Z*	*PS*	*PS*	*PB*
PB	*Z*	*PS*	*PS*	*PB*	*PB*

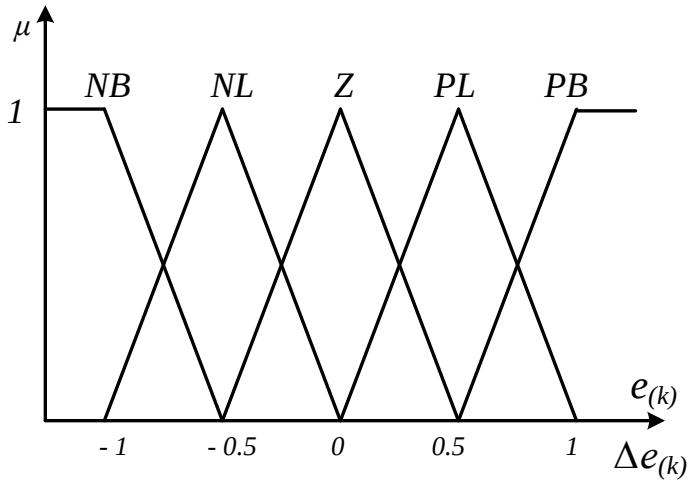

Fig. 5.3 Membership Function of FLC for the input variables

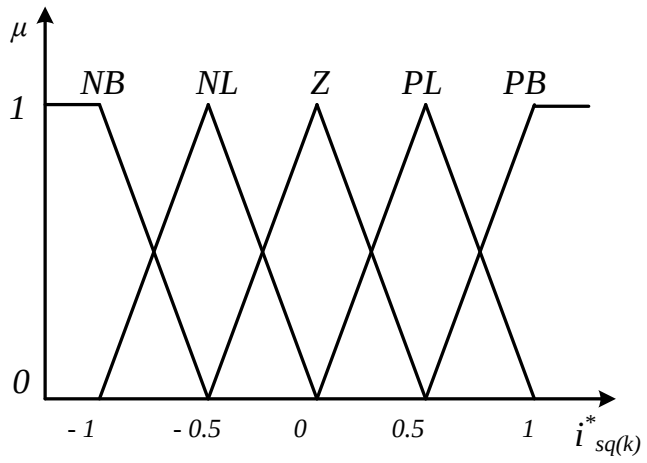

Fig. 5.4 Membership Function of FLC for the output variables

stage the rule base is applied to get the output fuzzy set which is finally identified using fuzzy implication method.

There are different methods that are used in the inference process such as max-min implication technique. Rules of the interface fuzzy memory which related to the proposed system are shown in Table 5.1.

In case the fuzzification process is over, output fuzzy range is located. On this stage defuzzification process is needed to convert to non-fuzzy value of control signal. Centroid defuzzification method is used to reverse the fuzzification process in the proposed solution of the signals.

5.4 Structure of the Proposed Technique

A good performance of FLC enable designers to use it in diversified hybrid system combined with neural network, genetic algorithm, adaptive and predictive controls to improve the output performance during uncertainty parameters of the system.

FPC system can manage the system model during controlling the output currents of both generator and grid. In this system two controllers have been used to perform the suggested algorithm, MSC and GSC. These controllers will be discussed in the following paragraphs.

5.4.1 Machine Side Control System

The Fuzzy predictive control of machine side is shown in Figure 5.5. The cascaded control loop has been used to control currents and speed of the machine. This can be divided to internal loop for currents and external loop for speed. The external speed loop can be controlled by traditional PI control to adjust the set value of rotor speed [237, 13]. Conversely, an internal control loop will operate to control the stator currents in the dq synchronous reference axis. Maximum torque at the minimum current can be obtained by adjusting d axis

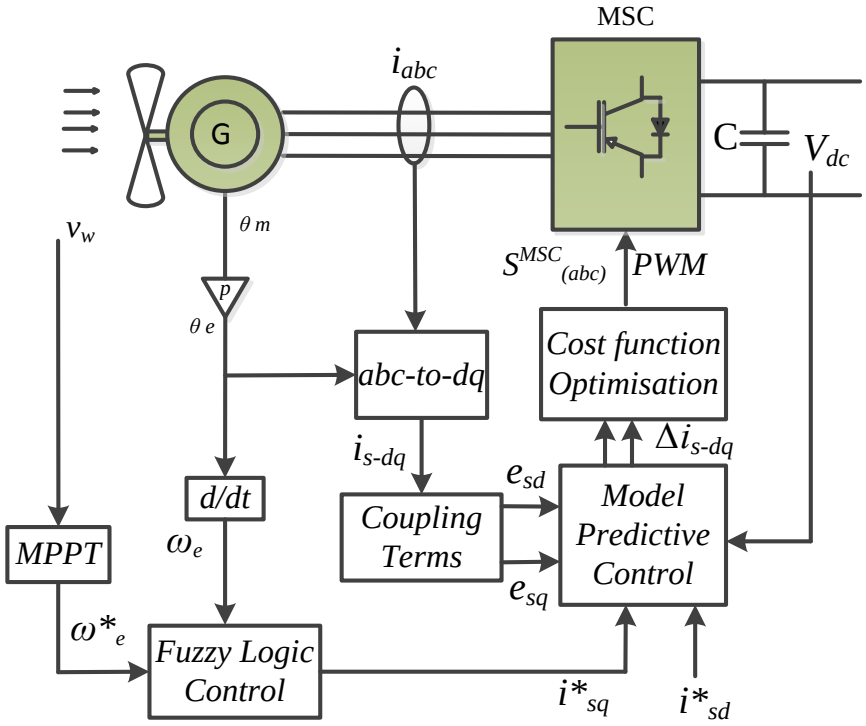

Fig. 5.5 FPC - MSC Schematic Diagram for the Machine Side

stator current reference i^*_{sd} to zero. The other current of the q axis stator current reference i^*_{sq} is computed via the outer loop of speed control loop.

5.4.1.1 Generator Current Loop Prediction Control

In order to obtain the digital predictive current controller algorithm the dq axis currents, the generator equations (3.43) and (3.44) can be rewritten as in equations (5.2) and (5.3) respectively:

$$\frac{di_{sd}}{dt} = \frac{1}{L_{sd}}(V_{sd} - R_s i_{sd} + \omega_{dq} L_{sq} i_{sq}) \tag{5.2}$$

$$\frac{di_{sq}}{dt} = \frac{1}{L_{sq}}(V_{sq} - R_s i_{sq} - \omega_{dq} L_{sq} i_{sd} + \omega_{dq} psi_f) \tag{5.3}$$

From the equations (5.2) and (5.3), using the forward Euler discretization method, the following prediction equations can be obtained:

$$i_{sd}[k+1] = \frac{T_s}{L_{sd}}(V_{sd}[k] - e_{sd}[k]) + (1 - \frac{T_s}{T_{sd}})i_{sd}[k] \tag{5.4}$$

$$i_{sq}[k+1] = \frac{T_s}{L_{sq}}(V_{sq}[k] - e_{sq}[k]) + (1 - \frac{T_s}{T_{sq}})i_{sq}[k] \tag{5.5}$$

where Ts is the sampling period. $i_{sd}[k+1]$ and $i_{sq}[k+1]$ are the predicted values of d and q stator current at the $(k+1)$ th sampling period. $i_{sd}[k]$ and $i_{sq}[k]$ are measured d and q stator current components during kth sampling period, $T_{sd} = L_{sd}/R_s$ and $T_{sq} = L_{sq}/R_s$ are time constant of d and q circuit respectively. The e_{sd} and e_{sq} terms refer to the d and q coupling terms and can be expressed in equations (5.6) and (5.7):

$$e_{sd}[k] = -L_{sq}\omega_{dq}[k]i_{sq}[k] \tag{5.6}$$

$$e_{sq}[k] = L_{sd}\omega_{dq}[k]i_{sd}[k] + \omega_{dq}[k]\phi_{rd}[k] \tag{5.7}$$

The growth of the d and q stator current values depends upon the applied stator voltage values $V_{sd}^{j}[k]$ and $V_{sq}^{j}[k]$ which have been determined at the k th sampling period. The values of these stator voltage can be expressed in the dq synchronous reference axis and can be estimated through the rotational angle equal to (θ_{dq}) to the $\alpha\beta$ components of the stator vectors of all voltages as shown in the equation (5.8) and Table 5.2.

$$\begin{bmatrix} V_{sd}^{j}[k] \\ V_{sq}^{j}[k] \end{bmatrix} = \begin{bmatrix} cos(\theta_{dq}[k]) & sin(\theta_{dq}[k]) \\ -sin(\theta_{dq}[k]) & cos(\theta_{dq}[k]) \end{bmatrix} \begin{bmatrix} V_{s\alpha}^{j}[k] \\ V_{s\beta}^{j}[k \end{bmatrix} \tag{5.8}$$

Taking in to account the eight switching states combinations of the MSC with two combinations V_0 and V_7 that lead to null stator voltage vector, then equations (5.4) and (5.5)

Table 5.2 Switching states and corresponding output voltages $V^{j}_{sdq(j=0...7)}$

Sa	**Sb**	**Sc**	$\mathbf{V}^{j}_{s\alpha}$	$\mathbf{V}^{j}_{s\beta}$	$\mathbf{V}_{j}$	$\mathbf{V}^{j}_{sdq}$
0	0	0	0	0	V_0	V^0_{dq}
1	0	0	$2V_{dc}/3$	0	V_1	V^1_{dq}
1	1	0	$V_{dc}/3$	$Vdc/\sqrt{3}$	V_2	V^2_{dq}
0	1	0	$-V_{dc}/3$	$Vdc/\sqrt{3}$	V_3	V^3_{dq}
0	1	1	$-2V_{dc}/3$	0	V_4	V^4_{dq}
0	0	1	$-V_{dc}/3$	$-Vdc/\sqrt{3}$	V_5	V^5_{dq}
1	0	1	$V_{dc}/3$	$-Vdc/\sqrt{3}$	V_6	V^6_{dq}
1	1	1	0	0	V_7	V^7_{dq}

can be represented for the different possibilities of the d and q stator voltage components space vector modulation $V^{j}_{sd}[k]$ and $V^{j}_{sq}[k]$ as shown in equations (5.9) and (5.10) respectively.

$$i^{j}_{sd}[k+1] = \frac{T_s}{L_{sd}}(V^{j}_{sd}[k] - e_{sd}[k]) + (1 - \frac{T_s}{T_{sd}})i_{sd}[k]_{(j=0...7)} \tag{5.9}$$

$$i^{j}_{sq}[k+1] = \frac{T_s}{L_{sq}}(V^{j}_{sq}[k] - e_{sq}[k]) + (1 - \frac{T_s}{T_{sq}})i_{sq}[k]_{(j=0...7)} \tag{5.10}$$

Consequently, it is able to predict the values of dq stator vector components $(\Delta i^{j}_{sd}[k+1])$ and $(\Delta i^{j}_{sq}[k+1])$ for all values of $(j = 0...7)$. The current errors are defined as the difference between the reference stator currents vectors $i^{*}_{sd}[k]$, $i^{*}_{sq}[k]$ during the k th sampling period of time and the predicted one at the $(k+1)$ th sampling period of time. These errors can be expressed as [238, 239]:

$$\Delta i^{j}_{sd}[k+1] = i^{*}_{sd}[k] - i^{j}_{sd}[k+1] \tag{5.11}$$

$$\Delta i^{j}_{sq}[k+1] = i^{*}_{sq}[k] - i^{j}_{sq}[k+1] \tag{5.12}$$

The errors estimated for all sectors values of $(j = 0...7)$. According to equations (5.11) and (5.12), a cost function g^{j} is applied to the obtained stator current error components. This cost function can be expressed in (5.13):

$$g^{j} = |\Delta i^{j}_{sd}[k+1]| + |\Delta i^{j}_{sq}[k+1]| \tag{5.13}$$

Finally, the selection of the optimal switching states combination $S(a,b,c)^{opt}$ can be obtained that leads to the minimal cost function $Min(g^j)$ for all values of $j = 0...7$.

5.4.1.2 Speed control loop

The block diagram of the outer loop of speed controller has been built as FLC system. The reference stator currents vectors $i^*_{sq}[k]$ during the k th sampling period of time can be determined by FLC which performs the adjusting process of the reference current as discussed in [240]. Input and output membership functions are shown in Figures 5.3 and 5.4 respectively.

5.4.2 Grid Side Control System

The MPC for the grid side is shown in Figure 5.6. A cascade control loops have been used, and a PI controller controls the dc link voltage V_{dc} in external loop. The main internal control loop an MPC based controls the currents of grid in the dq synchronous reference frame, where the d axis should be linked to the grid voltage vector. The q axis grid current reference i^*_{gq} is adjusted to be zero in order to satisfy a unity power factor and maximum power, whereas the d axis grid current referencei^*_{gd} is adjusted by the PI controller of the outer loop to control the dc-link voltage taking in to account that the primarily objective of the GSC to use both MPC or FPC algorithms is to control the active and reactive powers through the control of the d axis and q axis grid current components. Therefore both algorithms are predicting the values of grid currents [241–243].

5.4.2.1 Grid Current Loop Prediction Control

In the same manner that used in MSC, the current of GSC can be controlled by adjusting the predicted vales of d and q grid current components. During each sampling period, the evolution of the d and q grid current components depends on the applied converter voltage

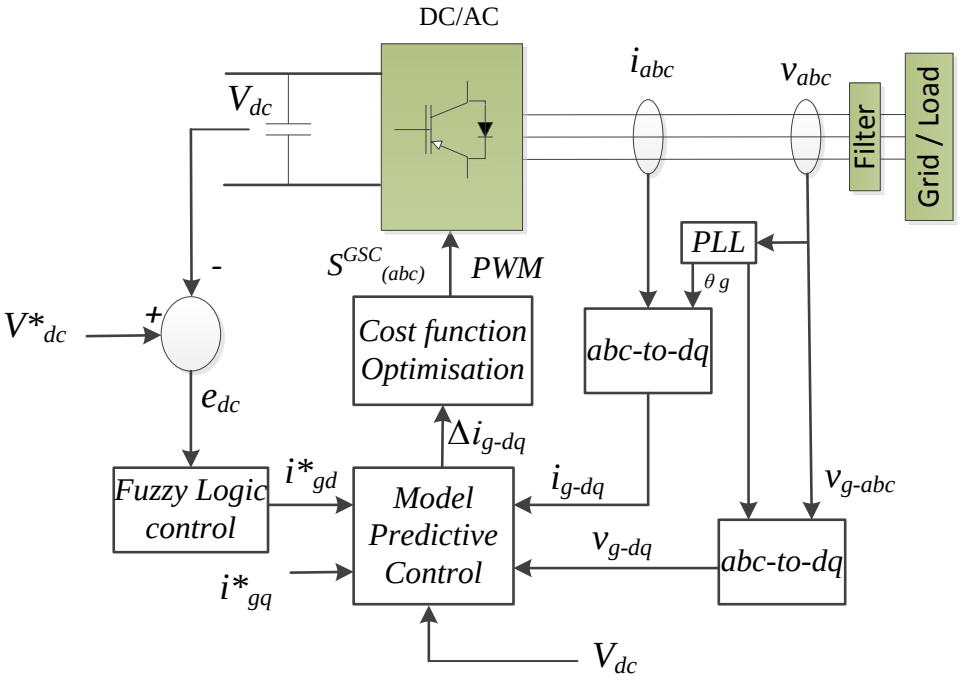

Fig. 5.6 FPC - GSC for the Grid Side

components $V_{conv_d}[k]$ and $V_{conv_q}[k]$ at the k^{th} sampling period. It is obvious that the voltage vectors $V_{conv_d}[k]$ and $V_{conv_q}[k]$ depend also on the dc-link voltage V_{dc} level using Park and Clarke transformation as in the following equations [244]:

$$\begin{bmatrix} V^j_{con-d}[k] \\ V^j_{con-q}[k] \end{bmatrix} = \begin{bmatrix} cos(\theta_{dq}[k] & sin(\theta_{dq}[k] \\ -sin(\theta_{dq}[k] & cos(\theta_{dq}[k] \end{bmatrix} \begin{bmatrix} V^j_{con-\alpha}[k] \\ V^j_{con-\beta}[k \end{bmatrix} \tag{5.14}$$

$$\begin{bmatrix} V^j_{con-\alpha}[k] \\ V^j_{con-\beta}[k] \end{bmatrix} = \frac{2}{3} V^*_{dc} \begin{bmatrix} 1 & -\frac{1}{2} & -\frac{1}{2} \\ 0 & \frac{\sqrt{3}}{2} & -\frac{\sqrt{3}}{2} \end{bmatrix} \begin{bmatrix} S_{ia}[k] \\ S_{ib}[k] \\ S_{ic}[k] \end{bmatrix} \tag{5.15}$$

where $V^{j}_{con-d}[k]$ and $V^{j}_{con-q}[k]$ are voltage vectors of d and q axis component, and $V^{j}_{con-\alpha}[k]$, $V^{j}_{con-\beta}[k]$ are the output converter voltage vectors in the stationary values of $\alpha$and β axis, and $S_{ia}[k], S_{ib}[k], S_{ic}[k]$ are the switching signals of the controller. Then, the forward Euler discretization method can be used to adjust the predictive values of currents as:

$$i^{j}_{gd}[k+1] = a_0[(V_{gd}[k] - V^{j}_{con-d}[k])] + a_1 i_{gd}[k]) \tag{5.16}$$

$$i^{j}_{gq}[k+1] = a_0[(V_{gq}[k] - V^{j}_{con-q}[k])] + a_1 i_{sq}[k]) \tag{5.17}$$

where a_0 is T_s/L_g and a_1 is $(1 - R_g.T_s/L_g)$.

The prediction process will give the predicted values of currents which will be manage the controller to find the values of signal voltages.

In the same sequence of analysis in MSC, it is possible to firstly predict the dq grid current error vector components $(\Delta i^{j}_{gd}[k+1])_{(j=0...7)}$ and $(\Delta i^{j}_{gq}[k+1])_{(j=0...7)}$ as shown in equations(5.18) and (5.19) :

$$\Delta i^{j}_{gd}[k+1] = i^{*}_{gd}[k] - i^{j}_{gd}[k+1]_{(j=0...7)} \tag{5.18}$$

$$\Delta i^{j}_{gq}[k+1] = i^{*}_{gq}[k] - i^{j}_{gq}[k+1]_{(j=0...7)} \tag{5.19}$$

Finally, the This cost function can be defined in equation:

$$g^{j} = |\Delta i^{j}_{gd}[k+1]| + |\Delta i^{j}_{gq}[k+1]| \tag{5.20}$$

Minimisation of the cost function can be achieved by selection the optimal values of the above switching signals considering that the applied switching signals during the previous sampling period so that the switching frequency is minimised.

5.4.2.2 DC voltage Control Loop

The DC link voltage equation can be expressed as a function of the voltage across the capacitor as shown in Figure 5.6. As discussed in MSC, the current can be controlled by adjusting the reference vales of d and q grid current components using FLC. The task of FLC is to obtain the reference value of $i^*_{sd}[k]$ to be as an input of MPC. In the same time $i^*_{sq}[k]$ is equal to zero to inject active power to the grid.

5.5 Simulation of the Proposed Controller

In this chapter, modelling of variable speed wind turbine PMSG connected to the grid through BTB will be discussed. The proposed control of FPC will be used in the design of the MSC control and GSC control. MATLAB/Simulink environment tool to show the effect of the proposed model of FPC. The input to the system is variable wind speed. To compare the proposed controller with the previous work of CH-3, the same parameters of WECS have been taken for whole system as shown:

(a) Wind turbine: blade radius $R_o = 39$ m, inertia $J_{eq} = 10,000\ kg.m^2$, air density $\rho = 1.205\ kg/m3$, rated wind speed $V_{w-rated} = 11.4\ m/s$, cut-in speed $V_{w,cut-in} = 5m/s$, and cut-out speed $V_{w,cut-out} = 24m/s$.

(b) Parameters of generator: rated power $P_{g-rated} = 2MW$, number of poles pair $p = 11$, stator resistance $Ra = 50\ \mu\Omega$, d-axis inductance $L_d = 0.0055\ H$ q-axis inductance $L_q = 0.00375\ H$, field flux $\psi = 135.25\ V.s/rad$, rotational damping $D = 0$.

(c) Parameters of power converter: PWM carrier frequency $fp = 10kHz$, rated DC-link voltage $V_{dc-rated} = 7.1kV$, DC-link capacitor $C = 15,000\mu F$.

(d) Parameters of PI Control schemes: MSC: speed loop controller $K_p = 33$, $K_I = 100$, current loop $K_p = 100$, $K_I = 5$. GSC: DC voltage loop controller $K_p = 2$, $K_I = 70$, current loop $K_p = 100$, $K_I = 10$.

The simulation shows that the effect of the controller during different values of wind speed. Some initial condition of simulation should be taken in to account to operate the system fairly.

5.5.1 Machine Side Converter Simulations

In MSC the set value of i_d is equal to zero to achieve Maximum torque at the minimum current.

The dc-link capacitor should be charged to rated value of dc voltage (V_{dc} = 7.1 kV). In GSC the set value of i_q is equal to zero to ensure a unity power factor. Mechanical power of wind turbine will be an input to the generator. Figure 5.7 shows the variation of wind speed with respect to time. As shown in Figure 5.8, the generator speed will be varied when the wind speed change, then the output generator current also be changed as shown in Figure 5.10. As a result to this variation, the generator speed will be varied when the wind speed changed as shown in Figure 5.8. The difference between mechanical and electromagnetic torque is approximately negligible as shown in Figure 5.9, while the output generator current also changed with the variation of the wind as shown in Figure 5.10.

The DC link voltage will be kept constant by the GSC to insure the constancy of output voltage. Figure 5.11 shows the measured and set values of V_{dc}.

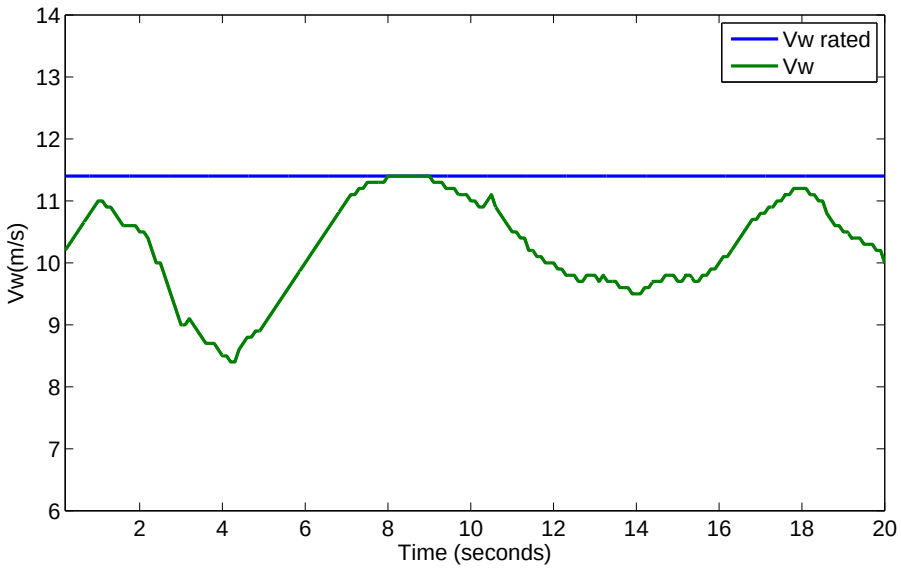

Fig. 5.7 Variation of wind speed

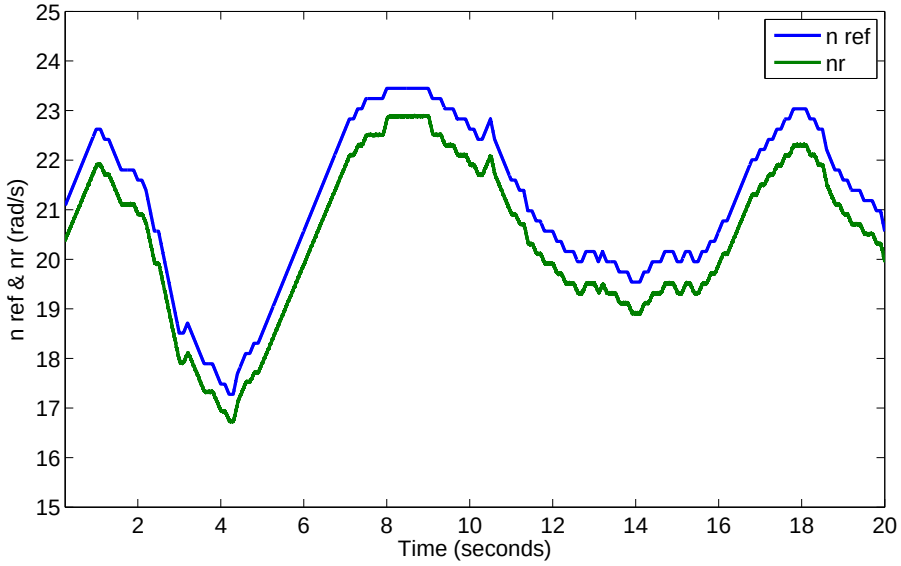

Fig. 5.8 Variation of the generator speed

5.5.2 Grid Side Converter Simulations

The DC link voltage will be imposed to be constant by the controller of GSC as shown in Figure 5.11, then output grid voltage will be fixed and in phase with grid current as shown in

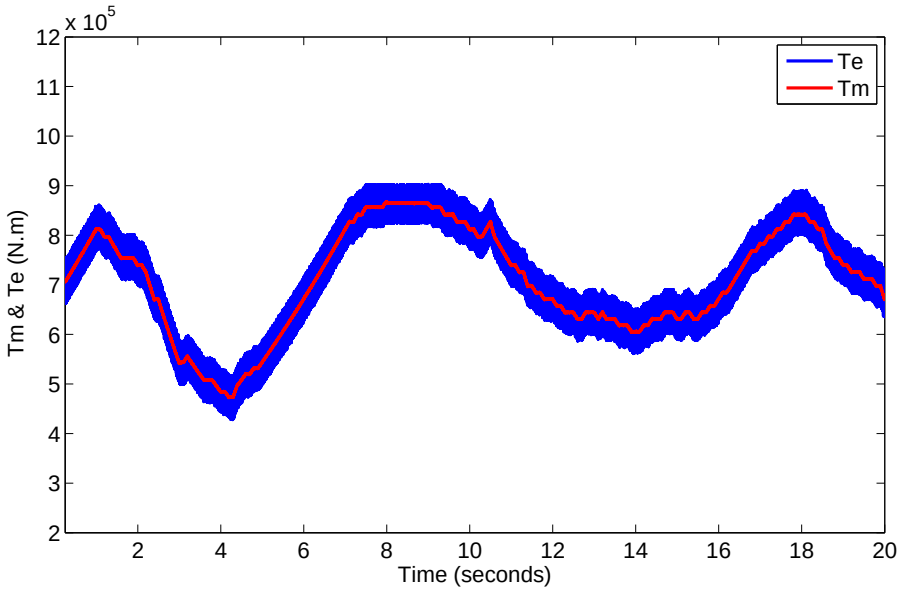

Fig. 5.9 Variation of mechanical torque and electromagnetic torque

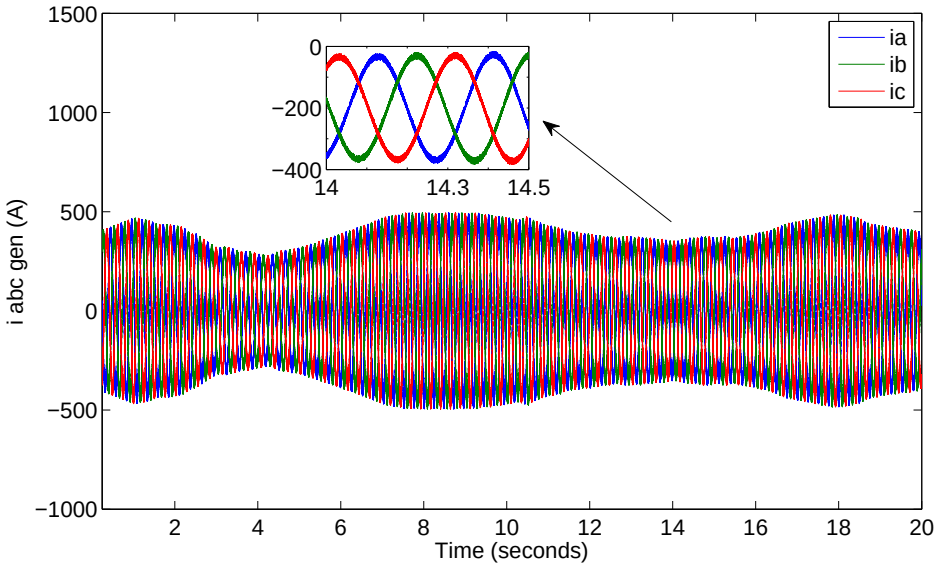

Fig. 5.10 Variation of the generator currents

Figure 5.12. Normal oscillation of grid frequency within acceptable limit is shown in Figure 5.14. Since the controller is designed to inject active power, injected reactive power will be

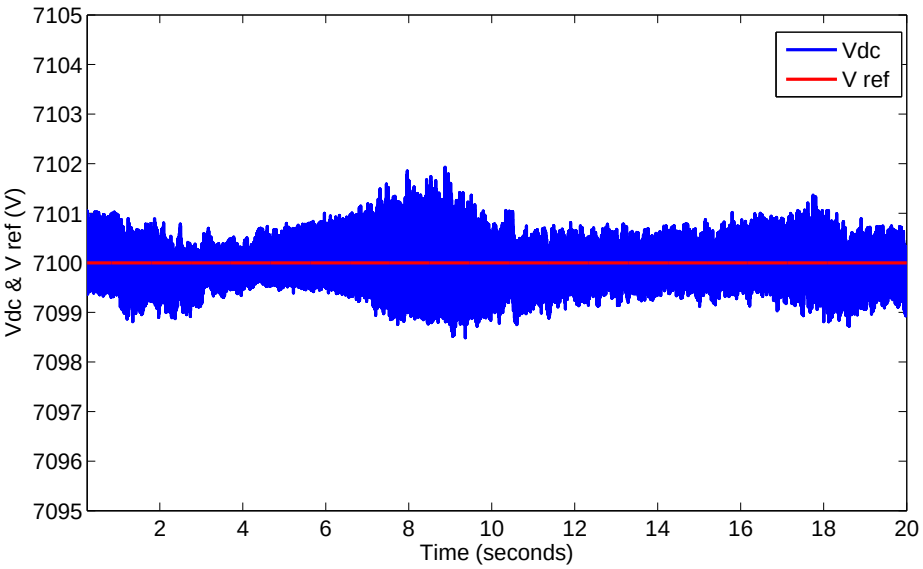

Fig. 5.11 Variation of DC link voltage

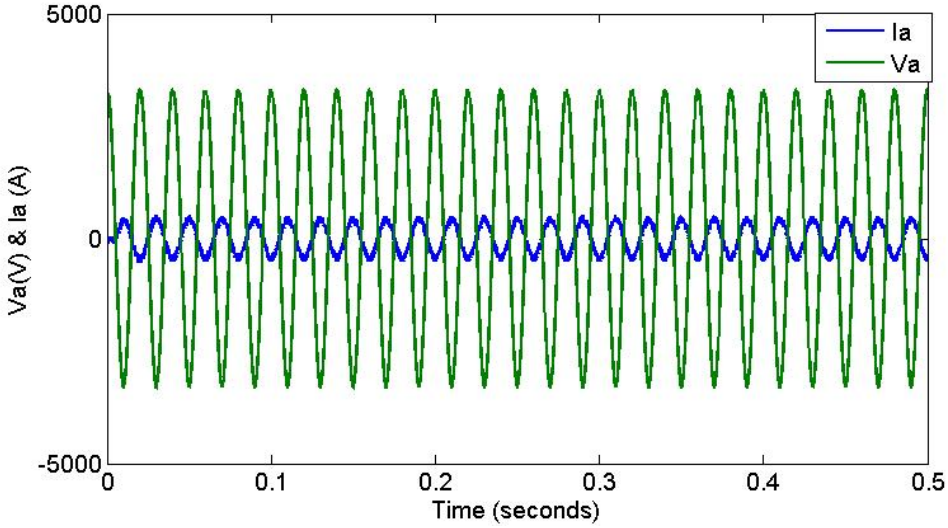

Fig. 5.12 Variation of grid voltage and current for a specific period of time

within zero value during the simulation. The active and reactive powers are shown in Figure 5.15.

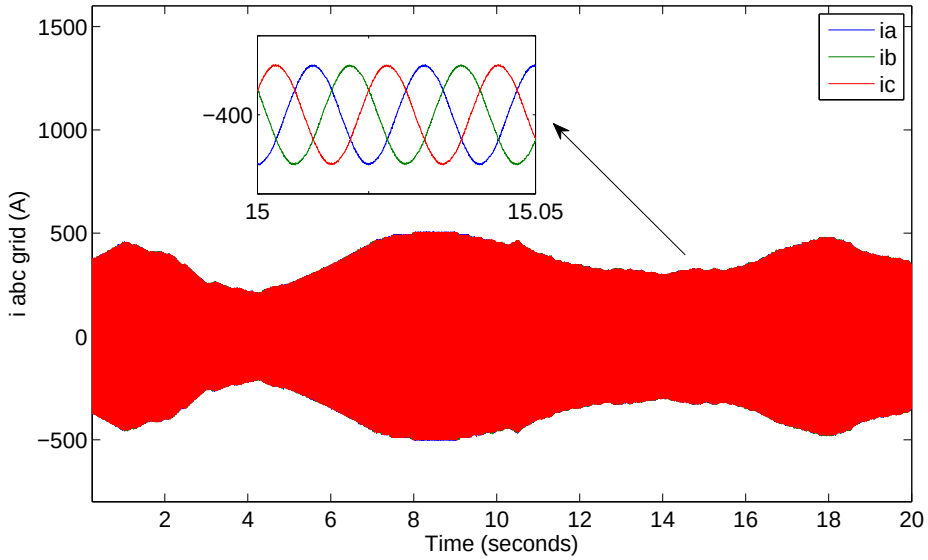

Fig. 5.13 Variation of grid current with respect to time

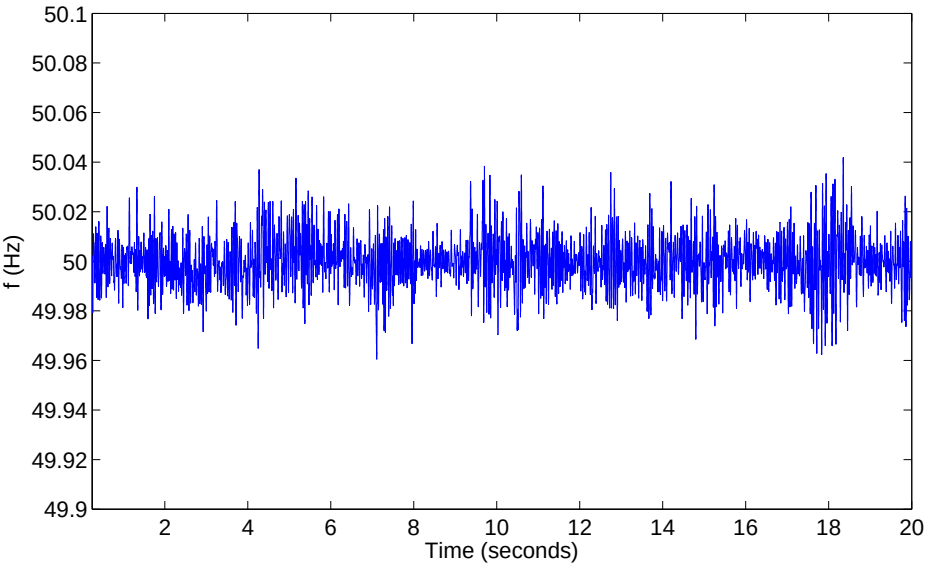

Fig. 5.14 Variation of grid frequency

5.5.3 Analysis of Results

The simulations show that the effect of controller during the change of different values of stochastic wind speed. At the beginning of simulation, the initial conditions should be fixed

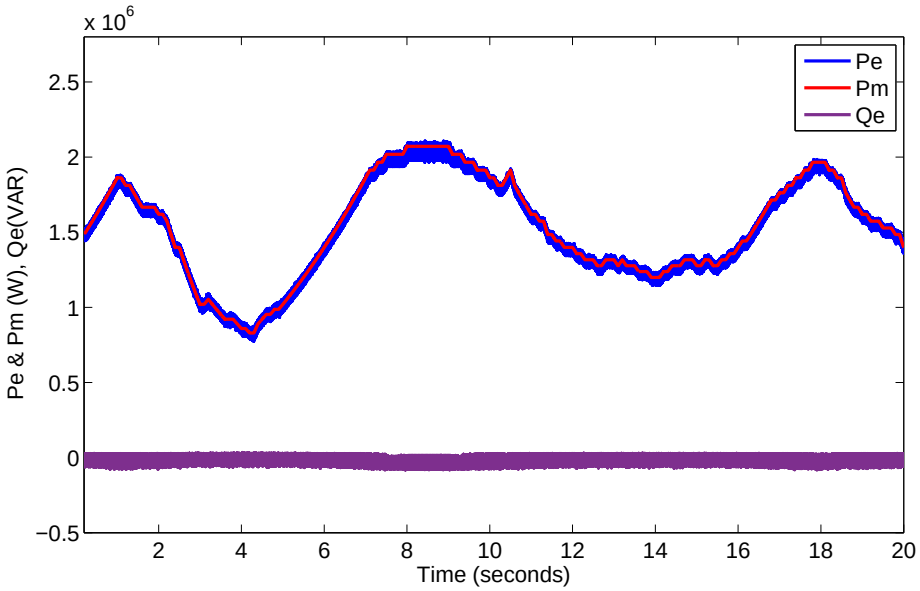

Fig. 5.15 Variation of grid active and reactive power

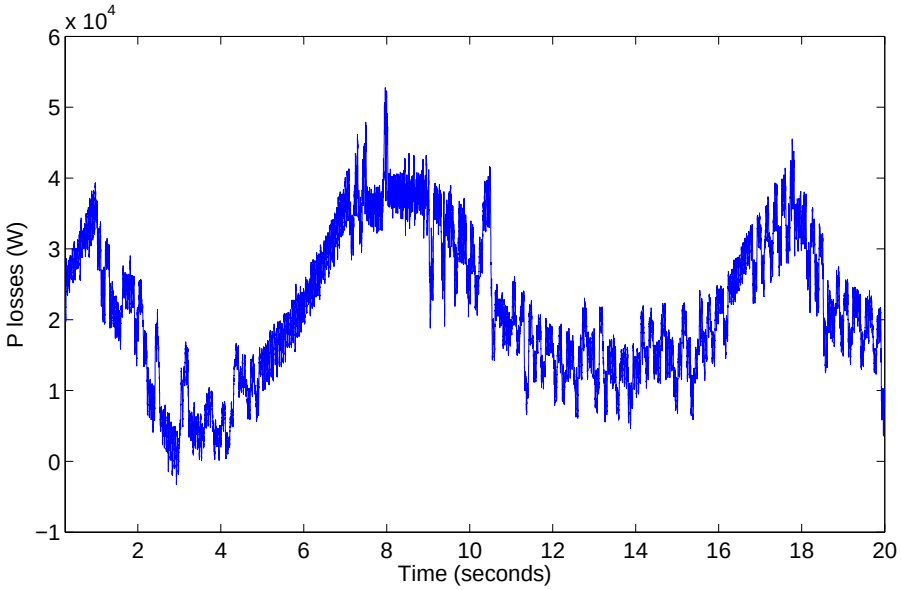

Fig. 5.16 Variation of grid active power losses

in order to operate the system within acceptable fluctuation. In MSC the set value of i_d is equal to zero to achieve maximum torque at the minimum current. The simulation also shows

Table 5.3 Variation of active power with respect to wind speeds for PI controller

Wind speed (m/s)	**5**	**6**	**7**	**8**	**9**	**10**	**11.4**
Pm (MW)	0.1748	0.3021	0.4798	0.71628	1.0199	1.3991	2.0728
Pe av. (MW)	0.1740	0.3005	0.473	0.702	0.995	1.368	2.025
P losses (KW)	0.8	1.6	6.8	14.28	24.9	31.1	47.8
Fluctuation (KW) ±	1.27	1.78	1.85	2.05	2.27	2.37	5.96
Overshoot %	1.6	0.711	0.97	1.593	0.94	1.77	1.94
Settling time (ms)	0.09	0.12	0.13	0.16	0.155	0.23	0.26

Table 5.4 Variation of active power with respect to wind speeds for FPC

Wind speed (m/s)	**5**	**6**	**7**	**8**	**9**	**10**	**11.4**
Pm (MW)	0.1748	0.3021	0.4798	0.71628	1.0199	1.3991	2.0728
Pe av. (MW)	0.1743	0.3015	0.478	0.71165	1.0105	1.3815	2.035
P losses (KW)	0.5	0.6	1.8	4.63	9.4	17.6	37.8
Fluctuation (KW) ±	1.15	1.36	1.45	1.75	1.85	2.15	5.3
Overshoot %	1.4	0.411	0.477	0.993	0.445	0.977	1.14
Settling time (ms)	0.06	0.08	0.08	0.1	0.085	0.15	0.18

that the grid currents demonstrated an obvious distortion using PI control compared with low distorted current using FPC as shown in Figure 5.13.

5.5.4 Comparison between FPC and traditional PI controller

The comparison have been made at rated wind speed 11.4 m/s first between the proposed model using FPC and the conventional model using PI controller.

1. Step change in wind speed

The variation of generated power with respect to the variable wind speed when subjected to step change variation for both PI controller and FPC can be tabulated in Tables 5.3 and 5.4 respectively. The data show reduction in settling time and overshoot as well as in power losses due to well tracking to the maximum power from the wind during variation.

The performance sensitivity of the controllers can be evaluated for some metrics such as overshoot, settling time and power fluctuation by taking their standard deviations as shown in Table 5.5. It is obvious from the table that standard deviations of these metrics are reduced

Table 5.5 Calculation of some metrics standard deviations for both controllers

	Overshoot %	**Settling Time (ms)**	**Fluctuation (kW)**
PI	0.4774	0.0609	1.5651
FPC	0.391	0.0435	1.4310

Table 5.6 Calculation of some metrics mean values for both controllers

	Overshoot %	**Settling Time (ms)**	**Fluctuation (kW)**
PI	1.3604	0.1636	2.5071
FPC	0.8347	0.105	2.1443

in case of FPC compared to PI controller. Therefore FPC is more consistent and robust than PI controller. The mean values of the same metrics are shown in Table 5.6. The table shows that the mean values of those metrics are reduced in case of FPC. Thus FPC performs better than PI controller across all operating points.

It is shown that the overshoot of the rotor speed is highly reduced from 2.1% in PI controller to 1.14% in FPC and settling time is also reduced from 0.5 to 0.18 for these controllers respectively while the error will be reduced from 0.8 to 0.4 respectively as shown in Table 5.7. At the same time, THD shows a small amount reduction from 1.1% in case of PI controller to 0.93% in case of FPC.

2. Variable wind speed

Different quantities have been compared with traditional models are shown in detailed for all period of time. In Figure 5.17 the frequencies of both controllers are shown. The values are varied within acceptable limit of 50 Hz where the maximum variation in case of FPC is $\pm 1.25\%$.

Figure 5.18 shows the rotor speed of the generator in both FPC and PI controller. Figure

Table 5.7 Calculation of change response for rated rotor speed for different controllers

	Overshoot %	**Settling Time (ms)**	**Error %**
PI	2.1	0.5	0.8
FPC	1.14	0.18	0.4

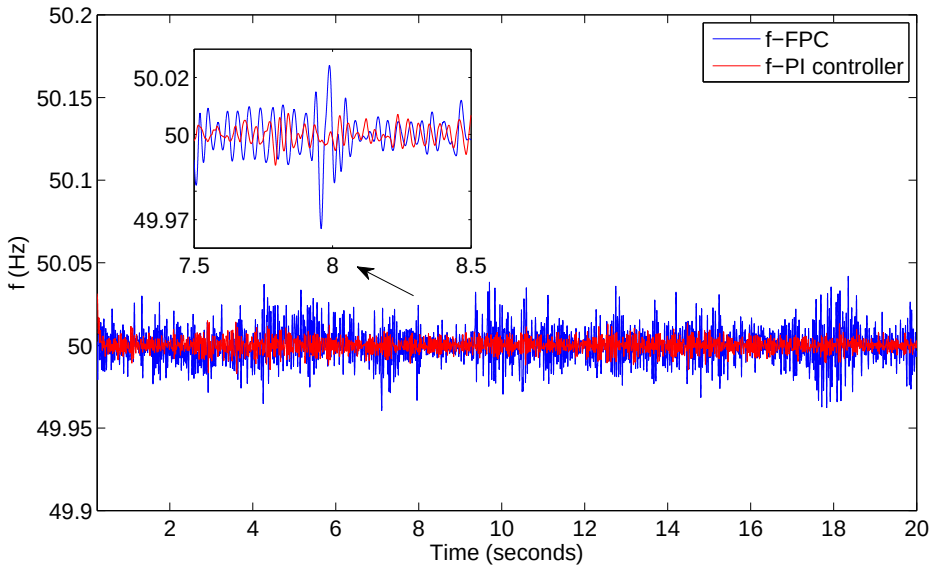

Fig. 5.17 Variation grid frequency compared to PI controller

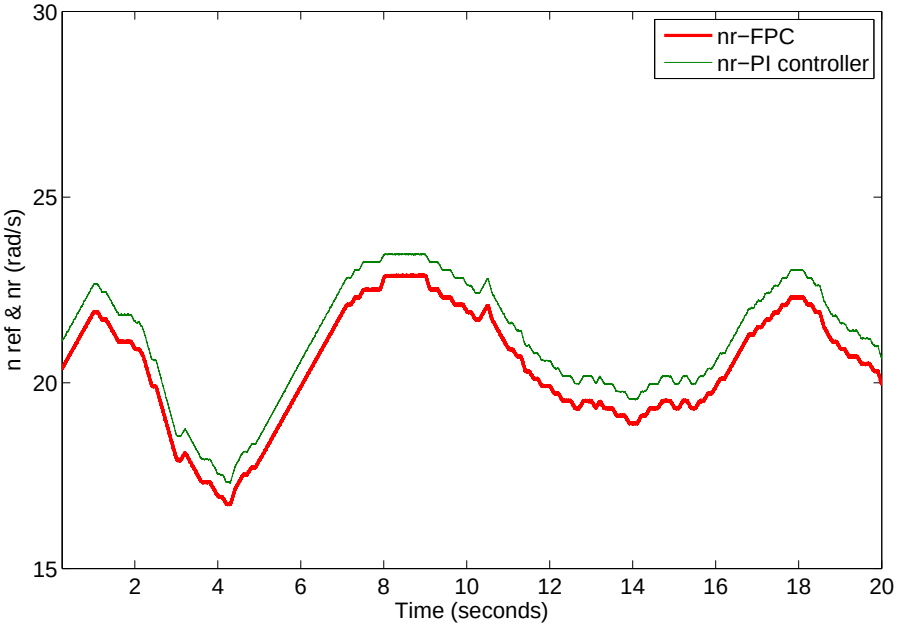

Fig. 5.18 Variation rotor speed compared to PI controller

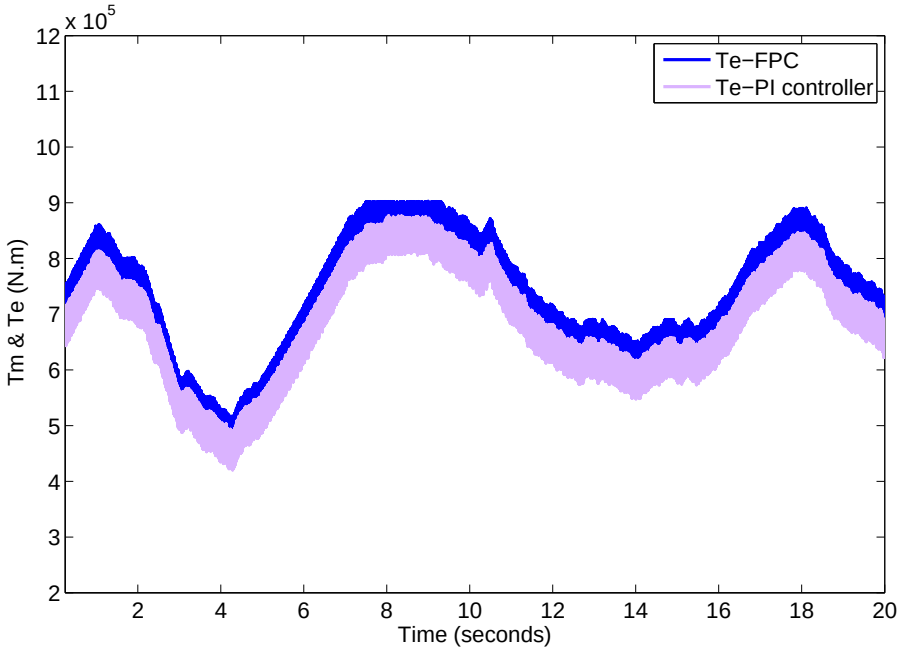

Fig. 5.19 Variation electromagnetic torque compared to PI controller

5.19 shows the generated electromagnetic torque in both ceases of FPC and PI controller. It is noticed that the torque increased in case of FPC compared to PI controller which leads to increase in generated active power.

The difference between the optimal active power and actual generated power can be expressed as:

$$\Delta P_e = P_{opt} - P_e \tag{5.21}$$

Figure 5.20 shows this power difference for the proposed FPC and PI controller. It is obvious that the oscillations in case of the proposed controller are reduced compared to PI controller.

Finally, the DC voltages are shown in Figure 5.21 of both FPC and PI controller. It is noticed that the DC voltage in case of FPC is more robust and varied by 1.5 V compared to PI controller which increased in rated speed by 7.5 V.

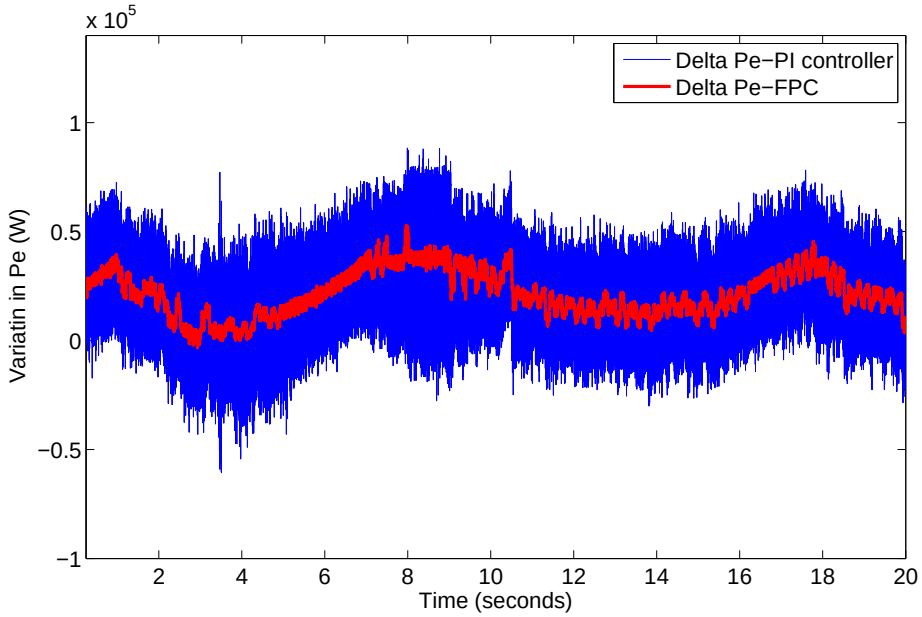

Fig. 5.20 Variation of ΔP_e of FPC compared to PI controller

Table 5.8 Standard deviation of the variation in DC voltage and active power

	Delta V dc (V)	**Delta Pe (W)**
PI	0.474	1.643 e4
FPC	0.322	1.520 e4

Compared to PI controller, the difference between of the set value of DC voltage and actual controlled DC voltage can be expressed:

$$\Delta V_{dc} = V_{dcref} - V_{dc} \tag{5.22}$$

The Standard deviation of ΔV_{dc} and ΔP_e for both controllers is tabulated in Table 5.8.

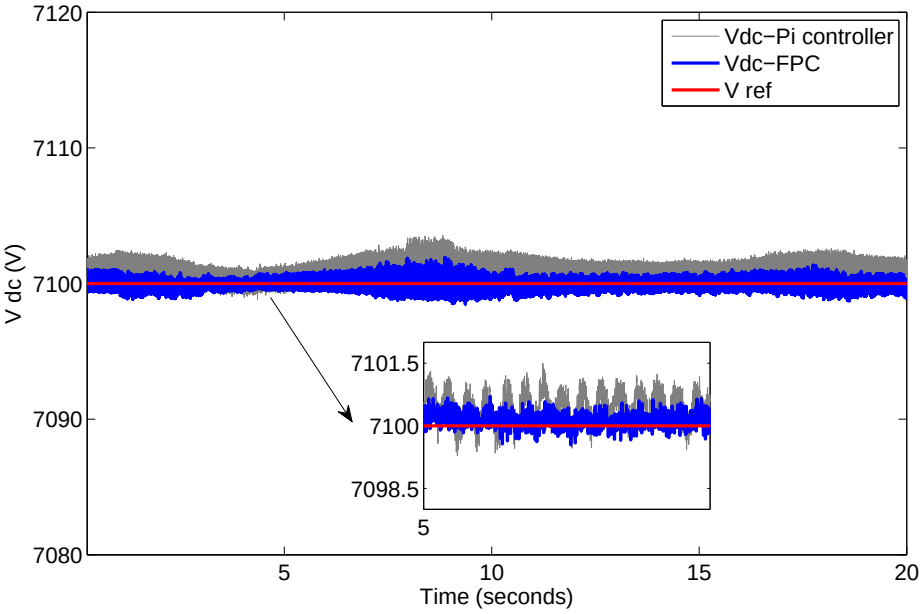

Fig. 5.21 Variation of ΔV_{dc} for both controllers

5.6 Summary

In this chapter, the state of the art converter control techniques are described, followed by the explanation of different types of the advanced and hybrid control schemes. Modelling and design of different schemes for the VSC control are presented with their main features and specifications. The operating principle of the MPC strategy is explained for designer point of view for different cases of operation. The discussions imply the potentiality of the cost function which plays a vital role in prediction process is discussed for different control and technical requirements. The main Fuzzy Logic techniques are describes with all definitions of the whole components of the system. Analysis presented in this chapter shows that the use MPC and FLC strategies have different benefits if they have been combined together to form a new scheme of FPC to satisfy high performance operation for various power converters technology. This type of control scheme has been simulated and tested in different cases studies to evaluate the operation of the whole system output during uncertainty.

Chapter 6

Conclusions and Future Works

This chapter concludes the work presented in this thesis and demonstrates some of the future research directions.

6.1 Conclusions

Currently wind energy industry indicates a trend towards the research and development of grid connected wind turbines. The major interests of the current wind turbine manufacturers include: variable speed (Type-4) technology, a direct-driven permanent magnet synchronous generator of medium voltage operation and development of sophisticated control systems to increase the efficiency of wind energy conversion and to meet grid code requirements. In this work, the proposed robust control schemes of Back-to-Back (BB) power converter configurations have been designed and simulated to validate the system model and deal with various operational conditions. The following notes can be addressed as conclusions:

- The fundamentals and principles of WECS have been explained in detail. Different types of generators and their connection categories, advantages and drawbacks are discussed through the chapters of this thesis. It is concluded from the literature review that Type-4 technology of BTB converters is more beneficial compared to

other technologies. This configuration has several benefits such as high efficiency, less mechanical parts and easy of control. Therefore the Type-4 has been selected in this thesis which fully decoupled PMSG.

- Due to ease of use, simple and low costs, conventional control schemes using PI controllers are common and show acceptable operational performance in the case of linear systems and constant loads. In cases of sudden change in wind or transient operation, PI controllers will not be suitable.

- Maximum power capturing from the wind can be obtained by adjusting the PI controller gain parameters of the speed control loop. Achieving MPPT leads to high efficiency in power conversion of generator side converter. Furthermore, smoothing of DC voltage in the grid or load side converter can be achieved by adjusting the PI controller parameters of DC link control loop in GSC control. The output results show a small oscillation in output active and reactive powers which are due to different factors such as parameters gain of PI controller, the value of DC link capacitor and the values of inductance and resistance of the grid. The DC output voltage will be stable after a small oscillation. The value of oscillation depends upon the size of DC link capacitor and the tuning of PI gain parameters in DC link control loop of GSC.

- Advanced control schemes have been developed to control the voltage source converter in a WECS. These control schemes have been applied to provide FOC for MSC control section. Various control schemes have been modelled and simulated in this these, namely traditional control scheme using PI controller, advanced control scheme using FLC, novel control scheme using MRFC and hybrid control scheme using FPC.

- Simulations show that the FLC scheme has good performance with regard to wind variation and reduces the overshoot in rotor speed compared to a conventional PI

controller. This reduction in errors gives more mechanical stability to the generator in the case of variable wind speed.

- At the same time the design of FOC using MRFC has a robust performance better than the traditional controller and FLC in reduction of errors, overshoot and THD for all operating conditions. Reduction in overshoot and error of rotor speed leads to an increase in the lifetime of the mechanical parts and provides more generator stability with variable wind speeds.

- From simulations, it is clear that the MRFC scheme is more stable in rotor speed and enable to capture more mechanical power from the wind due to the model reference signal that enhances the set points of the controller and finally improves the performance of the system with variable wind speeds.

- FLC has been combined with MPC to form a hybrid control scheme addressed as FPC. The system has been simulated using a mathematical model which has obtained a stable performance with high quality output of voltage and frequency during all operational conditions. This control scheme has been applied to grid connection and can be divided into two parts, MSC and GSC control. The first part of the scheme adjusts the rotor speed to achieve MPPT, whilst the second part of the scheme controls the DC-Link voltage in order to adjust the grid voltage as well. In cases of sudden change in wind or transient operation, PI controllers will not be suitable.

- Compared to the traditional PI controller of available BTB converter, the proposed hybrid control scheme configuration can be used to reduce the effects of disturbances of wind speed. For this reason, FPC scheme has been suggested to mitigate the effects of system variability and shows robust performance.

- Simulations show that the adjusted set value of rotor speed is more accurate where the speed error is small which enables the system to track the maximum power captured

from the wind. As a result, DC link voltage variation during variable wind speed is so small; therefore the grid voltage will be maintained at constant level.

- Moreover, FPC shows a good reduction in error and overshoot of rotor speed and gives higher output energy than the conventional controller. It is also noticed that FPC presents a fast response to wind speed variation.

6.2 Future Works

As a future work notes, the following points is suggested:

- The configuration of grid connected DFIG of Type 3 of WECS can be investigated, modelled and simulated as well as applying other types of controller such as sliding mode or hysteresis current controller to overcome oscillations in the output currents and improve the system stability and performance.

- One of the important issues with FLC is determining the values of input and output parameters of membership functions. Although simple technique has been used in adjusting an appropriate value of inputs and outputs parameters of membership function. It is important to analyse the system using an advanced algorithms to obtain the optimum values of the fuzzy system parameters and present better performance. Therefore, more general, accurate and robust methods in optimization algorithm are needed. For example, optimisation algorithms such as Particle Swarm Optimisation and Genetic Algorithms can be utilised to optimise the system.

- Investigation of WECS behaviour under unbalanced grid fault conditions and development of new control systems represent an important issue in research development to meet the emerging grid code requirements.

Bibliography

[1] Paul Gipe. *Wind energy basics*. Chelsea Green Pub. Co., 2009.

[2] Bin Wu, Yongqiang Lang, Navid Zargari, and Samir Kouro. *Power conversion and control of wind energy systems*. John Wiley & Sons, 2011.

[3] Rana Adib. Renewables 2015 global status report. 2015.

[4] Frede Blaabjerg and Ke Ma. Future on power electronics for wind turbine systems. *IEEE Journal of Emerging and Selected Topics in Power Electronics*, 1(3):139–152, 2013.

[5] Frede Blaabjerg, Marco Liserre, and Ke Ma. Power electronics converters for wind turbine systems. *IEEE Transactions on Industry Applications*, 48(2):708–719, 2012.

[6] Shigeo Morimoto, Yi Tong, Yoji Takeda, and Takao Hirasa. Loss minimization control of permanent magnet synchronous motor drives. *IEEE Transactions on industrial electronics*, 41(5):511–517, 1994.

[7] Zhe Chen and Frede Blaabjerg. Wind farm—a power source in future power systems. *Renewable and Sustainable Energy Reviews*, 13(6):1288–1300, 2009.

[8] V Galdi, A Piccolo, and P Siano. Exploiting maximum energy from variable speed wind power generation systems by using an adaptive takagi–sugeno–kang fuzzy model. *Energy Conversion and Management*, 50(2):413–421, 2009.

[9] Mukhtiar Singh and Ambrish Chandra. Application of adaptive network-based fuzzy inference system for sensorless control of pmsg-based wind turbine with nonlinear-load-compensation capabilities. *IEEE transactions on power electronics*, 26(1):165–175, 2011.

[10] Jose Rodriguez, Marian P Kazmierkowski, Jose R Espinoza, Pericle Zanchetta, Haitham Abu-Rub, Hector A Young, and Christian A Rojas. State of the art of finite control set model predictive control in power electronics. *IEEE Transactions on Industrial Informatics*, 9(2):1003–1016, 2013.

[11] Venkata Yaramasu, Bin Wu, Paresh C Sen, Samir Kouro, and Mehdi Narimani. High-power wind energy conversion systems: State-of-the-art and emerging technologies. *Proceedings of the IEEE*, 103(5):740–788, 2015.

[12] Venkata Narasimha Rao Yaramasu. *Predictive control of multilevel converters for megawatt wind energy conversion systems*. PhD thesis, Ryerson University, 2014.

[13] Marwan Rosyadi, SM Muyeen, Rion Takahashi, and Junji Tamura. A design fuzzy logic controller for a permanent magnet wind generator to enhance the dynamic stability of wind farms. *Applied Sciences*, 2(4):780–800, 2012.

[14] REN 21 Steering Committee et al. Renewables 2013, global status report. *Renewable Energy Policy Network for the 21st Century, Paris, Tech. Rep*, 2013.

[15] Yaxing Ren, Liuying Li, Joseph Brindley, and Lin Jiang. Nonlinear pi control for variable pitch wind turbine. *Control Engineering Practice*, 50:84–94, 2016.

[16] James F Manwell, Jon G McGowan, and Anthony L Rogers. *Wind energy explained: theory, design and application*. John Wiley & Sons, 2010.

[17] Lucy Y Pao and Kathryn E Johnson. Control of wind turbines. *IEEE Control Systems*, 31(2):44–62, 2011.

[18] Teresa Orłowska-Kowalska, Frede Blaabjerg, and José Rodríguez. *Advanced and intelligent control in power electronics and drives*, volume 531. Springer, 2014.

[19] Sandra Eriksson, Hans Bernhoff, and Mats Leijon. Evaluation of different turbine concepts for wind power. *Renewable and Sustainable Energy Reviews*, 12(5):1419–1434, 2008.

[20] Paul S Veers, Thomas D Ashwill, Herbert J Sutherland, Daniel L Laird, Donald W Lobitz, Dayton A Griffin, John F Mandell, Walter D Musial, Kevin Jackson, Michael Zuteck, et al. Trends in the design, manufacture and evaluation of wind turbine blades. *Wind Energy*, 6(3):245–259, 2003.

[21] Siegfried Heier. *Grid integration of wind energy: onshore and offshore conversion systems*. John Wiley & Sons, 2014.

[22] Zhe Chen, Josep M Guerrero, and Frede Blaabjerg. A review of the state of the art of power electronics for wind turbines. *IEEE Transactions on power electronics*, 24(8): 1859–1875, 2009.

[23] Eduard Muljadi and Charles P Butterfield. Pitch-controlled variable-speed wind turbine generation. *IEEE transactions on Industry Applications*, 37(1):240–246, 2001.

[24] Tomonobu Senjyu, Ryosei Sakamoto, Naomitsu Urasaki, Toshihisa Funabashi, Hideki Fujita, and Hideomi Sekine. Output power leveling of wind turbine generator for all operating regions by pitch angle control. *IEEE Transactions on Energy conversion*, 21 (2):467–475, 2006.

[25] Henk Polinder, Frank FA Van der Pijl, G-J De Vilder, and Peter J Tavner. Comparison of direct-drive and geared generator concepts for wind turbines. *IEEE Transactions on energy conversion*, 21(3):725–733, 2006.

[26] H Li and Zhe Chen. Overview of different wind generator systems and their comparisons. *IET Renewable Power Generation*, 2(2):123–138, 2008.

[27] BJ Chalmers and E Spooner. An axial-flux permanent-magnet generator for a gearless wind energy system. *IEEE Transactions on Energy Conversion*, 14(2):251–257, 1999.

[28] Lyndon Greedy and REV DATE. Review of electric drive-train topologies. project upwind. 2007.

[29] Lars Henrik Hansen, Lars Helle, Frede Blaabjerg, E Ritchie, Stig Munk-Nielsen, Henrik W Bindner, Poul Ejnar Sørensen, and Birgitte Bak-Jensen. Conceptual survey of generators and power electronics for wind turbines. Technical report, 2002.

[30] Henk Polinder, Jan Abraham Ferreira, Bogi Bech Jensen, Asger B Abrahamsen, Kais Atallah, and Richard A McMahon. Trends in wind turbine generator systems. *IEEE Journal of Emerging and Selected Topics in Power Electronics*, 1(3):174–185, 2013.

[31] Xu Yang, Dean Patterson, and Jerry Hudgins. Permanent magnet generator design and control for large wind turbines. In *Power Electronics and Machines in Wind Applications (PEMWA), 2012 IEEE*, pages 1–5. IEEE, 2012.

[32] TF Chan and LL Lai. An axial-flux permanent-magnet synchronous generator for a direct-coupled wind-turbine system. *IEEE Transactions on Energy Conversion*, 22(1): 86–94, 2007.

[33] L Soderlund, J-T Eriksson, J Salonen, H Vihriala, and R Perala. A permanent-magnet generator for wind power applications. *IEEE Transactions on Magnetics*, 32(4): 2389–2392, 1996.

[34] AA Rockhill, Marco Liserre, Remus Teodorescu, and Pedro Rodriguez. Grid-filter design for a multimegawatt medium-voltage voltage-source inverter. *IEEE Transactions on Industrial Electronics*, 58(4):1205–1217, 2011.

[35] Soeren Baekhoej Kjaer, John K Pedersen, and Frede Blaabjerg. A review of single-phase grid-connected inverters for photovoltaic modules. *IEEE transactions on industry applications*, 41(5):1292–1306, 2005.

[36] Ryosei Sakamoto, Tomonobu Senjyu, Tatsuto Kinjo, Naomitsu Urasaki, Toshihisa Funabashi, Hideki Fujita, and Hideomi Sekine. Output power leveling of wind turbine generator for all operating regions by pitch angle control. In *Power Engineering Society General Meeting, 2005. IEEE*, pages 45–52. IEEE, 2005.

[37] Concettina Buccella, Carlo Cecati, and Hamed Latafat. Digital control of power converters—a survey. *IEEE Transactions on Industrial Informatics*, 8(3):437–447, 2012.

[38] Eric Monmasson, Lahoucine Idkhajine, Marcian N Cirstea, Imene Bahri, Alin Tisan, and Mohamed Wissem Naouar. Fpgas in industrial control applications. *IEEE Transactions on Industrial informatics*, 7(2):224–243, 2011.

[39] Willy Tjiu, Tjukup Marnoto, Sohif Mat, Mohd Hafidz Ruslan, and Kamaruzzaman Sopian. Darrieus vertical axis wind turbine for power generation ii: Challenges in hawt and the opportunity of multi-megawatt darrieus vawt development. *Renewable Energy*, 75:560–571, 2015.

[40] William Erdman and M Behnke. Low wind speed turbine project phase ii: The application of medium-voltage electrical apparatus to the class of variable speed multi-megawatt low wind speed turbines; 15 june 2004–30 april 2005. Technical report, National Renewable Energy Laboratory (NREL), Golden, CO., 2005.

[41] Marina Tsili and S Papathanassiou. A review of grid code technical requirements for wind farms. *IET Renewable Power Generation*, 3(3):308–332, 2009.

[42] Müfit Altin, Ömer Göksu, Remus Teodorescu, Pedro Rodriguez, Birgitte-Bak Jensen, and Lars Helle. Overview of recent grid codes for wind power integration. In *Optimization of Electrical and Electronic Equipment (OPTIM), 2010 12th International Conference on*, pages 1152–1160. IEEE, 2010.

[43] Anca D Hansen and Lars H Hansen. Wind turbine concept market penetration over 10 years (1995–2004). *Wind energy*, 10(1):81–97, 2007.

[44] Thomas Ackermann. *Wind power in power systems*. John Wiley & Sons, 2005.

[45] Olimpo Anaya-Lara, Nick Jenkins, Janaka Ekanayake, Phill Cartwright, and Michael Hughes. *Wind energy generation: modelling and control*. John Wiley & Sons, 2011.

[46] A Abedini and A Nasiri. Pmsg wind turbine performance analysis during short circuit faults. In *Electrical Power Conference, 2007. EPC 2007. IEEE Canada*, pages 160–165. IEEE, 2007.

[47] DP Kadam and BE Kushare. Overview of different wind generator systems and their comparisons. *International Journal of Engineering Science & Advanced Technology,[IJESAT]*, 2(4):1076–1081, 2012.

[48] Yao Duan and Ronald G Harley. Present and future trends in wind turbine generator designs. In *Power Electronics and Machines in Wind Applications, 2009. PEMWA 2009. IEEE*, pages 1–6. IEEE, 2009.

[49] Daniel J Trudnowski, Andrew Gentile, Jawad M Khan, and Eric M Petritz. Fixed-speed wind-generator and wind-park modeling for transient stability studies. *IEEE Transactions on Power Systems*, 19(4):1911–1917, 2004.

[50] Juan Dixon, Luis Moran, Jose Rodriguez, and Ricardo Domke. Reactive power compensation technologies: State-of-the-art review. *Proceedings of the IEEE*, 93(12): 2144–2164, 2005.

[51] Stavros A Papathanassiou and Michael P Papadopoulos. Mechanical stresses in fixed-speed wind turbines due to network disturbances. *IEEE Transactions on Energy Conversion*, 16(4):361–367, 2001.

[52] M Jahangir Hossain, Hemanshu R Pota, Valeri A Ugrinovskii, and Rodrigo A Ramos. Simultaneous statcom and pitch angle control for improved lvrt capability of fixed-speed wind turbines. *IEEE Transactions on sustainable energy*, 1(3):142–151, 2010.

[53] Marta Molinas, Jon Are Suul, and Tore Undeland. Extending the life of gear box in wind generators by smoothing transient torque with statcom. *IEEE Transactions on Industrial Electronics*, 57(2):476–484, 2010.

[54] Mohamed Ridha Khadraoui and Mohamed Elleuch. Comparison between optislip and fixed speed wind energy conversion systems. In *Systems, Signals and Devices, 2008. IEEE SSD 2008. 5th International Multi-Conference on*, pages 1–6. IEEE, 2008.

[55] R Pena, JC Clare, and GM Asher. Doubly fed induction generator using back-to-back pwm converters and its application to variable-speed wind-energy generation. *IEE Proceedings-Electric Power Applications*, 143(3):231–241, 1996.

[56] Set Muller, M Deicke, and Rik W De Doncker. Doubly fed induction generator systems for wind turbines. *IEEE Industry applications magazine*, 8(3):26–33, 2002.

[57] Rajib Datta and VT Ranganathan. Variable-speed wind power generation using doubly fed wound rotor induction machine-a comparison with alternative schemes. *IEEE transactions on Energy conversion*, 17(3):414–421, 2002.

[58] Jesus Lopez, Pablo Sanchis, Xavier Roboam, and Luis Marroyo. Dynamic behavior of the doubly fed induction generator during three-phase voltage dips. *IEEE Transactions on Energy conversion*, 22(3):709–717, 2007.

[59] Resham R Wandile, Sandeep V Karemore, and G Shriwastawa Rakesh. Direct active and reactive power control of dfig for wind energy generation. *International Journal Of Innovative Research In Electrical, Electronics, Instrumentation And Control Engineering*, 3(5), 2015.

[60] Shibashis Bhowmik, Rene Spee, and Johan HR Enslin. Performance optimization for doubly fed wind power generation systems. *IEEE Transactions on Industry Applications*, 35(4):949–958, 1999.

[61] Rajib Datta and VT Ranganathan. A method of tracking the peak power points for a variable speed wind energy conversion system. *IEEE Transactions on Energy Conversion*, 18(1):163–168, 2003.

[62] Janaka Ekanayake and Nick Jenkins. Comparison of the response of doubly fed and fixed-speed induction generator wind turbines to changes in network frequency. *IEEE Transactions on Energy conversion*, 19(4):800–802, 2004.

[63] L Holdsworth, XG Wu, Janaka Bandara Ekanayake, and Nick Jenkins. Comparison of fixed speed and doubly-fed induction wind turbines during power system disturbances. *IEE Proceedings-Generation, Transmission and Distribution*, 150(3):343–352, 2003.

[64] Patrick S Flannery and Giri Venkataramanan. A fault tolerant doubly fed induction generator wind turbine using a parallel grid side rectifier and series grid side converter. *IEEE Transactions on Power Electronics*, 23(3):1126–1135, 2008.

[65] Roberto Cardenas, Rubén Pena, Salvador Alepuz, and Greg Asher. Overview of control systems for the operation of dfigs in wind energy applications. *IEEE Transactions on Industrial Electronics*, 60(7):2776–2798, 2013.

[66] Monica Chinchilla, Santiago Arnaltes, and Juan Carlos Burgos. Control of permanent-magnet generators applied to variable-speed wind-energy systems connected to the grid. *IEEE Transactions on energy conversion*, 21(1):130–135, 2006.

[67] Emilio J Bueno, Santiago Cobreces, Francisco J RodrÍguez, Alvaro Hernandez, and Felipe Espinosa. Design of a back-to-back npc converter interface for wind turbines with squirrel-cage induction generator. *IEEE Transactions on Energy conversion*, 23 (3):932–945, 2008.

[68] Venkata Yaramasu, Bin Wu, Marco Rivera, and Jose Rodriguez. A new power conversion system for megawatt pmsg wind turbines using four-level converters and a simple control scheme based on two-step model predictive strategy—part ii: Simulation and experimental analysis. *IEEE Journal of Emerging and Selected Topics in Power Electronics*, 2(1):14–25, 2014.

[69] Hua Geng, Dewei Xu, Bin Wu, and Geng Yang. Active damping for pmsg-based wecs with dc-link current estimation. *IEEE Transactions on Industrial Electronics*, 58(4): 1110–1119, 2011.

[70] Eftichios Koutroulis and Kostas Kalaitzakis. Design of a maximum power tracking system for wind-energy-conversion applications. *IEEE transactions on industrial electronics*, 53(2):486–494, 2006.

[71] Kelvin Tan and Syed Islam. Optimum control strategies in energy conversion of pmsg wind turbine system without mechanical sensors. *IEEE transactions on energy conversion*, 19(2):392–399, 2004.

[72] Elkhatib Kamal, Magdy Koutb, Abdul Azim Sobaih, and Belal Abozalam. An intelligent maximum power extraction algorithm for hybrid wind–diesel-storage system. *International journal of electrical power & energy systems*, 32(3):170–177, 2010.

[73] Juan Manuel Carrasco, Leopoldo Garcia Franquelo, Jan T Bialasiewicz, Eduardo Galván, Ramón Carlos PortilloGuisado, MA Martin Prats, José Ignacio León, and Narciso Moreno-Alfonso. Power-electronic systems for the grid integration of renewable energy sources: A survey. *IEEE Transactions on industrial electronics*, 53(4): 1002–1016, 2006.

[74] Ming Cheng and Ying Zhu. The state of the art of wind energy conversion systems and technologies: A review. *Energy Conversion and Management*, 88:332–347, 2014.

[75] Bikash Kumar Sahu, Moonmoon Hiloidhari, and DC Baruah. Global trend in wind power with special focus on the top five wind power producing countries. *Renewable and Sustainable Energy Reviews*, 19:348–359, 2013.

[76] Frede Blaabjerg and Zhe Chen. Power electronics for modern wind turbines. *Synthesis Lectures on Power Electronics*, 1(1):1–68, 2005.

[77] Jun Kang, Noriyuki Takada, Eiji Yamamoto, and Eiji Watanabe. High power matrix converter for wind power generation applications. In *Power Electronics and ECCE Asia (ICPE & ECCE), 2011 IEEE 8th International Conference on*, pages 1331–1336. IEEE, 2011.

[78] Eiji Yamamoto, Hidenori Hara, Takahiro Uchino, Masahiro Kawaji, Tsuneo Joe Kume, Jun Koo Kang, and Hans-peter Krug. Development of mcs and its applications in industry [industry forum]. *IEEE Industrial Electronics Magazine*, 5(1):4–12, 2011.

[79] Bin Wu, Jorge Pontt, José Rodríguez, Steffen Bernet, and Samir Kouro. Current-source converter and cycloconverter topologies for industrial medium-voltage drives. *IEEE Transactions on Industrial Electronics*, 55(7):2786–2797, 2008.

[80] Samir Kouro, Jose Rodriguez, Bin Wu, Steffen Bernet, and Marcelo Perez. Powering the future of industry: High-power adjustable speed drive topologies. *IEEE industry applications magazine*, 18(4):26–39, 2012.

[81] Eng Ahmed Masmoudi, ZQ Zhu, and Jiabing Hu. Electrical machines and power-electronic systems for high-power wind energy generation applications: Part i–market penetration, current technology and advanced machine systems. *COMPEL-The international journal for computation and mathematics in electrical and electronic engineering*, 32(1):7–33, 2012.

[82] H Polinder, H Lendenmann, R Chin, and WM Arshad. Fault tolerant generator systems for wind turbines. In *Electric Machines and Drives Conference, 2009. IEMDC'09. IEEE International*, pages 675–681. IEEE, 2009.

[83] Andrew Kusiak and Wenyan Li. The prediction and diagnosis of wind turbine faults. *Renewable Energy*, 36(1):16–23, 2011.

[84] Jose I Leon, Samir Kouro, Mariusz Malinowski, K Gopakumar, Josep Pou Félix, LG Franquelo, Bin Wu, José Rodríguez, and Marcelo A Pérez. Recent advances and industrial applications of multilevel converters. *IEEE transactions on industrial electronics*, 57(8):2553–2580, 2010.

[85] José Rodríguez, Steffen Bernet, Bin Wu, Jorge O Pontt, and Samir Kouro. Multilevel voltage-source-converter topologies for industrial medium-voltage drives. *IEEE Transactions on industrial electronics*, 54(6):2930–2945, 2007.

[86] Remus Teodorescu, Marco Liserre, and Pedro Rodriguez. *Grid converters for photovoltaic and wind power systems*, volume 29. John Wiley & Sons, 2011.

[87] Venkata Yaramasu and Bin Wu. Predictive control of a three-level boost converter and an npc inverter for high-power pmsg-based medium voltage wind energy conversion systems. *IEEE Transactions on Power Electronics*, 29(10):5308–5322, 2014.

[88] Hern?? n De Battista and Ricardo J Mantz. *Wind Turbine Control Systems: Principles, Modelling and Gain Scheduling Design. Advances in Industrial Control*. Springer, 2007.

[89] Patrick J Moriarty and Sandy B Butterfield. Wind turbine modeling overview for control engineers. In *American Control Conference, 2009. ACC'09.*, pages 2090–2095. IEEE, 2009.

[90] Yuan-zhang Sun, Jin Lin, Guo-jie Li, and Xiong Li. A review on the integration of wind farms with variable speed wind turbine systems into power systems. In *Sustainable Power Generation and Supply, 2009. SUPERGEN'09. International Conference on*, pages 1–6. IEEE, 2009.

[91] Jinyun Yan, Jian Chen, Hongzhong Ma, Haihua Liu, and Lin Chen. The survey of electrical control systems of wind turbine generators. In *Sustainable Power Generation and Supply, 2009. SUPERGEN'09. International Conference on*, pages 1–5. IEEE, 2009.

[92] Yuan-zhang Sun, Zhao-sui Zhang, Guo-jie Li, and Jin Lin. Review on frequency control of power systems with wind power penetration. In *Power System Technology (POWERCON), 2010 International Conference on*, pages 1–8. IEEE, 2010.

[93] Jason H Laks, Lucy Y Pao, and Alan D Wright. Control of wind turbines: Past, present, and future. In *American Control Conference, 2009. ACC'09.*, pages 2096–2103. IEEE, 2009.

[94] Yu Ling, Guoxiang Wu, and Xu Cai. Comparison of wind turbine efficiency in maximum power extraction of wind turbines with doubly fed induction generator. *Prze gląd Elektro techniczny Electrical Review*, page 5, 2012.

[95] MNY Murthy. A review on power electronics application on wind turbines. *International Journal of Research in Eng. &Technology*, 2(11):09, 2013.

[96] Luis Arturo Soriano, Wen Yu, and Jose de Jesus Rubio. Modeling and control of wind turbine. *Mathematical Problems in Engineering*, 2013, 2013.

[97] Venugopal J Kante and DZJ Khan. A review paper on modeling and simulation of permanent magnet synchronous generator based on wind energy conversion system. *International Jour. of Engg. Research and Appl*, 4(6):34–43, 2014.

[98] Mazhar Hussain Baloch, Jie Wang, and Ghulam Sarwar Kaloi. A review of the state of the art control techniques for wind energy conversion system. *International Journal of Renewable Energy Research (IJRER)*, 6(4):1276–1295, 2016.

[99] IK Buehring and LL Freris. Control policies for wind-energy conversion systems. In *IEE Proceedings C (Generation, Transmission and Distribution)*, volume 128, pages 253–261. IET, 1981.

[100] I Tsoumas, A Safacas, E Tsimplostefanakis, and E Tatakis. An optimal control strategy of a variable speed wind energy conversion system. In *Electrical Machines and Systems, 2003. ICEMS 2003. Sixth International Conference on*, volume 1, pages 274–277. IEEE, 2003.

[101] Jau-Woei Perng, Guan-Yan Chen, and Shan-Chang Hsieh. Optimal pid controller design based on pso-rbfnn for wind turbine systems. *Energies*, 7(1):191–209, 2014.

[102] Avishek Kumar and Karl Stol. Scheduled model predictive control of a wind turbine. In *47th AIAA Aerospace Sciences Meeting Including The New Horizons Forum and Aerospace Exposition*, page 481, 2009.

[103] Arne Korber and Rudibert King. Model predictive control for wind turbines. In *European Wind Energy Conference*, 2010.

[104] Jason Laks, Lucy Pao, Eric Simley, Alan Wright, Neil Kelley, and Bonnie Jonkman. Model predictive control using preview measurements from lidar. In *49th AIAA Aerospace Sciences Meeting including the New Horizons Forum and Aerospace Exposition*, page 813, 2011.

[105] Le Xie and Marija D Ilic. Model predictive dispatch in electric energy systems with intermittent resources. In *Systems, Man and Cybernetics, 2008. SMC 2008. IEEE International Conference on*, pages 42–47. IEEE, 2008.

[106] M Khalid and AV Savkin. A model predictive control approach to the problem of wind power smoothing with controlled battery storage. *Renewable Energy*, 35(7): 1520–1526, 2010.

[107] M Bayat and H Kazemi Karegar. Predictive control of wind energy conversion system. In *Developments in Renewable Energy Technology (ICDRET), 2009 1st International Conference on the*, pages 1–5. IEEE, 2009.

[108] EB Muhando, T Senjyu, K Uchida, H Kinjo, and T Funabashi. Stochastic inequality constrained closed-loop model-based predictive control of mw-class wind generating system in the electric power supply. *IET renewable power generation*, 4(1):23–35, 2010.

[109] J Novak and P Chalupa. Mimo predictive control of a wind turbine. *International Journal of Energy and Environment*, 8:1–10, 2014.

[110] Kamel Ouari, Mohand Ouhrouche, Toufik Rekioua, and Taib Nabil. Nonlinear predictive control of wind energy conversion system using dfig with aerodynamic torque observer. *Journal of Electrical Engineering*, 65(6):333–341, 2014.

[111] Miguel Angel Mayosky and IE Cancelo. Direct adaptive control of wind energy conversion systems using gaussian networks. *IEEE Transactions on neural networks*, 10(4):898–906, 1999.

[112] M Sedighizadeh, A Rezazadeh, and M Khatibi. A self-tuning pid control for a wind energy conversion system based on the lyapunov approach. In *Universities Power Engineering Conference, 2008. UPEC 2008. 43rd International*, pages 1–4. IEEE, 2008.

[113] M Sedighizadeh, D Arzaghi-Harris, and M Kalantar. Adaptive pid control of wind energy conversion systems using rasp1 mother wavelet basis function networks. In *TENCON 2004. 2004 IEEE Region 10 Conference*, volume 100, pages 524–527. IEEE, 2004.

[114] Farzia Karim, Md Faruk Hossain, and Md Shah Alam. Modified hill climb searching method for tracking maximum power point in wind energy conversion systems. In *Proceedings International Conference on Mechanical Engineering (ICME)*, pages 18–20, 2011.

[115] KS Reddy, Madhusudan Kumar, TK Mallick, H Sharon, and S Lokeswaran. A review of integration, control, communication and metering (iccm) of renewable energy based smart grid. *Renewable and Sustainable Energy Reviews*, 38:180–192, 2014.

[116] Francisco Díaz-González, Melanie Hau, Andreas Sumper, and Oriol Gomis-Bellmunt. Participation of wind power plants in system frequency control: Review of grid code requirements and control methods. *Renewable and Sustainable Energy Reviews*, 34: 551–564, 2014.

[117] Ronilson Rocha et al. A multivariable h/sub/spl infin//control for wind energy conversion system. In *Control Applications, 2003. CCA 2003. Proceedings of 2003 IEEE Conference on*, volume 1, pages 206–211. IEEE, 2003.

[118] R Rocha, MV Bortolus, et al. Optimal multivariable control for wind energy conversion system-a comparison between h 2 and h - infinity controllers. In *Decision and Control, 2005 and 2005 European Control Conference. CDC-ECC'05. 44th IEEE Conference on*, pages 7906–7911. IEEE, 2005.

[119] Ronilson Rocha, Peterson Resende, Jos6 Luiz Silvino, and Marcos Vinicius Bortolus. Control of stall regulated wind turbine through h/sub/spl infin//loop shaping method. In *Control Applications, 2001.(CCA'01). Proceedings of the 2001 IEEE International Conference on*, pages 925–929. IEEE, 2001.

[120] Chao-hao CAI and Jian YANG. H - infinity control for doubly-fed wind power generators with variable speed and constant frequency. *Small & Special Electrical Machines*, 2:003, 2011.

[121] Dimitrios Bourlis and JAM Bleijs. Gain scheduled controller with wind speed estimation via kalman filtering for a stall regulated variable speed wind turbine. In *Universities Power Engineering Conference (UPEC), 2009 Proceedings of the 44th International*, pages 1–5. IEEE, 2009.

[122] H Nguyen Tien, CW Scherer, and JMA Scherpen. Robust performance of self-scheduled lpv control of doubly-fed induction generator in wind energy conversion systems. In *Power Electronics and Applications, 2007 European Conference on*, pages 1–10. IEEE, 2007.

[123] Shahab Ghasemi, Ahmadreza Tabesh, and Javad Askari-Marnani. Application of fractional calculus theory to robust controller design for wind turbine generators. *IEEE Transactions on Energy Conversion*, 29(3):780–787, 2014.

[124] Hamed Moradi and Gholamreza Vossoughi. Robust control of the variable speed wind turbines in the presence of uncertainties: A comparison between h - infinity and pid controllers. *Energy*, 90:1508–1521, 2015.

[125] Mahmood Mirzaei, Hans Henrik Niemann, Niels Kj, et al. Dk-iteration robust control design of a wind turbine. In *Control Applications (CCA), 2011 IEEE International Conference on*, pages 1493–1498. IEEE, 2011.

[126] Mahmoud M Hussein, Tomonobu Senjyu, Mohamed Orabi, Mohamed AA Wahab, and Mohamed M Hamada. Control of a grid connected variable speed wind energy conversion system. In *Renewable Energy Research and Applications (ICRERA), 2012 International Conference on*, pages 1–5. IEEE, 2012.

[127] Hassan K Khalil. *Noninear Systems*. Prentice-Hall, New Jersey, 1996.

[128] Hernán De Battista and Ricardo Julián Mantz. Sliding mode control of torque ripple in wind energy conversion systems with slip power recovery. In *Industrial Electronics Society, 1998. IECON'98. Proceedings of the 24th Annual Conference of the IEEE*, volume 2, pages 651–656. IEEE, 1998.

[129] Hernán De Battista, Pablo F Puleston, Ricardo J Mantz, and Carlos F Christiansen. Sliding mode control of wind energy systems with doig-power efficiency and torsional dynamics optimization. *IEEE Transactions on Power Systems*, 15(2):728–734, 2000.

[130] SF Pinto, L Aparicio, and P Esteves. Direct controlled matrix converters in variable speed wind energy generation systems. In *Power Engineering, Energy and Electrical Drives, 2007. POWERENG 2007. International Conference on*, pages 654–659. IEEE, 2007.

[131] Brice Beltran, Tarek Ahmed-Ali, and Mohamed El Hachemi Benbouzid. Sliding mode power control of variable-speed wind energy conversion systems. *IEEE Transactions on Energy Conversion*, 23(2):551–558, 2008.

[132] Iulian Munteanu, Seddik Bacha, Antoneta Iuliana Bratcu, Joel Guiraud, and Daniel Roye. Energy-reliability optimization of wind energy conversion systems by sliding mode control. *IEEE Transactions on Energy Conversion*, 23(3):975–985, 2008.

[133] Hui Li, KL Shi, and PG McLaren. Neural-network-based sensorless maximum wind energy capture with compensated power coefficient. *IEEE transactions on industry applications*, 41(6):1548–1556, 2005.

[134] YF Ren and GQ Bao. Control strategy of maximum wind energy capture of direct-drive wind turbine generator based on neural-network. In *Power and Energy Engineering Conference (APPEEC), 2010 Asia-Pacific*, pages 1–4. IEEE, 2010.

[135] Jogendra Singh Thongam, Pierre Bouchard, Hassan Ezzaidi, and M Ouhrouche. Artificial neural network-based maximum power point tracking control for variable speed wind energy conversion systems. In *Control Applications,(CCA) & Intelligent Control,(ISIC), 2009 IEEE*, pages 1667–1671. IEEE, 2009.

[136] Nikola Celanovic and Dushan Boroyevich. A fast space-vector modulation algorithm for multilevel three-phase converters. *IEEE transactions on industry applications*, 37 (2):637–641, 2001.

[137] Amal Z Mohamed, Mona N Eskander, and Fadia A Ghali. Fuzzy logic control based maximum power tracking of a wind energy system. *Renewable energy*, 23(2):235–245, 2001.

[138] MM Prats, JM Carrasco, E Galvan, JA Sanchez, and LG Franquelo. A new fuzzy logic controller to improve the captured wind energy in a real 800 kw variable speed-variable pitch wind turbine. In *Power Electronics Specialists Conference, 2002. pesc 02. 2002 IEEE 33rd Annual*, volume 1, pages 101–105. IEEE, 2002.

[139] AH Besheer, HM Emara, and MM Abdel_Aziz. Fuzzy based output feedback control for wind energy conversion system: an lmi approach. In *Power Systems Conference and Exposition, 2006. PSCE'06. 2006 IEEE PES*, pages 2030–2037. IEEE, 2006.

[140] AH Besheer, HM Emara, and MM Abdel Aziz. Fuzzy-based output-feedback h-infinity control for uncertain nonlinear systems: an lmi approach. *IET Control Theory & Applications*, 1(4):1176–1185, 2007.

[141] Xinyan Zhang, Weiqing Wang, and Ye Liu. Fuzzy control of variable speed wind turbine. In *Intelligent Control and Automation, 2006. WCICA 2006. The Sixth World Congress on*, volume 1, pages 3872–3876. IEEE, 2006.

[142] Xinyan Zhang, Xiaobo Zhang, Peiyi Zhou, Jing Cheng, Weiqing Wang, Suonan Jiale, and Ye Liu. Fuzzy control used in variable speed wind turbine. In *Automation and Logistics, 2009. ICAL'09. IEEE International Conference on*, pages 1194–1198. IEEE, 2009.

[143] CAM Amandola and DP Gonzaga. Fuzzy-logic control system of a variable-speed variable-pitch wind-turbine and a double-fed induction generator. In *Intelligent Systems Design and Applications, 2007. ISDA 2007. Seventh International Conference on*, pages 252–257. IEEE, 2007.

[144] Nimit Boonpirom and Kitti Paithoonwattanakij. Wind farm generator control using self-tuning fuzzy controller. In *Electrical and Computer Engineering, 2006. ICECE'06. International Conference on*, pages 221–224. IEEE, 2006.

[145] V Calderaro, V Galdi, A Piccolo, and P Siano. A fuzzy controller for maximum energy extraction from variable speed wind power generation systems. *Electric Power Systems Research*, 78(6):1109–1118, 2008.

[146] Antoneta Iuliana Bratcu, Iulian Munteanu, Emil Ceanga, and Silviu Epure. Energetic optimization of variable speed wind energy conversion systems by extremum seeking control. In *EUROCON, 2007. The International Conference on" Computer as a Tool"*, pages 2536–2541. IEEE, 2007.

[147] R Chedid, F Mrad, and M Basma. Intelligent control of a class of wind energy conversion systems. *IEEE Transactions on Energy Conversion*, 14(4):1597–1604, 1999.

[148] Santiago Sánchez, Maximiliano Bueno, Edilson Delgado, and Eduardo Giraldo. Optimal pi control of a wind energy conversion system using particles swarm. In *Electronics, Robotics and Automotive Mechanics Conference, 2009. CERMA'09.*, pages 332–337. IEEE, 2009.

[149] Mahmoud M Hussein, Tomonobu Senjyu, Mohamed Orabi, Mohamed AA Wahab, and Mohamed M Hamada. Simple sensor less maximum power extraction control for a variable speed wind energy conversion system. *Int. Jour. of Sustainability & Green Energy*, 1(1):1–10, 2012.

[150] SAFIULLAH Faqirzay and HD Patel. Maximum power extraction from wind generation system using mppt control scheme through power electronics converters. *International Jou. of Innovative Res. in Elect., Electr., Instrumentation and Control Engineering*, 3(3), 2015.

[151] Carlo L Bottasso, Alessandro Croce, Barbara Savini, Walter Sirchi, and Lorenzo Trainelli. Aero-servo-elastic modeling and control of wind turbines using finite-element multibody procedures. *Multibody System Dynamics*, 16(3):291–308, 2006.

[152] David Schlipf, Dominik Johannes Schlipf, and Martin Kühn. Nonlinear model predictive control of wind turbines using lidar. *Wind Energy*, 16(7):1107–1129, 2013.

[153] Matthias D Galus, Raffael La Fauci, and Göran Andersson. Investigating phev wind balancing capabilities using heuristics and model predictive control. In *Power and Energy Society General Meeting, 2010 IEEE*, pages 1–8. IEEE, 2010.

[154] Wei Qi, Jinfeng Liu, Xianzhong Chen, and Panagiotis D Christofides. Supervisory predictive control of standalone wind/solar energy generation systems. *IEEE transactions on control systems technology*, 19(1):199–207, 2011.

[155] Massimo Canale, Lorenzo Fagiano, and Mario Milanese. Power kites for wind energy generation. *IEEE Control Systems Magazine*, 27(6):25–38, 2007.

[156] Lars Christian Henriksen. Model predictive control of a wind turbine (with constraints). *In Proc. of European Wind Energy Conference, Brussels, Belgium*, 2007.

[157] Bonnie J Jonkman. Turbsim user's guide: Version 1.50. 2009.

[158] Subho Upadhyay and MP Sharma. A review on configurations, control and sizing methodologies of hybrid energy systems. *Renewable and Sustainable Energy Reviews*, 38:47–63, 2014.

[159] Debashisha Jena and Saravanakumar Rajendran. A review of estimation of effective wind speed based control of wind turbines. *Renewable and Sustainable Energy Reviews*, 43:1046–1062, 2015.

[160] Ilhami Colak, Ersan Kabalci, Gianluca Fulli, and Stavros Lazarou. A survey on the contributions of power electronics to smart grid systems. *Renewable and Sustainable Energy Reviews*, 47:562–579, 2015.

[161] Bhavna Jain, Shailendra Jain, and RK Nema. Control strategies of grid interfaced wind energy conversion system: An overview. *Renewable and Sustainable Energy Reviews*, 47:983–996, 2015.

[162] Gabriele Michalke. *Variable speed wind turbines-modelling, control, and impact on power systems*. PhD thesis, Technische Universität, 2008.

[163] Hoa M Nguyen and D Subbaram Naidu. Advanced control strategies for wind energy systems: an overview. In *Power Systems Conference and Exposition (PSCE), 2011 IEEE/PES*, pages 1–8. IEEE, 2011.

[164] Sathyajith Mathew. *Wind energy: fundamentals, resource analysis and economics*, volume 1. Springer, 2006.

[165] H-B Zhang, John Fletcher, N Greeves, SJ Finney, and BW Williams. One-power-point operation for variable speed wind/tidal stream turbines with synchronous generators. *IET renewable power generation*, 5(1):99–108, 2011.

[166] Tao Sun, Zhe Chen, and Frede Blaabjerg. Voltage recovery of grid-connected wind turbines after a short-circuit fault. In *Industrial Electronics Society, 2003. IECON'03. The 29th Annual Conference of the IEEE*, volume 3, pages 2723–2728. IEEE, 2003.

[167] Magdi Ragheb and Adam M Ragheb. *Wind turbines theory-the betz equation and optimal rotor tip speed ratio*. INTECH Open Access Publisher, 2011.

[168] Samuel Ofordile Ani. *Low cost small wind turbine generators for developing countries*. TU Delft, Delft University of Technology, 2013.

[169] Iulian Munteanu, Antoneta Iuliana Bratcu, Nicolaos-Antonio Cutululis, and Emil Ceanga. *Optimal control of wind energy systems: towards a global approach*. Springer Science & Business Media, 2008.

[170] Juha Pyrhonen, Tapani Jokinen, and Valeria Hrabovcova. *Design of rotating electrical machines*. John Wiley & Sons, 2009.

[171] Thomas A Lipo. *Analysis of synchronous machines*. CRC Press, 2012.

[172] E Spooner and AC Williamson. Direct coupled, permanent magnet generators for wind turbine applications. *IEE Proceedings-Electric Power Applications*, 143(1):1–8, 1996.

[173] Reza Zeinali. *Design and Optimization of High Torque Density Generator for Direct Drive Wind Turbine Applications*. PhD thesis, MIDDLE EAST TECHNICAL UNIVERSITY, 2016.

[174] Naomitsu Urasaki, Tomonobu Senjyu, and Katsumi Uezato. Relationship of parallel model and series model for permanent magnet synchronous motors taking iron loss into account. *IEEE Transactions on Energy Conversion*, 19(2):265–270, 2004.

[175] Jorge Oliveira Estima. *Development and analysis of permanent magnet synchronous motor drives with fully integrated inverter fault-tolerant capabilities*. PhD thesis, University of Coimbra, 2012.

[176] Xiangyu Zhang, Yi Wang, and Heming Li. Control of pmsg-based wind turbines to damp the power system oscillations. In *IEEE PEDS*, 2011.

[177] Ned Mohan and Tore M Undeland. *Power electronics: converters, applications, and design*. John Wiley & Sons, 2007.

[178] SA Azmi, KH Ahmed, SJ Finney, and BW Williams. Comparative analysis between voltage and current source inverters in grid-connected application. In *Renewable Power Generation (RPG 2011), IET Conference on*, pages 1–6. IET, 2011.

[179] Jingya Dai, Dewei Xu, and Bin Wu. A novel control scheme for current-source-converter-based pmsg wind energy conversion systems. *IEEE Transactions on Power Electronics*, 24(4):963–972, 2009.

[180] Hak-Jun Lee, Sungho Jung, and Seung-Ki Sul. A current controller design for current source inverter-fed pmsm drive system. In *Power Electronics and ECCE Asia (ICPE & ECCE), 2011 IEEE 8th International Conference on*, pages 1364–1370. IEEE, 2011.

[181] A Dreschinski. *Comparison of Different Control Strategies for Permanent Magnet Synchronous Generators for Use in Wind Turbines*. PhD thesis, Master thesis, Department of Renewable Energies, Technical University of Darmstadt, 2005.

[182] Anders Grauers and Sven Landström. The rectifiers influence on the size of direct-driven generators. In *EWEC 99-Conference proceedings*, pages 829–832, 1999.

[183] S Jöckel. Calculation of different generator systems for wind turbines with particular reference to low-speed permanent-magnet machines, technische universität darmstadt, diss., 2003.

[184] Ahmed S Al-Toma, Gareth A Taylor, and Maysam Abbod. Modelling and simulation of load connected fixed blade wind turbine with permanent magnet synchronous generators. In *Power Engineering Conference (UPEC), 2015 50th International Universities*, pages 1–6. IEEE, 2015.

[185] F Blaabjerg and F Iov. Wind power–a power source now enabled by power electronics. *Proc. COBEP 2007*, 2007.

[186] Stefano Bifaretti, Pericle Zanchetta, Alan Watson, Luca Tarisciotti, and Jon C Clare. Advanced power electronic conversion and control system for universal and flexible power management. *IEEE Transactions on Smart Grid*, 2(2):231–243, 2011.

[187] Jon Clare. Advanced power converters for universal and flexible power management in future electricity networks. In *Power Electronics and Applications, 2009. EPE'09. 13th European Conference on*, pages 1–29. IEEE, 2009.

[188] Ned Mohan. *Advanced electric drives: analysis, control, and modeling using MATLAB/Simulink*. John wiley & sons, 2014.

[189] Gabriele Michalke, Anca D Hansen, and Thomas Hartkopf. Control strategy of a variable speed wind turbine with multipole permanent magnet synchronous generator. In *Proceedings of European Wind Energy Conference and Exhibition*, 2007.

[190] M Kasmierkowski and Henryk Tunia. Automatic control of converter fed drives. *ELECTRONIC ENGINEERING*, 4:6, 1994.

[191] DD Banham-Hall, GA Taylor, CA Smith, and MR Irving. Towards large-scale direct drive wind turbines with permanent magnet generators and full converters. In *Power and Energy Society General Meeting, 2010 IEEE*, pages 1–8. IEEE, 2010.

[192] Surya Baktiono. *A Study of Field-Oriented Control of a Permanent Magnet Synchronous Generator and Hysteresis Current Control for Wind Turbine Application*. PhD thesis, The Ohio State University, 2012.

[193] Shyam Janakiraman and Wajiha Shireen. An optimal speed wind turbine test bench system for pmsg machines with mpp control. In *2014 IEEE PES General Meeting| Conference & Exposition*, pages 1–5. IEEE, 2014.

[194] Ashish Kumar Agrawal. *Study of wind Turbine Driven DFIG using AC/DC/AC converter*. PhD thesis, National Institute of Technology Rourkela, 2006.

[195] Anders Carlsson. The back-to-back converter. *Lund: Department of Industrial Electrical Engineering and Automation Lund Institute of Technology*, 7, 1998.

[196] Frede Blaabjerg, Remus Teodorescu, Marco Liserre, and Adrian V Timbus. Overview of control and grid synchronization for distributed power generation systems. *IEEE Transactions on industrial electronics*, 53(5):1398–1409, 2006.

[197] Antonio Gómez Expósito, Antonio Gomez-Exposito, Antonio J Conejo, and Claudio Canizares. *Electric energy systems: analysis and operation*. CRC Press, 2016.

[198] Zhenbin Zhang, Ralph Kennel, and Christoph Hackl. Two direct torque and power control methods for back-to-back power converter pmsg wind turbine systems. In *Power Electronics and Motion Control Conference (IPEMC-ECCE Asia), 2016 IEEE 8th International*, pages 1515–1520. IEEE, 2016.

[199] Mihai Ciobotaru, Remus Teodorescu, and Vassilios G Agelidis. Offset rejection for pll based synchronization in grid-connected converters. In *Applied Power Electronics Conference and Exposition, 2008. APEC 2008. Twenty-Third Annual IEEE*, pages 1611–1617. IEEE, 2008.

[200] Ahmed S Al-Toma, Gareth A Taylor, and Maysam Abbod. Intelligent pitch angle control scheme for variable speed wind generator systems. In *Power Engineering Conference (UPEC), 2017 52th International Universities*. IEEE, 2017 Accepted.

[201] AI Stan, DI Stroe, T Stanciu, and L Shuai. *Variable speed wind turbine equipped with synchronous generator*. PhD thesis, Master's thesis, Institute of Energy Technology, Aalborg, Denmark (June 2009), 2009.

[202] Abdul Motin Howlader, Naomitsu Urasaki, Atsushi Yona, Tomonobu Senjyu, and Ahmed Yousuf Saber. Design and implement a digital h infinity robust controller for a mw-class pmsg-based grid-interactive wind energy conversion system. *Energies*, 6(4): 2084–2109, 2013.

[203] Akie Uehara, Alok Pratap, Tomonori Goya, Tomonobu Senjyu, Atsushi Yona, Naomitsu Urasaki, and Toshihisa Funabashi. A coordinated control method to smooth wind power fluctuations of a pmsg-based wecs. *IEEE Transactions on energy conversion*, 26(2):550–558, 2011.

[204] Bin Wu and Mehdi Narimani. *High power converters and AC drives*. John Wiley & Sons, 2016.

[205] Bimal K Bose. *Power electronics and motor drives: advances and trends*. Academic press, 2010.

[206] JD Irwin, Marian P Kazmierkowski, Ramu Krishnan, and Frede Blaabjerg. *Control in power electronics: selected problems*. Academic press, 2002.

[207] Ion Boldea and Syed A Nasar. *Electric drives*. CRC press, 2016.

[208] Jose Rodriguez and Patricio Cortes. *Predictive control of power converters and electrical drives*, volume 40. John Wiley & Sons, 2012.

[209] Tevhid Atalik, Mustafa Deniz, Erkan Koc, Cem Özgur Gercek, Burhan Gultekin, Muammer Ermis, and Isik Cadirci. Multi-dsp and-fpga-based fully digital control system for cascaded multilevel converters used in facts applications. *IEEE transactions on industrial informatics*, 8(3):511–527, 2012.

[210] Bimal K Bose. Modern power electronics and ac drives. 2002.

[211] Marcian Cirstea, Andrei Dinu, Malcolm McCormick, and Jeen Ghee Khor. *Neural and fuzzy logic control of drives and power systems*. Newnes, 2002.

[212] Peter Vas. *Artificial-intelligence-based electrical machines and drives: application of fuzzy, neural, fuzzy-neural, and genetic-algorithm-based techniques*, volume 45. Oxford university press, 1999.

[213] Zafer Civelek, Murat Lüy, Ertuğrul Çam, and Necaattin Barışçı. Control of pitch angle of wind turbine by fuzzy pid controller. *Intelligent Automation & Soft Computing*, 22 (3):463–471, 2016.

[214] Li Zhen and Longya Xu. Fuzzy learning enhanced speed control of an indirect field-oriented induction machine drive. *IEEE transactions on control systems technology*, 8 (2):270–278, 2000.

[215] JL Silva Neto and H Le-Huy. An improved fuzzy learning algorithm for motion control applications [pm synchronous motors]. In *Industrial Electronics Society, 1998. IECON'98. Proceedings of the 24th Annual Conference of the IEEE*, volume 1, pages 1–5. IEEE, 1998.

[216] Ahmed S Al-Toma, Gareth A Taylor, and Maysam Abbod. A comparison of pi and fuzzy logic control schemes for field oriented permanent magnet synchronous generator wind turbines. In *IEEE PES ISGT Europe 2017, 7th IEEE International Conference on Innovative Smart Grid Technologies*. IEEE, Accepted 2017.

[217] Liu Mingji, Cai Zhongqin, Cheng Ximing, and Ouyang Minggao. Adaptive position servo control of permanent magnet synchronous motor. In *American Control Conference, 2004. Proceedings of the 2004*, volume 1, pages 84–89. IEEE, 2004.

[218] Sidney R Bowes and Jian Li. New robust adaptive control algorithm for high-performance ac drives. *IEEE Transactions on Industrial Electronics*, 47(2):325–336, 2000.

[219] H Le-Huy, P Viarouge, and I Kamwa. Model reference adaptive fuzzy control of a permanent-magnet synchronous motor. In *Industrial Electronics, Control, and Instrumentation, 1995., Proceedings of the 1995 IEEE IECON 21st International Conference on*, volume 2, pages 1440–1445. IEEE, 1995.

[220] Ioan Doré Landau, Rogelio Lozano, Mohammed M'Saad, and Alireza Karimi. *Adaptive control*, volume 51. Springer New York, 1998.

[221] Nitin J Patil, Rajan H Chile, and Laxman M Waghmare. Hybrid model reference adaptive fuzzy controller. In *Emerging Trends in Engineering and Technology (ICETET), 2009 2nd International Conference on*, pages 698–703. IEEE, 2009.

[222] Jeffrey T Spooner, Raúl Ordónez, and Kevin M Passino. Stable direct adaptive control of a class of discrete time nonlinear systems. In *Proc. of the 13th IFAC world congress, San Francisco*, pages 343–348, 1996.

[223] Marián Tárnık—Ján Murgaš. Model reference adaptive control of permanent magnet synchronous motor. *Journal of Electrical Engineering*, 62(3):117–125, 2011.

[224] Arne Linder, Rahul Kanchan, Ralph Kennel, and Peter Stolze. *Model-based predictive control of electric drives*. Cuvillier, 2010.

[225] Patricio Cortés, Marian P Kazmierkowski, Ralph M Kennel, Daniel E Quevedo, and José Rodríguez. Predictive control in power electronics and drives. *Industrial Electronics, IEEE Transactions on*, 55(12):4312–4324, 2008.

[226] S Joe Qin and Thomas A Badgwell. An overview of nonlinear model predictive control applications. In *Nonlinear model predictive control*, pages 369–392. Springer, 2000.

[227] James Blake Rawlings and David Q Mayne. *Model predictive control: Theory and design*. Nob Hill Pub., 2009.

[228] Manfred Morari and Jay H Lee. Model predictive control: past, present and future. *Computers & Chemical Engineering*, 23(4):667–682, 1999.

[229] Samir Kouro, Patricio Cortés, René Vargas, Ulrich Ammann, and José Rodríguez. Model predictive control—a simple and powerful method to control power converters. *IEEE Transactions on Industrial Electronics*, 56(6):1826–1838, 2009.

[230] Arne Linder, Rahul Kanchan, Ralph Kennel, and Peter Stolze. *Model-based predictive control of electric drives*. Cuvillier, 2010.

[231] Ahmed S Al-Toma, Gareth A Taylor, and Maysam Abbod. Development of space vector modulation control schemes for grid connected variable speed permanent magnet synchronous generator wind turbines. In *Power Engineering Conference (UPEC), 2016 51th International Universities*, pages 1–6. IEEE, 2016.

[232] Eduardo F Camacho and Carlos Bordons Alba. *Model predictive control*. Springer Science & Business Media, 2013.

[233] Sergio Vazquez, Jose I Leon, Leopoldo G Franquelo, Jose Rodriguez, Hector A Young, Abraham Marquez, and Pericle Zanchetta. Model predictive control: A review of its applications in power electronics. *IEEE Industrial Electronics Magazine*, 8(1):16–31, 2014.

[234] Sofiane Bououden, Salim Filali, and Mohammed Chadli. Fuzzy predictive control of a variable speed wind turbine. *Energy Procedia*, 42:357–366, 2013.

[235] S Bououden, M Chadli, S Filali, and A El Hajjaji. Fuzzy model based multivariable predictive control of a variable speed wind turbine: Lmi approach. *Renewable Energy*, 37(1):434–439, 2012.

[236] Ritu Shakya, Kritika Rajanwal, Sanskriti Patel, and Smita Dinkar. Design and simulation of pd, pid and fuzzy logic controller for industrial application. *International Journal of Information and Computation Technology ISSN*, pages 0974–2239, 2014.

[237] Harish Kumar, Ankit Gupta, Rupendra Kumar Pachauri, and Yogesh K Chauhan. Pi/fl based blade pitch angle control for wind turbine used in wind energy conversion system. In *Recent Developments in Control, International Conference on Automation and Power Engineering (RDCAPE)*, pages 15–20. IEEE, 2015.

[238] Zhenbin Zhang, Christoph Hackl, Fengxiang Wang, Zhe Chen, and Ralph Kennel. Encoderless model predictive control of back-to-back converter direct-drive permanent-magnet synchronous generator wind turbine systems. In *Power Electronics and Applications (EPE), 2013 15th European Conference on*, pages 1–10. IEEE, 2013.

[239] Ahmed Lasheen and Abdel Latif Elshafei. Wind-turbine collective-pitch control via a fuzzy predictive algorithm. *Renewable Energy*, 87:298–306, 2016.

[240] Ahmed Lasheen and Abdel Latif Elshafei. Fuzzy predictive control of the collective pitch in large wind turbines. In *Control Conference (ECC), 2015 European*, pages 1528–1533. IEEE, 2015.

[241] P Antoniewicz and MP Kazmierkowski. Predictive direct power control of three phase boost rectifier. *Bull. Polisch Acad. Sci*, 54(3), 2006.

[242] Johanna Carolina Salazar Salas. *MPC-BASED ENERGY MANAGEMENT SYSTEM FOR HYBRID RENEWABLE ENERGIES*. PhD thesis, University of Valladolid, 2015.

[243] Naziha Harrabi, Mansour Souissi, Abdel Aitouche, and Mohamed Chabaane. Intelligent control of wind conversion system based on pmsg using ts fuzzy scheme. *International Journal Of Renewable Energy Research*, 5(4):952–960, 2015.

[244] Texas Instruments. Clarke & park transforms on the tms320c2xx. *Application Report Literature Number: BPRA048*, 1996.